5.2.4. Cross-linker

The crosslinking agent used for the trials was MBAm instead of EGDMA. The choice of MBAm over EGDMA is due to the proved influence that this hydrophilic crosslinking agent has on the hydrogels' hydrophilicity character.[22,30] The efficacy in using MBAm in these systems was tested and concentration effect was evaluated. It has been observed that there is a range of possible concentration for the MBAm crosslinking agent, which is 1-2wt% with respect to HEMA's quantity. Low concentrations of MBAm lead to hydrogels, which have scarce control of the liquid diffusion (example of 233PVP50* and 400PVP50* samples), while high amounts of cross-linker in the gel formulation lead to rigid and friable gels. It has been observed that when gel formulations are constituted by high amounts of PVP with respect to water and HEMA and high water content (e.g. 233PVP65*, see table 5.8), the MBAm concentration should be increased to a maximum of 2wt% with respect to HEMA's amount.

5.3. Selected formulations of SIPN p(HEMA)/PVP hydrogels

It has been confirmed from the synthesis trials that SIPNs can be effectively designed by varying their component ratios (water, PVP, HEMA, and cross-linker quantities) in order to tune their characteristics in terms of mechanical behavior (softness, elasticity, and resistance to tensile strength) and affinity to water. The selected hydrogels formulations, which are already presented and discussed in peer-reviewed research papers[31–33], were designed to answer different demands in the cleaning of Cultural Heritage (see formulations and weight ratios in tables 5.8 and 5.9).

Table 5.8. Compositions (wt%) of the selected SIPN hydrogels. XPVPY designation, where "X" refers to the weight percentage of PVP with respect of HEMA and "Y" refers to the weight percentage of water in the composition.

Gel	Short name	PVP (wt%)	HEMA (wt%)	H_2O (wt%)	MBA (wt%)	AIBN (wt%)
100PVP50*	**H50**	24.86	24.86	49.72	0.25	0.31
150PVP58*	**H58**	25.09	16.72	57.73	0.25	0.21
233PVP65*	**H65**	24.42	10.46	64.78	0.21	0.13

* AIBN is added in a 1:0.01 HEMA/AIBN molar ratio.

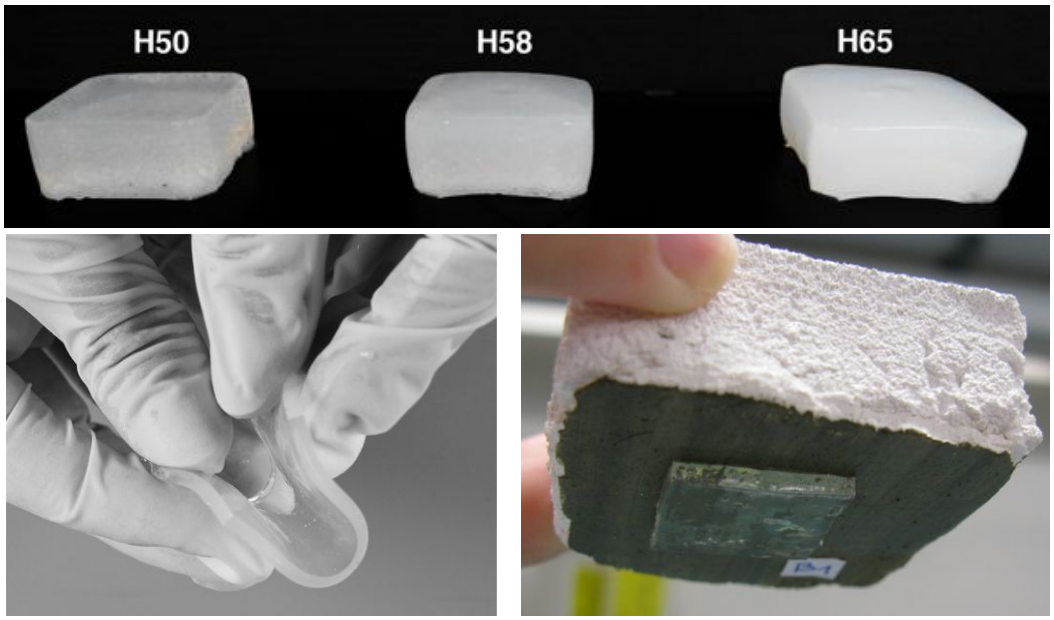

Figure 5.6. Some of the visible physical characteristics of the selected SIPN p(HEMA)/PVP hydrogels.

Table 5.9. Weight ratios between components for the selected SIPN hydrogel formulations.

Gel	HEMA/MBA ratio	HEMA/PVP ratio	H_2O/PVP ratio
H50	1:0.01	1:1	1:0.50
H58	1:0.015	1:1.5	1:0.43
H65	1:0.02	1:2.3	1:0.38

Generally speaking, the macroscopic characteristics of these selected systems are the following: ***H50*** hydrogel is more rigid and less water content so is suitable to treat extremely water-sensitive materials, under the condition of a somewhat flat surface (e.g. paper manuscripts and parchment); ***H58*** is soft and with appropriate water content for the cleaning of water-sensitive surfaces, and it may adhere on slightly rough surfaces (e.g. paintings on canvas or wood); ***H65*** is the most soft and with high water content, which allows more liquid interchange with the surface to clean and permits the adherence of the gel in rough surfaces (e.g. wall-paintings). The investigated hydrogels are transparent or translucent and easy to manipulate (see figure 5.6). It is also possible to observe that SIPN hydrogels remain attached to the surface even in downward position.

Furthermore, the SIPN p(HEMA)/PVP hydrogels are able to load other liquids than water, including pure and mixtures of organic solvents and nanostructured fluids. All the nominated characteristics were investigated through a comprehensive physicochemical characterization, using several methods and techniques, presented in the next chapter. The characterization of the physicochemical and mechanical properties of SIPN gels was limited to the selected gel formulations. Where needed, specific gel formulations were prepared to evaluate the influence on varying the components in the composition.

5.3.1. Water release

A water release test was performed using the selected hydrogel formulations (***H50***, ***H58*** and ***H65***) and two commonly used physical gels in the conservation and restoration field for the cleaning of artifacts, based on polysaccharide polymers, known by the commercial grades AgarArt and Kelcogel. In order to assess the real amount of water released to a highly hydrophilic surface, a paper surface was chosen, which is also a water-sensitive material. The values of the amount of water release by cm^2 of contact area are presented in figure 5.7. The results show that physical polysaccharide gels release water at least twice as much as semi-IPN hydrogels.

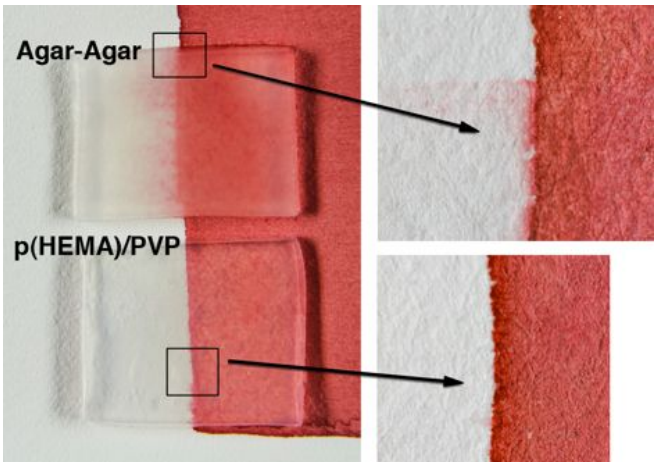

Gel	Water released (mg/cm^2)
H50	8
H58	15
H65	16
AgarArt	30
Kelcogel	33

Figure 5.7. Five minutes application of agar-agar (2wt%) and ***H50*** p(HEMA)/PVP hydrogel on paper painted with brazilwood ink, which is partially soluble in water. In the right, water release test results are presented for SIPN hydrogels and polysaccharide gels.

All SIPN hydrogels performed a homogeneous release of water restricted to the paper contact area, that is, without spreading in the X-Y axis, while physical gels showed an evident water spreading much over the gel contact area. In order to further investigate on this, a painted paper sample was prepared and water-swollen gels were applied (see figure 5.7). Only after 5 minutes of gel contact the polysaccharide gels showed an evident paint leaching, while the painted surface where SIPN hydrogels were applied remained without changes.

5.4. Materials and methods

5.4.1. Synthesis of gels

5.4.1.1. Materials

2-Hydroxyethyl methacrylate (HEMA) (assay 97%), poly(vinylpyrrolidone) (PVP) (average $M_w \approx 1.3 \times 10^6$Da) and ammonium persulfate (APS) (assay 98%) were obtained from Sigma-Aldrich. 2,2-azobis(2-methylpropionitrile) (AIBN) (assay 98%), N,N-methylene-bis(acrylamide) (MBAm) (assay 99%) and *N*,*N*,*N*',*N*'-tetramethylethylenediamine (TEMED) (assay ≥99%) were obtained from Fluka. AIBN was recrystallized twice from methanol prior to use. All the other chemicals were used as received. Water was purified by a Millipore MilliRO-6 Milli-Q gradient system (resistivity >18 MΩ cm).

5.4.1.2. Preparation procedure

Hydrogels synthesis was carried out in two different types of molds to obtain (i) hydrogels with 2.5×2.5×1cm parallelepiped shape used for the physicochemical measurements and (ii) flat hydrogel films having 2 mm thickness used for the cleaning tests presented in the chapters 7 and 8 (see figure 5.8). All the products and radical initiator were mixed together, and the solution was bubbled with nitrogen for 5 min to remove dissolved oxygen that could inhibit the radical polymerization of HEMA. The solutions were stored at 4ºC for 2 days in order to decrease the formed nitrogen gas bubbles in the reaction mixture, due to the solution's high viscosity. Then, they were gently sonicated for 30min in pulsed mode to eliminate the last remained gas bubbles. The free-radical polymerization reaction, initiated by thermal homolysis of AIBN, occurred at 60°C for 4h. After polymerization, hydrogels were washed and placed in containers filled with

distilled water. The water was renewed twice a day for 7 days to remove any residue of unreacted monomer and the free PVP.

5.4.2. Preparation of polysaccharide-based gels

Polysaccharide-based physical gels (agar–agar and gellan gum) were also prepared by dispersion of dry powders in water with 3wt%. Powders were supplied by C.T.S. Italy (trademarks AgarArt and Kelcogel).

5.4.3. Water release

For the evaluation of water release properties, fully swollen hydrogels were gently surface dried and then positioned on four sheets of Whatman filter paper and covered with a lid to avoid water evaporation. The sheets of filter paper were weighted before and after 30min of gel application. The released water is normalized by unit area.

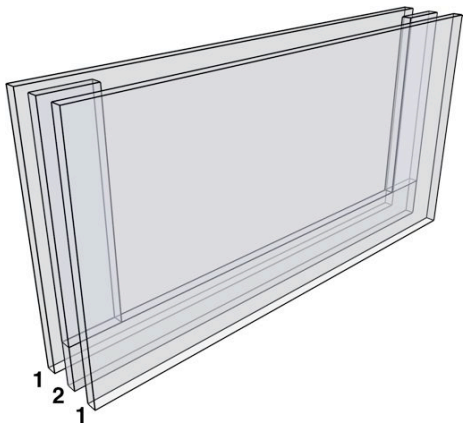

Figure 5.8. Schematic representation of the constructed mold for casting 2mm thick hydrogel films, constituted by: (1) glass plates; (2) 2mm thickeners of PMMA; and blinder clips to hold the components tight.

5.5. Bibliography

(1) Pizzorusso, G. Synthesis and Characterization of Systems for the Micro-Confinement of Detergents for the Cleaning of Canvas Paintings. PhD thesis on Science for the Conservation of Cultural Heritage, University of Florence: Florence, 2010.

(2) Bonini, M.; Lenz, S.; Giorgi, R.; Baglioni, P. Nanomagnetic Sponges for the Cleaning of Works of Art. *Langmuir* **2007**, *23*, 8681–8685.

(3) Pizzorusso, G.; Fratini, E.; Eiblmeier, J.; Giorgi, R.; Chelazzi, D.; Chevalier, A.; Baglioni, P. Physicochemical Characterization of Acrylamide/Bisacrylamide Hydrogels and their Application for the Conservation of Easel Paintings. *Langmuir* **2012**, *28*, 3952–3961.

(4) Material Safety Data Sheet: Acrylamide. In *Fisher Scientific*. https://extranet.fisher.co.uk/chemicalProductData_uk/wercs?itemCode=10235203&lang=EN (accessed Nov 27, 2014).

(5) Material Safety Data Sheet: 2-Hydroxyethyl methacrylate. In *Fischer Scientific*. https://extranet.fisher.co.uk/chemicalProductData_uk/wercs?itemCode=10559433&lang=EN (accessed Nov 27, 2014).

(6) Tighe, B. J. Hydrogels as Contact Lens Materials. In *Hydrogels in Medicine and Pharmacy*; Peppas, N. A., Ed.; Vol. III, Properties and applications; CRC Press: Boca Raton, FL, 1987; pp 53–82.

(7) Mack, E. J.; Okano, T.; Kim, S. W. Biomedical Applications of Poly(2-Hydroxyethyl Methacrylate) and its Copolymers. In *Hydrogels in Medicine and Pharmacy*; Peppas, N. A., Ed.; Vol. II, Polymers; CRC Press: Boca Raton, FL, 1987; pp 65–93.

(8) Peppas, N. A.; Moynihan, H. J.; Lucht, L. M. The Structure of Highly Crosslinked Poly(2-Hydroxyethyl Methacrylate) Hydrogels. *J. Biomed. Mater. Res.* **1985**, *19*, 397–411.

(9) Wichterle, O.; LíM, D. Hydrophilic Gels for Biological Use. *Nature* **1960**, *185*, 117–118.

(10) Refojo, M. F.; Yasuda, H. Hydrogels from 2-Hydroxyethyl Methacrylate and Propylene Glycol Monoacrylate. *J. Appl. Polym. Sci.* **1965**, *9*, 2425–2435.

(11) Okay, O. Macroporous Copolymer Networks. *Prog Polym Sci* **2000**, *25*, 711–779.

(12) Material Safety Data Sheet: N-Vinyl-2-pyrrolidone. In *Fisher Scientific*. https://extranet.fisher.co.uk/chemicalProductData_uk/wercs?itemCode=10773694&lang=EN (accessed Nov 27, 2014).

(13) Haaf, F.; Sanner, A.; Straub, F. Polymers of N-Vinylpyrrolidone: Synthesis, Characterization and Uses. *Polym J* **1985**, *17*, 143–152.

(14) Lai, Y.-C. A Novel Crosslinker for UV Copolymerization of N-vinyl Pyrrolidone and Methacrylates To Give Hydrogels. *J. Polym. Sci. Part Polym. Chem.* **1997**, *35*, 1039–1046.

(15) Al-Issa, M. A.; Davis, T. P.; Huglin, M. B.; Yip, D. C. F. Copolymerizations Involving N-Vinyl-2-Pyrrolidone. *Polymer* **1985**, *26*, 1869–1874.

(16) Raju, M. P.; Raju, K. M. Design and Synthesis of Superabsorbent Polymers. *J. Appl. Polym. Sci.* **2001**, *80*, 2635–2639.

(17) Gregonis, D. E.; Chen, C. M.; Andrade, J. D. The Chemistry of Some Selected Methacrylate Hydrogels. In *Hydrogels for Medical and Related Applications* 0-8412-0338-5, 0-8412-0311-3; Andrade, J. D., Ed.; American Chemical Society: Washington, DC, 1976; Vol. 31, pp 88–104. http://pubs.acs.org/doi/abs/10.1021/bk-1976-0031.ch007 (accessed Nov 29, 2014).

(18) Korbar, A.; Malavašič, T. Influence of Different Initiators on Methyl Methacrylate Polymerization, Studied by Differential Scanning Calorimetry. *J. Therm. Anal.* **1995**, *44*, 1357–1365.

(19) Schneider, M.; Graillat, C.; Boutti, S.; McKenna, T. F. Decomposition of APS and H2O2 for Emulsion Polymerisation. *Polym. Bull.* **2001**, *47*, 269–275.

(20) Chu, H.-H.; Lin, C.-S. The Effect of Initiators on the Emulsion Polymerization of 2-hydroxyethyl Methacrylate. *J. Polym. Res.* **2003**, *10*, 283–287.

(21) Čoupek, J.; Křiváková, M.; Pokorný, S. New Hydrophilic Materials for Chromatography: Glycol Methacrylates. *J. Polym. Sci. Polym. Symp.* **1973**, *42*, 185–190.

(22) Çaykara, T.; Turan, E. Effect of the Amount and Type of the Crosslinker on the Swelling Behavior of Temperature-Sensitive Poly(N-tert-Butylacrylamide-co-Acrylamide) Hydrogels. *Colloid Polym. Sci.* **2006**, *284*, 1038–1048.

(23) Hoare, T. R.; Kohane, D. S. Hydrogels in Drug delivery: Progress and Challenges. *Polymer* **2008**, *49*, 1993–2007.

(24) Sperling, L. H. Interpenetrating Polymer Networks: An Overview. In *Interpenetrating Polymer Networks*; Klempner, D.; Sperling, L. H.; Utracki, L. A., Eds.; American Chemical Society: Washington, DC, 1994; Vol. 239, pp 3–38.

(25) Gong, J. P.; Osada, Y. Surface Friction of Polymer Gels. *Prog Polym Sci* **2002**, *27*, 3–38.

(26) Fujimoto, D.; Mizuno, Y.; Danjoubara, K.; Murai, H. *Process for Producing Resin Varnish Containing Semi-IPN Composite Thermosetting Resin and, Provided Using the Same, Resin Varnish for Printed Wiring Board, Prepreg and Metal-Clad Laminate*. **EP2141198 A1**. 2010.

(27) Yin, L.; Fei, L.; Cui, F.; Tang, C.; Yin, C. Superporous Hydrogels Containing Poly(Acrylic Acid-co-Acrylamide)/O-Carboxymethyl Chitosan Interpenetrating Polymer Networks. *Biomaterials* **2007**, *28*, 1258–1266.

(28) Yanez, F.; Concheiro, A.; Alvarez-Lorenzo, C. Macromolecule Release and Smoothness of Semi-Interpenetrating PVP–pHEMA Networks for Comfortable Soft Contact Lenses. *Eur J Pharm Biopharm* **2008**, *69*, 1094–1103.

(29) Jovaševića, J. S.; Dimitrijevića, S. I.; Filipovića, J. M.; Tomića, S. L.; Mićićb, M. M.; Suljovrujića, E. H. Swelling, Mechanical and Antimicrobial Studies of Ag/P (HEMA/IA)/PVP Semi-IPN Hybrid Hydrogels. *Acta Phys. Pol. A* **2011**, *120*.

(30) Erbil, C.; Toz, E.; Akdemir, Ö.; Uyanık, N. An Investigation into the Influence of Crosslinker Type and Solvent Composition on Physical Properties and Phase Transition Behavior of Poly(N-isopropylacrylamide) Hydrogels. In *Advances in Silicones and Silicone-Modified Materials* 0-8412-2559-1, 0-8412-2560-5; Clarson, S. J.; Owen, M. J.; Smith, S. D.; Van Dyke, M. E., Eds.; American Chemical Society: Washington, DC, 2010; Vol. 1051, pp 167–180. http://pubs.acs.org/doi/abs/10.1021/bk-2010-1051.ch014 (accessed Dec 3, 2014).

(31) Domingues, J. A. L.; Bonelli, N.; Giorgi, R.; Fratini, E.; Gorel, F.; Baglioni, P. Innovative Hydrogels Based on Semi-Interpenetrating p(HEMA)/PVP Networks for the Cleaning of Water-Sensitive Cultural Heritage Artifacts. *Langmuir* **2013**, *29*, 2746–2755.

(32) Domingues, J.; Bonelli, N.; Giorgi, R.; Baglioni, P. Chemical Semi-IPN Hydrogels for the Removal of Adhesives from Canvas Paintings. *Appl. Phys. A* **2014**, *114*, 705–710.

(33) Domingues, J.; Bonelli, N.; Giorgi, R.; Fratini, E.; Baglioni, P. Innovative Method for the Cleaning of Water-Sensitive Artifacts: Synthesis and Application of Highly Retentive Chemical Hydrogels. *Int. J. Conserv. Sci.* **2013**, *4*, 715–722.

CHAPTER 6
Physicochemical Characterization of Selected SIPN p(HEMA)/PVP Hydrogels

6.1. Introduction

A comprehensive investigation of the physicochemical characteristics of hydrogels based on Semi-Interpenetrating Polymer Networks (SIPN) comprised by p(2-hydroxyethyl methacrylate) (pHEMA), as the constituent polymer network, and by poly(vinylpyrrolidone) (PVP), as the embedded linear polymer, is described here. The potential application of these hydrogels as containers for the cleaning of different surfaces using a wide range of cleaning systems (e.g. microemulsions and micellar solutions) is also evidenced. Special attention is made to SIPN hydrogels loaded with nanostructured fluids: possible interactions between polymeric chains and these cleaning systems are evidenced using rheology and scattering techniques. This chapter will be mainly focused on the selected formulations of SIPN p(HEMA)/PVP hydrogels, which have shown the most promising applicative characteristics during cleaning trials: ***H50***, ***H58*** and ***H65***. However, some specific gel formulations were also prepared to evaluate the influence of varying the composition, mainly the change in HEMA and crosslinking agent, which directly influence the gel network.

Table 6.1. Compositions (wt%) of the selected SIPN hydrogels.

Gel	PVP (wt%)	HEMA (wt%)	H_2O (wt%)	MBA (wt%)	AIBN (wt%)
H50	24.86	24.86	49.72	0.25	0.31
H58	25.09	16.72	57.73	0.25	0.21
H65	24.42	10.46	64.78	0.21	0.13

The composition for the preparation of the selected SIPN hydrogels is presented in table 6.1, and weight ratios between the components are shown in table 6.2. The materials and methods describing the experimental procedures and defining the parameters used hereafter are reported at the end of this chapter.

Table 6.2. Weight ratios between components for the selected SIPN hydrogel formulations.

Gel	HEMA/MBA ratio	HEMA/PVP ratio	H_2O/PVP ratio
H50	1:0.01	1:1	1:0.50
H58	1:0.015	1:1.5	1:0.43
H65	1:0.02	1:2.3	1:0.38

6.2. SIPN chemical composition

Due to the fact that these hydrogels are semi-interpenetrating polymer networks it is not possible to discuss about the reaction yield using gravimetric measurements, since PVP is also part of the polymer network, but it is inert during the polymerization reaction of the HEMA monomer. Knowing the exact composition of SIPN hydrogels is not possible without using complex chromatography techniques.[1] In fact, it should be noticed that a fraction of the added PVP is lost after the synthesis procedure, due to the fact that PVP is water-soluble and that its addition in high quantities may result in poor polymer interpenetration. Nonetheless, its addition in high quantities in the composition, as demonstrated in the previous chapter, is necessary to increase the water content of the reaction mixture during synthesis and to avoid water-polymer phase separation.

Attempts to obtain approximate values of the real formulation of the obtained SIPN systems were made through the calculation of the gel content (*G*) and the extrapolation of a calibration curve from pHEMA/PVP ratios by Fourier transform infrared spectroscopy in attenuated total reflectance (ATR-FTIR).

6.2.1. Gel content

Semi-IPN hydrogels are similar to polymer blends, that is, there is no chemical reaction, such as the formation of covalent bonds, between the forming network of HEMA and linear polymer PVP, during the polymerization reaction. Therefore,

linear PVP could be separated from the constituent network of pHEMA without cleavage of the polymer network. Formation of hydrogen bonds between the carbonyl group of PVP and the hydroxyl group of HEMA has already been reported in the literature.[2] This kind of interaction leads to an efficient embedding of linear PVP into the pHEMA network. In SIPN hydrogels, the final polymeric fraction of the gel is constituted by both polymerized pHEMA (with a relative reaction yield) and the imbedded PVP. Therefore, *G* is the most appropriate paramater to describe the efficiency of the polymer gel synthesis with the simultaneous polymer interpenetration. The results for *G* are: 90% for ***H50***, 78% for ***H58*** and 74% for ***H65***.

Even if the initial p(HEMA)/PVP ratio in ***H50*** is 50/50, its gel content is substantially high. It is clear that with increasing of PVP content in the reaction mixture it lowers *G* of the gel formed, since some of the PVP will be washed off after synthesis. As already stressed, high amounts of PVP are needed to keep the water content high, thus avoiding the phase separation.

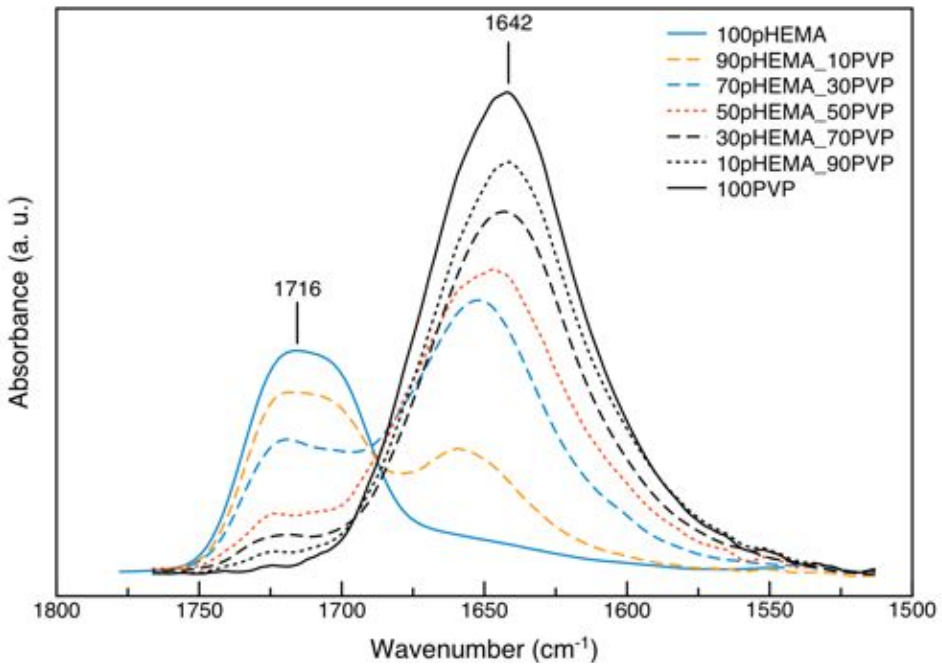

Figure 6.1. Selected wavenumber range of the ATR-FTIR spectra of pHEMA, PVP and their mixtures with known quantities, with characteristic peaks corresponding to the carbonyl stretching vibrations.

6.2.2. SIPN hydrogel composition

The gel content (*G*) does not give information on the real composition of the final formulation of the gel, since the major loss is due to the not embedded PVP. Considering that the reaction yield of the polymerization of pHEMA remains constant in all formulations (i.e ≈93wt% for an analogous pHEMA homopolymer), it is possible to estimate the real amount of PVP in the final hydrogel composition, through FTIR spectroscopy (see materials and methods). pHEMA and PVP show two distinct intense peaks in the carbonyl stretching mode FTIR range: pHEMA show a maximum peak at 1716cm^{-1}, while PVP an intense broad peak at 1642cm^{-1}. The peak of unreacted C=C bonds (at ≈1640 cm^{-1}) was not observed. (see figure 6.1).

In order to extrapolate a calibration curve, able to correlates the PVP/pHEMA ratio to the wt% of PVP in the final gel formulation, samples comprised by mixtures of known quantities of pHEMA and PVP were characterized through ATR-FTIR spectroscopy, which spectra are shown in figure 6.1. PVP/pHEMA ratios were calculated by Gaussian areas (see materials and methods) and then fitted to an exponential function, which is showed in the graphic of figure 6.2.

All the selected SIPN hydrogels (figure 6.3) featured the characteristic peaks of pHEMA, at ≈1723 cm^{-1} and of PVP at ≈1647 cm^{-1}. PVP peak increased as its content in the HEMA/PVP ratio is higher. The estimated wt% PVP in the PVP/pHEMA ratio could be calculated using the above calibration curve. Then, the amount of PVP in the hydrogel formulation was deducted from the obtained PVP amount with respect to the weight of polymerized pHEMA (considered to be 93wt% of the initial content). The weight percentage of PVP loss was assessed through weighting the estimated PVP in the formulation over the total added PVP in the reaction mixture. The obtained results are listed in table 6.3.

As expected, there is a major loss of PVP (from 71 to 79wt%). This means that the amount of chains of the HEMA network, which interacts with PVP chains, at a specific HEMA/PVP ratio will not be enough to contain further PVP. In this case it seems that the added PVP is already in saturation for all three formulations. Even if a comparison between the selected hydrogels is imprecise due to differences in the composition, a certain PVP loss increase is noted from ***H50*** to ***H65*** formulations, where HEMA/PVP ratios varies from 1:1 to 1:2.3, respectively. To sustain the hypothesis that the HEMA/PVP ratio influences on the loss of PVP, an hydrogel synthesis series was prepared by varying HEMA weight concentration in the composition (20-3.3%), above and below the analogous composition of ***H65***. These hydrogel series are presented in table 6.4 and PVP estimated proportions are listed in table 6.5.

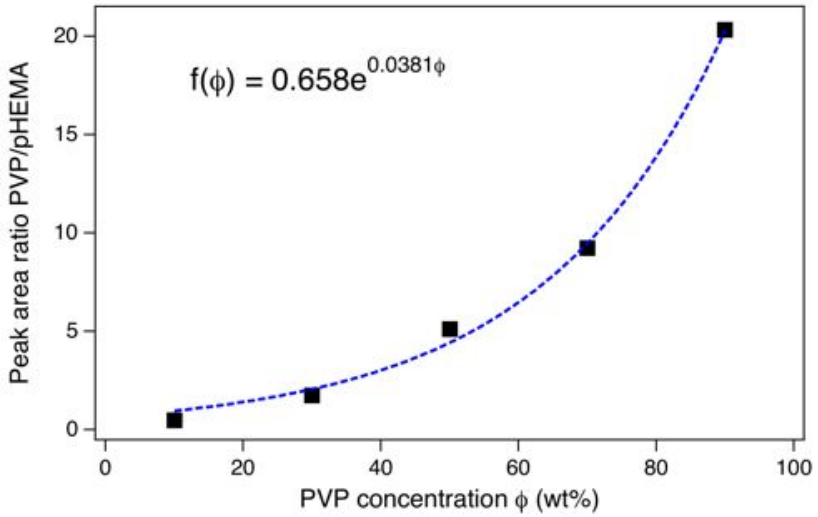

Figure 6.2. Calibration curve (blue line) derived from experimental data (squares) obtained from characteristic peak area ratios of PVP/pHEMA, in function of PVP concentration (wt%) with respect to pHEMA.

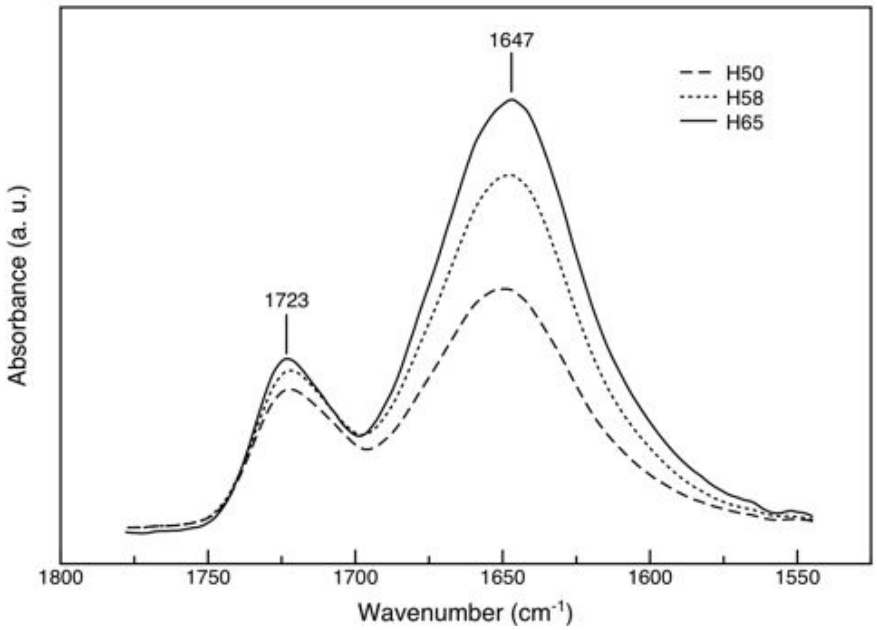

Figure 6.3. ATR-FTIR spectra of the selected hydrogels with assigned peaks for HEMA (1723 cm^{-1}, $\nu_{C=O}$) and PVP (1647 cm^{-1}, $\nu_{C=O}$).

Table 6.3. Comparison between added PVP and estimated PVP amount in the PVP/pHEMA ratio and in the selected SIPN hydrogel formulations, according to the calibration curve of ATR-FTIR.

Gel	Initial PVP in PVP/pHEMA (wt%)	Estimated PVP in PVP/pHEMA (wt%)	Estimated PVP in composition (wt%)	PVP loss with respect to added PVP (wt%)
H50	50	24.06	7.33	70.53
H58	60	32.08	7.34	70.73
H65	70	34.50	5.12	79.01

Table 6.4. Composition (wt%) of SIPN hydrogels for the series "HEMA" (***HM***).

	PVP (wt%)	HEMA (wt%)	H_2O (wt%)	MBAm (wt%)	AIBN (wt%)	HEMA/PVP ratio	H_2O/PVP ratio
HM20	24.42	20.00	54.93	0.40	0.25	1:1.2	1:0.44
HM17.5	24.42	17.50	57.51	0.35	0.22	1:1.4	1:0.42
HM15	24.42	15.00	60.09	0.30	0.19	1:1.6	1:0.41
HM12.5	24.42	12.50	62.67	0.25	0.16	1:2.0	1:0.39
HM7.5	24.42	7.50	67.84	0.15	0.09	1:3.3	1:0.36
HM5	24.42	5.00	70.42	0.10	0.06	1:4.9	1:0.35
HM4.1	24.42	4.10	71.35	0.08	0.05	1:6.0	1:0.34
HM3.3	24.42	3.30	72.17	0.07	0.04	1:7.4	1:0.34

As anticipated, there is an increase as well of the amount of lost PVP in these gel formulations, after hydrogel preparation, as the weight percentage of HEMA decreases, and consequently the HEMA/PVP ratio decreases too. Yañez et al.[3] reported the synthesis of semi-IPN p(HEMA)/PVP hydrogels for soft contact lenses, using PVP with an analogous M_w, but the HEMA/PVP ratio did not exceed 1:0.05 even if they observed that higher amounts of PVP in SIPN hydrogels are responsible for the observed characteristics of hydrophilicity and softness. So, considering the aim of this thesis, it is important to know that a high amount of PVP is lost after gel preparation, but is more important that its initial concentration remains high in order to obtain hydrogels with improved softness and hydrophilicity.

Table 6.5. Comparison between added PVP and estimated amount of PVP in the HEMA/PVP ratio and in the compositions of "HEMA" gel series, according to calculated values from the calibration curve of ATR-FTIR.

Gel	Initial PVP in PVP/HEMA (wt%)	Estimated PVP in PVP/HEMA (wt%)	Estimated PVP in composition (wt%)	PVP loss with respect to added PVP (wt%)
HM20	54.98	22.91	5.53	77.36
HM17.5	58.25	25.85	5.67	76.76
HM15	61.95	29.50	5.84	76.10
HM12.5	66.14	27.27	4.36	82.15
H65	**70**	**34.50**	**5.12**	**79.01**
HM7.5	76.50	30.51	3.06	87.46
HM5	83.00	31.95	2.18	91.06
HM4.1	85.62	34.37	2.00	91.82
HM3.3	88.10	35.12	1.66	93.20

6.3. Liquid-polymer interactions

An important characteristic of hydrogels is its liquid portion, since it is directly in relation with gels function. In fact, it is usually the liquid that has an active role, while the polymer fraction acts as a liquid carrier/container (e.g. drug delivery gels, contact lenses, etc.). Studying the swelling kinetics of hydrogels provides essential information on how is water diffusing inside gels, until equilibrium is reached. Each gel formulation is thermodynamically limited to a certain Equilibrium Solvent Content (ESC), which is named also Equilibrium Water Content (EWC) if the solvent is water. This value provides an important indication of the hydrophilicity of the system. Finally, dehydration kinetics is directly related to application features of gels used in Cultural Heritage cleaning, since the retention capability, that is, the strong interactions between polymer structure and liquid fraction, are also responsible for restraining liquid spreading/evaporation. All these features are discussed below.

6.3.1. Swelling kinetics

In drug delivery field, the development of polymeric devices able to release controlled quantities of active agents to their surroundings over a period of time, requires an analysis of the diffuse behavior of the drug in the polymer. This characteristic is in concordance with the required features for hydrogels used for

cleaning of water-sensitive artifacts, so water diffusion behavior evaluation is necessary. Some of the factors influencing liquid diffusion in polymers are chain mobility, chain entanglement, crosslinking density, porosity, presence of fillers and plasticizers and the affinity of the liquid with the polymer.[4]

In order to evaluate water-loading differences between the selected hydrogels, two formulations, ***H50*** and ***H65*** with the lowest and higher water content, respectively, were used for the evaluation of the swelling ratio, when placed in containers filled with deionized water. This was carried out in two distinct phases: water swelling immediately after SIPN hydrogels preparation (hydration) and with lyophilized gels (rehydration), as expressed in figure 6.4.

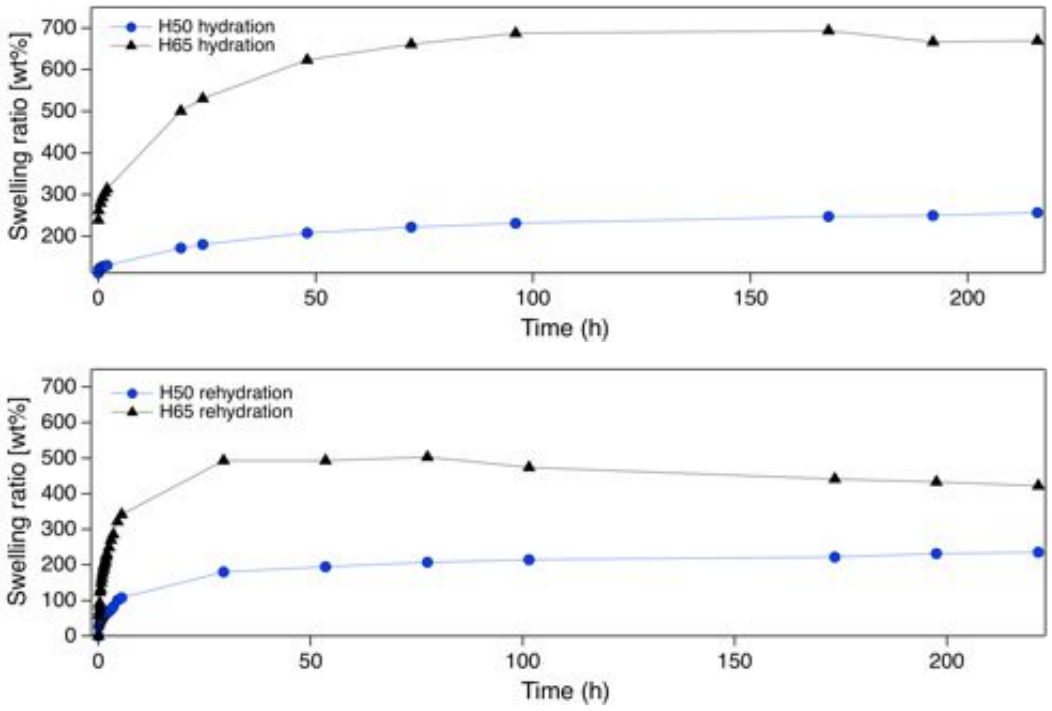

Figure 6.4. Swelling ratio of the gel's hydration after synthesis and gel's rehydration after a freeze-drying process. Two gel formulations (***H50*** and ***H65***) are shown.

From the swelling ratio over time ***H65*** hydrogel shows an higher swelling than ***H50***. This is particularly evidenced when EWC is reached, where ***H65*** has swelled ≈700wt% over its dry weight, while ***H50*** swelled ≈250wt%. This means that the EWC is higher for ***H65*** than for ***H50***, as demonstrated in the following sub-section. Since the swelling kinetics of hydrogels after preparation begins at a certain water

content, which is different for the selected hydrogels (see hydration SR in figure 6.4 when i = 0), in order to evaluate the interaction of water molecules and polymer network in the early phases of swelling, i.e. the diffusion phenomena, xerogels, obtained by a freeze-drying process, were used for the rehydration SR (see figure 6.4, bottom graph).

The rehydration swelling behavior is quite different than the hydration one, which is especially evident for ***H65***, which has a swelling ratio maximum at ≈500wt%, and then decreases over time. ***H50***, on the other hand, has a swelling ratio of ≈235wt%, when EWC is reached, and remains constant over time. These results indicate that the freeze-drying process induces some modifications on the hydrogel's structure. In fact, during freeze-drying, as a consequence of the water to ice expansion, some of the microporosity may collapse. Furthermore, ***H65*** shows a continuous decrease in weight after a SR maximum is reached, which may indicate that PVP is being release in considerable amounts. This confirms the fact that some structure is collapsed and, thus, some PVP is lost because not anymore efficiently interpenetrated.

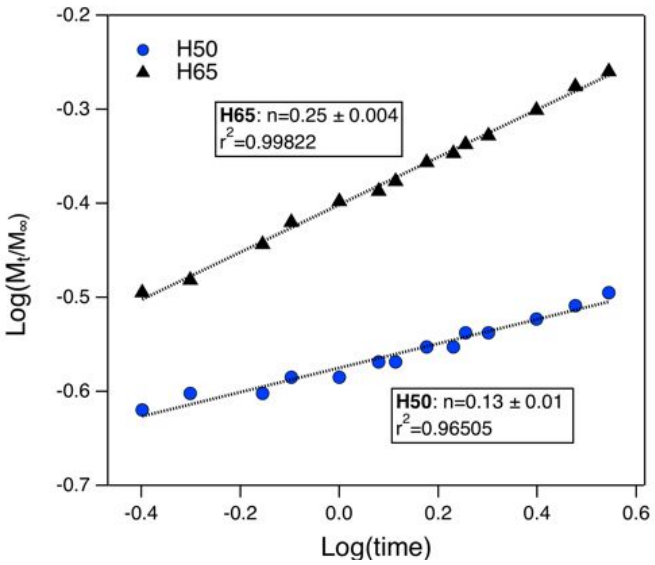

Figure 6.5. Log-log plot of the rehydration data with the linear fitting according to thee dynamics of water sorption expressed in equation 6.4.

In order to have a perception of the water transport process within the selected SIPN hydrogels, the Fickian power law of diffusion (see equation 6.4) was fitted to

the data of the early phases of the rehydration swelling kinetics, presented in figure 6.5. When the dried hydrogel is in contact with liquid water, the water molecules penetrate first into hydrogel's surface, creating, thus, a moving solvent front, which separates the dried glassy polymer region from the swollen rubber-like polymer phase. In the interface between water molecules front and dried polymer there is a glass-rubber transition, which can be slower or faster than the water diffusion rate. In Fickian power law, the swelling exponent *n* provides information about the mechanism of swelling kinetics.[5] Alfrey et al.[6] distinguished three classes of diffusion:

- *n*=0.5, Fickian diffusion: the diffusion of water is slower than the polymer relaxation rate. In this case, the system is controlled by a diffusion phenomenon.
- *n*=0.5-1.0, non-Fickian diffusion: describes the those cases in which the diffusion and relaxation rates are comparable.
- *n*=1.0, case II transport: anomalous diffusion, in which the solvent front penetrates at a constant velocity, in the early swelling phase.

The obtained exponent *n* for the selected SIPN systems is 0.13 and 0.25 for ***H50*** and ***H65*** hydrogels, respectively. These values indicate that the diffusion mechanism is Fickian type, thus diffusion controlled. In fact, the presence of hydrophilic polymer chains of PVP in SIPN makes the water-sorption process from relaxation controlled to diffusion controlled. In other words, the high number of PVP chains in the SIPN hydrogels reduces the diffusion of high amounts of water molecules from the swelling medium to the interior of the SIPN, due to its high hydrophilicity, thereby making the swelling process diffusion controlled. The phenomenon of water sorption in this kind of systems depends also on the relaxation of the macromolecular chains of the polymer network. The amount of HEMA increases from ***H65*** to ***H50***, which is in parallel with a decrease of the diffusion exponent, *n*, in the Fickian region, thus indicating a shift of the swelling process from more Fickian to less Fickian diffusion. This may be explained by the fact that HEMA is slightly hydrophobic, so in the presence of a more compact network of HEMA chains, the mobility of the macromolecular chains is reduced, and, at the same time, water affinity is decreased, resulting in a slow diffusion of water molecules within the gel along with a slow relaxation rate of the polymer. Diffusion exponent values lower than the ideal Fickian diffusion (i.e. $n<0.5$) have also been reported for other IPNs.[7,8]

6.3.2. Equilibrium Water Content

The EWC in semi-IPN hydrogels is due to both porosity and hydrophilic character of the final polymer network. The water content of ***H50*** increased from the initial 50wt% to 73wt%, of ***H58*** from 58wt% to 77wt% and of ***H65*** from 65wt% to 87wt%, without any loss of transparency. This is a noteworthy feature considering that there is a water content limit for the reaction mixture: larger amounts of water produce phase separation during polymerization leading to a totally white opaque hydrogelS.[3,9] By adding highly hydrophilic linear PVP into the reaction mixture, it is possible to increase both the water content and the network hydrophilicity with the result of an increase in the final porosity.

In order to evaluate how may these hydrogels be handled and stored from a practical point of view, it was relevant to study differences in swelling capacity after two different processes of dehydration have taken place: conventional non-controlled dehydration, carried out at 40*C for 48h, and dehydration through a freeze-drying process. In the swelling kinetics, it was already demonstrated that the freeze-drying of hydrogels might cause some collapse in the porosity of the system. In order to quantify the effects that these dehydration processes have in SIPN hydrogels, the EWC was calculated from the selected hydrogels, after reaching swelling equilibrium (results are expressed in table 6.6 in comparison with the initial EWC).

Table 6.6. EWC values of the selected hydrogels as obtained after hydration (EWC_{hydr}) and after rehydration (EWC_{rehydr}). The difference between them is expressed by ΔEWC.

Gel	Initial water content (wt%)	EWC_{hydr} (wt%)	EWC^*_{rehydr} (wt%)	EWC^{**}_{rehydr} (wt%)	ΔEWC* (wt%)	ΔEWC** (wt%)
H50	50	73,1	72.1	72.9	1.0	0.2
H58	58	76.6	76.4	76.0	0.2	0.6
H65	65	87.2	80.9	85.0	6.3	2.2

* After conventional dehydration.
** After dehydration through a freeze-drying process.

The results obtained indicate that the dehydration through a non-controlled conventional method, which simulates the gel dehydration occurring in a restorer's laboratory if exposed to air, produces non-controlled modifications of the polymer's EWC, thus affecting the final gel porosity. This is mainly noticed with ***H65*** hydrogel, which shows a loss of 6.3% in EWC. The freeze-drying process

seems to decrease the dehydration damage effect with respect to conventional drying. In this case, from ***H50*** to ***H65*** there is a decrease of the EWC and, while in ***H50*** and ***H58*** this decrease in negligible, in ***H65*** it is considerable (2.2%). For the above reasons and from a practical point of view, it is convenient to use the prepared SIPN hydrogels without letting them passing through a dehydration process. Thus, hydrogels should be stored in containers, immersed in excess amount of deionized water.

6.3.3. Dehydration kinetics

The dehydration kinetics of the hydrogels was evaluated to verify if during the time required for the cleaning process, the amount of water inside hydrogels is enough to perform a cleaning procedure. Dehydration curves of ***H50*** and ***H65*** hydrogel films are presented in figure 6.6. An analogous amount of water was put in a Petri dish inside the dehydration chamber in order to have a comparison with the evaporation kinetics of bulk water.

The dehydration kinetics confirmed that for the first hours the amount of water inside hydrogels is still above 95% of the initial value (see inset of figure 6.6), while the dehydration equilibrium was reached after 6 days. The clear difference between bulk water and hydrogels confirms that not only these systems are able to contain the liquid fraction but also to restrain its evaporation rate.

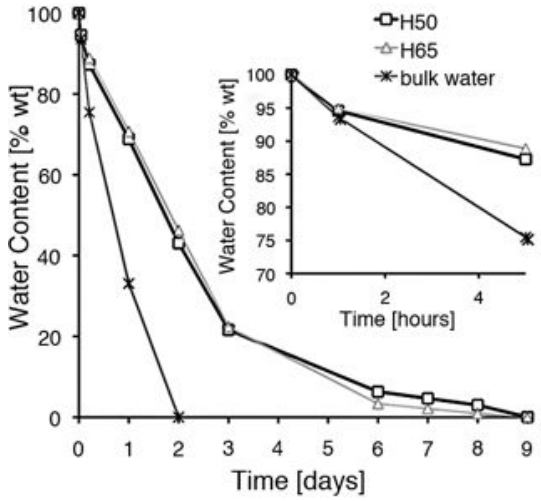

Figure 6.6. Dehydration curves for ***H50*** and ***H65*** SIPN hydrogels and for bulk water. Inset: dehydration curves within the first 5h.

6.3.4. Loading of solvents and nanofluids

Semi-IPN p(HEMA)/PVP hydrogels are capable to load liquid systems other than water, such as organic solvents and oil-in-water nanostructured fluids (nanofluids). In order to evaluate this hydrogels' characteristic, the hydrogels swelling capacity for different liquid systems was investigated on ***H58*** hydrogel, which is the selected gel composition in more close relation to both ***H50*** and ***H65*** physicochemical characteristics. The swelling capacity of ***H58*** hydrogel is represented in table 6.7 by the Equilibrium Solvent Content (ESC). As expected, only the most polar solvents are loaded in the SIPN hydrogel.

Table 6.7. Amount of loaded solvents in hydrogel ***H58*** and loading percentage with respect to the water loaded gel. In bold the water-based systems (nanostructured fluids and surfactants aqueous solutions).

Liquid system	ESC	Loading with respect to water-loaded gel (wt%)
Benzyl alcohol	93.74	22.32
Acetic acid	93.64	22.19
Water/DDAO (1:0.08)	**86.22**	**12.51**
Ethylene glycol	84.64	10.45
Water/SDS (1:0.05)	**83.97**	**9.58**
MEB system	**83.85**	**9.42**
2-Methoxyethanol	82.73	7.96
Ethanolamine	80.72	5.33
EAPC system	**80.22**	**4.69**
Propylene glycol	79.45	3.68
Ethyl alcohol	79.19	3.34
Water	**76.63**	**0**
Methyl alcohol	75.04	-2.09
2-Butanol	68.89	-10.10
Acetone	n.l	n.l
Butyl Acetate	n.l	n.l
Cyclohexane	n.l.	n.l
Ethyl acetate	n.l.	n.l.
Heptane	n.l	n.l
2-Butanone	n.l	n.l
1-Penthanol	n.l.	n.l.
Propylene carbonate	n.l	n.l
Toluene	n.l	n.l
p-Xylene	n.l	n.l

n.l.=not loaded; SDS=sodium dodecyl sulfate; DDAO=*N*,*N*-dimethyldodecan-1-amine oxide.

The study of the swelling behavior of SIPN p(HEMA)/PVP hydrogels loaded with oil-in-water nanofluids is also considered. The selected nanofluid systems are named EAPC and MEB. The EAPC system is a nanostructured fluid, which was previously formulated, and several papers can be found in the literature about its nanostructure and cleaning properties[10–13]. EAPC is a five-component system including water, sodium dodecyl sulfate (SDS), 1-pentanol (PeOH), propylene carbonate (PC) and ethyl acetate (EA). The assessment of this cleaning fluid had mainly dealt with the removal of acrylic, vinyl and silicone coatings from inorganic porous substrates, such as stones or wall paintings. Therefore the evaluation of its effectiveness in the removal of varnishes from canvas, wood or paper is of great interest, in order to expand its applicative range.

On the other hand, MEB system is a new aqueous nanofluid, based on *N,N*-dimethyldodecan-1-amine oxide (DDAO) as the surfactant, and a 1:1:1 mixture of methylethyl ketone (MEK), ethyl acetate and butyl acetate (BAc). DDAO was recently proposed as a promising surfactant for cleaning purposes in conservation of cultural heritage,[14] in view of its properties. Amine oxides are considered as nonionic surfactants, but at low pH they become cationic, due to the protonation of the N-O moiety. In some cases they are also classified as zwitterionic surfactants.[15,16] Moreover, amine oxide surfactants possess a high dispersing power towards several water-insoluble organic substances, and are dermatologically benign.[17] Finally, this class of surfactants is easily biodegraded by aerobic microorganisms in typically less than a week.[17] These features are particularly appreciated because they guarantee low toxicity and eco-compatibility to DDAO-based cleaning system. For what concerns the MEB solvent mixture, on the other side, MEK was chosen according to the good results of recent studies, as was done for ethyl acetate, which is one of the key ingredients that contribute to the effectiveness of the EAPC formulation. Finally, BAc was included in the MEB solvent mixture for two main reasons: 1) its slightly less polar nature with respect to MEK and EA widens the range of materials that can be removed by the cleaning system; 2) due to its quite high vapor pressure, its evaporation is not too quick, so that a restorer has the time to intervene on the treated area to perform a possible subsequent mechanical cleaning action.

Both nanofluids-loaded hydrogels remain transparent which indicates that these nanostructured systems are not considerably disturbed by the presence of the polymer fraction. In fact, if micelle size increased, micelles would be scattered by light which would result in less transparent gels. Moreover, from table 6.7 it is evident that these organic solvents alone cannot be loaded in SIPN hydrogels, due to their low polarity. On the other hand, when combined in the nanofluid

system, it is possible to use both the low polarity of these systems and the control of the cleaning action by confining them into SIPN hydrogels. Both EAPC and MEB systems show major hydrogel swelling with respect to deionized water, which can be associated to a more affinity of the surfactant to the polymeric fraction, as also evidenced by the swelling capacity given with water/SDS and water/DDAO solutions. The efficiency in loading microemulsion systems into a HEMA's polymer network has been already reported.[18]

6.3.5. Quantification of water states

Water inside swollen hydrogels can be classified into three different states: free, bound-freezable, and unfreezable water. This classification takes into account the extent of interactions of water molecules with the polar part of the polymer chains: free water is defined as the water with the same thermodynamic properties of bulk water; freeze-bound water interacts weakly with the polymer chains of the hydrogels so that its freezing point is lower than 0°C; unfreezable water is strongly hydrogen bonded, and no phase transition is observed from –70 to 50°C.[19,20] Because only free water contributes to the cleaning process, the knowledge of the bound-freezable and free water fractions inside hydrogels is important to quantify the hydrogel capability to exchange the solvent at the surface and thus to prevent any excessive wetting. The distribution of "water states" inside hydrogels can be estimated through the calculation of freezable water, from the Free Water Index (FWI) and Freeze-Bound Water Index (FBWI) parameters, both determined via Thermoanalysis. In Differential Scanning Calorimetry (DSC) thermograms, free water shows a freezing point equal to that of bulk water, while the freezing point of bound-freezable water is lower than 0°C, due to the water interactions with polymer chains or to its confinement in the gel porosity.[20]

The DSC thermograms, obtained from the water-swollen ***H50*** and ***H65*** hydrogels, are shown in figure 6.7. Two distinct sample preparation protocols were used to determine both FWI and FBWI parameters as described in materials and methods. The DSC thermograms in figure 6.7 (left panel) show a shoulder below 0°C, which is associated with a minor fraction of free water that has indirect interactions with the polymer network and, therefore, has a behavior close to freeze-bound water.

The FWI results are reported in table 6.8. The FWI values obtained highlight that free water inside swollen hydrogels is to a large extent higher than bound water. Therefore, aqueous systems inside hydrogels behave mostly as free water. In fact, the free water content is around 73% in ***H50*** and 77% in ***H65*** with respect to the total water inside the swollen hydrogels.

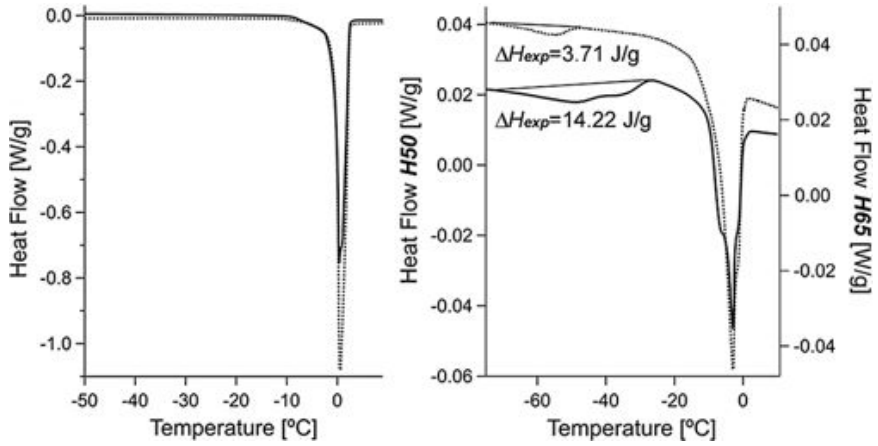

Figure 6.7. DSC thermograms for the fully swollen hydrogels (left) and partially rehydrated hydrogels (right) for ***H50*** (solid line) and ***H65*** (dotted line). Both thermograms were normalized to sample weight.

On the other hand, to better understand the freeze-bound water behavior in hydrogels, FBWI was calculated from the freeze-bound water fusion peak presented in figure 6.7 (right panel). Freeze-bound water is evidenced by the broad freezing peak visible between –70 and –20°C, in addition to the more intense freezing peak for free water. It is evident that the area associated with the freeze-bound water peak is larger for ***H50*** hydrogel. The results are listed in table 6.8. ***H50*** hydrogel has a higher FBWI than ***H65*** as a consequence of a greater number of water molecules in contact with pore walls due to smaller pore dimensions and to the higher surface to volume ratio.

Table 6.8. Free Water Index (FWI), Freeze-Bound Water Index (FBWI) and correlated parameters for fully swollen (Hxx) and partially rehydrated hydrogels (Hxx*). A is the weight fraction of water. FBWI was calculated using the partially rehydrated hydrogels.

	FWI			FBWI	
Gel	***A***	ΔH_{exp} **(J/g)**	**FWI**	ΔH_{exp} **(J/g)**	**FBWI**
H50	$0.758 \pm 20 \times 10^{-3}$	184.7 ± 5.9	$0.730 \pm 4 \times 10^{-3}$	-	-
H65	$0.859 \pm 13 \times 10^{-3}$	220.8 ± 0.6	$0.770 \pm 9 \times 10^{-3}$	-	-
H50*	$0.396 \pm 22 \times 10^{-3}$	40.7 ± 5.8	$0.309 \pm 63 \times 10^{-3}$	13.7 ± 1.7	$0.161 \pm 18 \times 10^{-3}$
H65*	$0.475 \pm 33 \times 10^{-3}$	47.1 ± 2.6	$0.304 \pm 6 \times 10^{-3}$	4.1 ± 0.6	$0.045 \pm 4 \times 10^{-3}$

6.4. Mechanical analysis

In order to investigate the dynamic mechanical properties of the selected formulations of SIPN p(HEMA)/PVP hydrogels (***H50***, ***H58*** and ***H65***), oscillatory frequency sweep tests were carried out in the linear viscoelastic regime (see materials and methods) and the dependence of the complex moduli G' (storage modulus) and G'' (loss modulus) on the frequency of the applied shear perturbation was investigated.

It is evidenced in figure 6.8 that all the investigated systems have a similar mechanical behavior: G' is always higher than the G'' and both moduli are relatively independent from the angular frequency of the applied shear stress. For viscoelastic fluids a characteristic frequency dependence of the elastic and loss modulus that is $G' \propto \omega^1$ and $G'' \propto \omega^2$, is observed at low frequencies,[21] while in this case the rheological behavior of the systems is characterized by an invariance of the G' modulus from the frequency ($G' \propto \omega^0$) and $G' >> G''$ over the explored frequency range, i.e. deformation in the linear viscoelastic range will be essentially elastic or recoverable. Thus, all the investigated SIPN p(HEMA)/PVP systems, show a gel-like behavior.[22] This means that they hold their shape, likewise to a solid, which is related to the fact that the stress relaxation time tends towards infinity. The stress relaxation time, τ, is the time required for viscous flow to occur, when the material is subject to strain, which is expressed by the Deborah number (D_e):[21]

$$D_e = \frac{\tau}{t} \tag{6.1}$$

where t is the time of the applied strain, also called observation time. Therefore, when $D_e \rightarrow 0$ the material behaves as a Newtonian fluid, while when $D_e \rightarrow \infty$, as a Hookean solid. The strain can be caused by the gravity's force of the material's own weight, so the time of the strain is infinite. Thus, after a certain time, even the more solid-like material will deform permanently, already mentioned in the song by prophetess Deborah, from whom the name derived:

"The mountains flowed down at the presence of the Lord, even yon Sinai at the presence of the Lord, the God of Israel." (Judges 5.5)

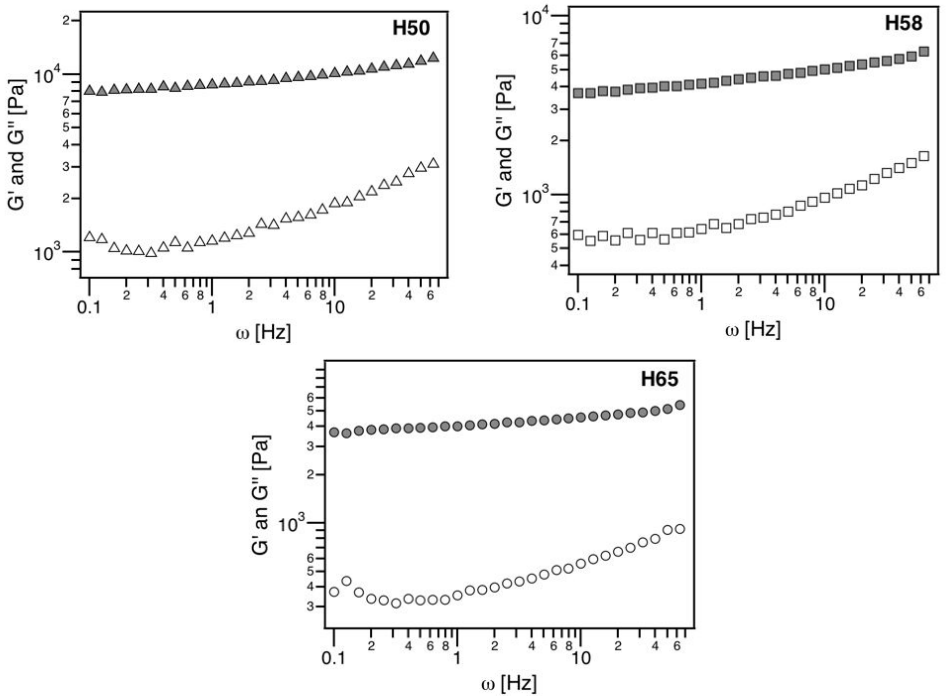

Figure 6.8. Log-log plot of storage *G′* (filled marks) and loss *G′′* (empty marks) moduli of the selected hydrogel formulations.

Accordingly, from a practical point of view, when a SIPN hydrogel is applied in vertical position, it will not deform for considerably long times, so the contact area remains constant during the cleaning application time.

In order to understand the effect of the hydrogel's chemical network on the mechanical behavior of these systems, their viscoelastic properties were investigated both as a function of the cross-linker MBAm (HEMA and PVP content is constant, see compositions in table 6.9), and of the monomer HEMA, an hydrogel series already presented before (HEMA/MBAm ratio and PVP content are constant, see compositions in table 6.4. Gel formulations ***CL2*** and ***HM10.5***, which are not expressed in the tables, yet are showed in the graphs (figure 6.9), are equivalent to ***H65*** hydrogel.

The oscillatory frequency-sweep measurements for both hydrogel series (***CL*** and ***HM***) are presented in figure 6.9, where is possible to notice that all formulations produced gel-like systems. Figure 6.10 shows the trend of the intrinsic elastic modulus, G_0, which is calculated from the five points average of *G′* obtained at the high frequency regime, as a function of the MBAm concentration, whereas the amount of HEMA is constant at 10.5wt% (***CL*** series). The G_0 values indicate that over the explored composition range, the system is sufficiently elastic

to be handled without being damage, which is particularly important during applications in restoration field. In fact, a gel when subject to strain by handling should have enough elasticity, in order to be placed and peeled off from a painted surface without being disrupted. For MBAm concentrations above what appears to be a critical cross-linker concentration at ≈0.1wt%, the slope of the curve increases dramatically with increasing MBAm content. This behavior can be attributed to the progressive formation of an infinite 3D polymer network induced by the chemical connection of the previously formed HEMA oligomeric clusters.

Table 6.9. Composition (wt%) of SIPN hydrogels for the series "cross-linker" (***CL***) used for the mechanical analysis.

	PVP (wt%)	HEMA (wt%)	H_2O (wt%)	MBAm (wt%)	AIBN (wt%)	HEMA/MBAm ratio
CL0	24.42	10.46	64.99	0	0.13	-
CL0.01	24.42	10.46	64.98	0.01	0.13	$1:1x10^{-3}$
CL0.05	24.42	10.46	64.94	0.05	0.13	$1:5x10^{-3}$
CL0.1	24.42	10.46	64.89	0.10	0.13	$1:1x10^{-2}$
CL0.15	24.42	10.46	64.84	0.15	0.13	$1:1.5x10^{-2}$

A remark should be made to hydrogel ***CL0***, which is a physical gel, since no permanent crosslinks exists between HEMA chains, due to the absence of the crosslinking agent. Nonetheless, it presents a solid-like behavior. In order to investigate if this effect is influenced by the incorporation of PVP in the formulation, an analogous gel was prepared, without PVP in the composition. The obtained frequency sweep is showed in figure 6.11, where it is possible to notice a solid-like behavior, as well. The obtained gel is, in fact, characterized by an high mechanical strength. The formation of a solid-like gel, which is more characteristic of chemical gels, may be explained by the fact that long HEMA chains are formed and inter-entangled to some extent, producing a more elastic than viscous structure.

A difference of the dynamic moduli of ***CL0*** and ***CL0**** (without PVP) is observed. ***CL0**** shows higher values for both G' (in the order of 10^4) and G'', which means that is more elastic than the analogous gel with PVP. This result provides enlightenment on the effect that the addition of PVP has on the mechanical properties of the SIPN hydrogels. Since an higher complex modulus is proportional with an higher entanglement density of the polymer gel,[23] the

presence of PVP during the formation of the polymer network appears to be an obstacle that forces the distance between its topological points, resulting in a more flexible gel.

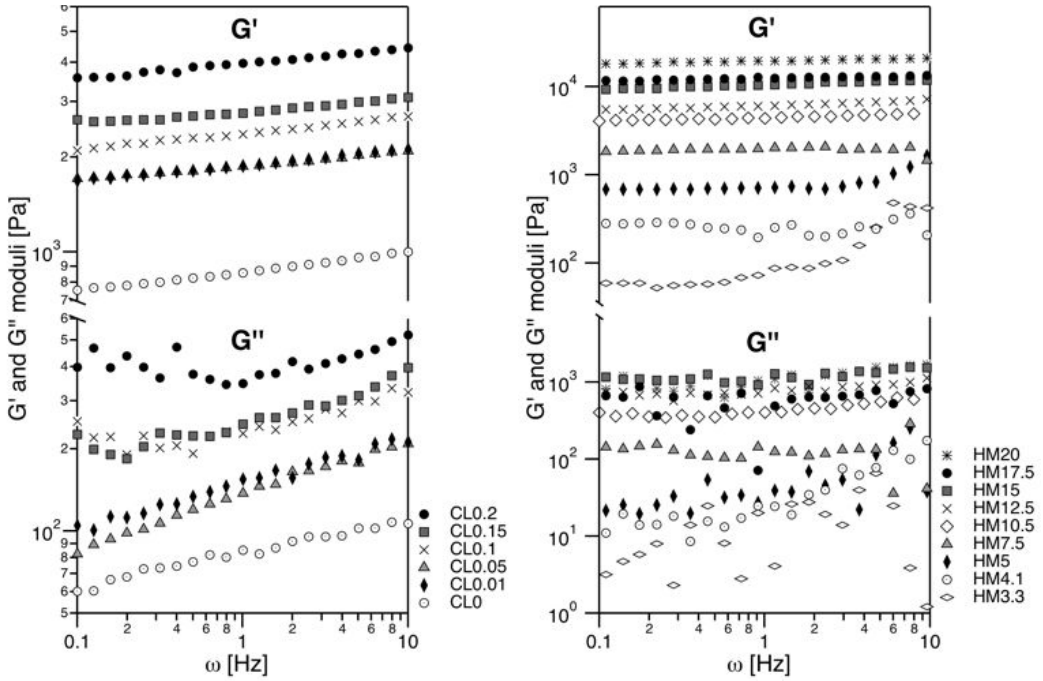

Figure 6.9. Log-log plot of storage *G′* and loss *G″* moduli of the MBAm (left) and HEMA (right) series (for hydrogels' composition see tables 6.9 and 6.4).

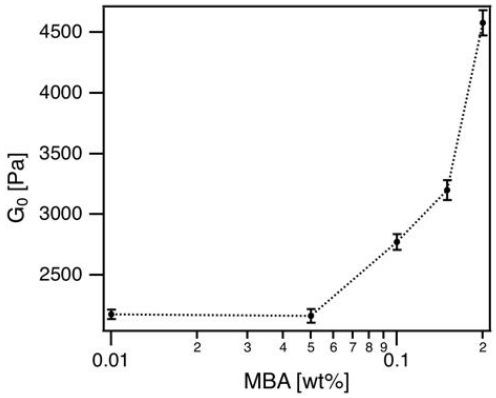

Figure 6.10. The intrinsic elastic modulus, G_0, on the dependency of cross-linker MBAm concentration.

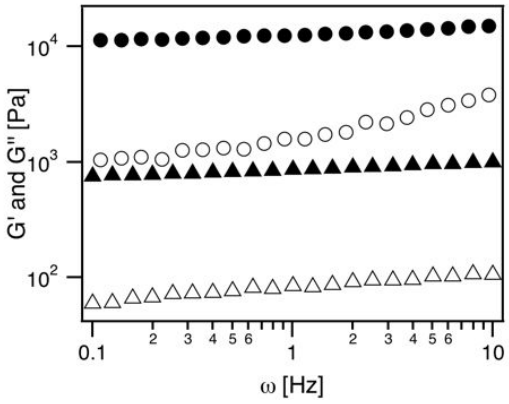

Figure 6.11. Log-log plot of the dynamic moduli of ***CL0**** (without PVP) (●) and of CL (with PVP) (▲) gel formulations.

As for the HEMA series, even small amounts of HEMA (from 3.1wt%) are enough to build a cross-linked polymer network and form a solid-like hydrogel. This behavior is probably due to the ability of PVP, as interpenetrating polymer, to improve the mechanical properties of polymer networks due to the formation of hydrogen bonds, as additional physical crosslinks.[24]

The elastic modulus *G′* shows a strong dependence on HEMA concentration as well (figure 6.9, right panel): as the monomer concentration increases (the molar ratio HEMA/MBAm was always equal to 1:1.7x10^{-2}), the increase of *G′* (from 55 to 19500 Pa upon increasing the monomer concentration from 3.1wt% to 20wt%) may indicate an enhanced elasticity of the system due to the increased density of the chemical entanglements in the network.[23,25]

There exists considerable literature on the dependence of the *G′* modulus on the polymer concentration for various polymers and solvents.[26] In most cases, a power law describes the dependence of *G′* from the polymer concentration (ϕ): $G' \propto \phi^n$, where *n* varies from 1.8-2.0.[27] In figure 6.12 *G′* is shown as a function of the polymer concentration, ϕ (the estimated total HEMA plus PVP in gel's formulation, see subchapter 6.2.2). Figure 6.12 shows two polymer composition regimes, in which the increasing of ϕ in the composition is described by a power law. The power law indicated by the blue line in the graphic of figure 6.12 accounts for gel formulations above a critical polymer concentration of ≈7wt% (in which, ≈2wt% are PVP) and is characteristic of the selected SIPN hydrogels since the amount of polymer fraction is at least as twice as that critical value. In this case, the data are well fitted by a curve with *n*=2.54±0.08. This value suggests that the expansion of

the of the SIPN p(HEMA)/PVP's network, occurs through a percolation mechanism.[28] This model, which relies upon a critical phenomenon of connectivity, has been applied to account for the formation of chemically cross-linked networks, which compositions are exactly known.[27] Therefore, due to the complexity of the selected systems, it must be emphasized that this consideration remains preliminary.

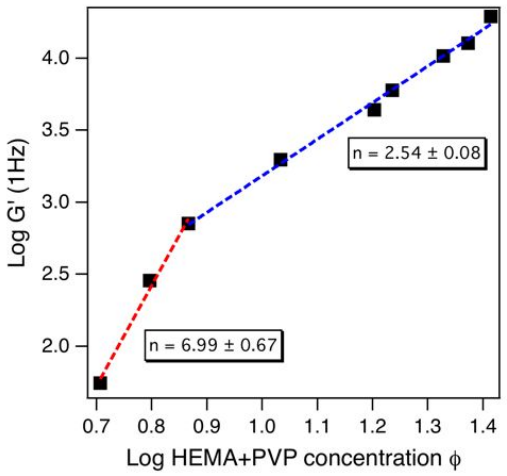

Figure 6.12. Log-log plot of the *G′* (obtained at 1Hz) dependence on polymer concentration (HEMA and PVP) ϕ. The double-logarithmic scale highlights two power law regimes.

6.4.1. Effects on loading nanofluids

The above mentioned swelling tests (see under sub-chapter 6.3.4) have showed that these hydrogels are capable of loading different cleaning systems, other than water, which allows a broad range of application possibilities.[29] Therefore, it is important to evaluate the effects that this combined system, that is, nanofluid-loaded SIPN hydrogel, has on the mechanical features of the gel. Thus, oscillatory measurements were carried out, within the viscoelastic region, to study the properties of the combined systems ***H58*** and ***H65*** hydrogels loaded with two different nanofluids (EAPC and MEB systems), and are presented in figure 6.13.

The storage moduli of water-loaded hydrogels and of nanofluid-loaded hydrogels are very similar, while *G″* is slightly different for the nanofluid-loaded hydrogels, as highlighted by the tanδ shown in the below graphics of figure 6.13. Since tanδ accounts for the gel character, it appears that in the case of ***H65*** both

microemulsions act like a structuring agent, increasing the gel character, while in ***H58*** the reverse occurs.

The similarity of *G′* between gels and nanofluid-loaded gels confirms that viscoelastic features of the hydrogels do not change considerably when loaded with the nanofluids and that no substantial difference exists between two different SIPN hydrogels. The invariance of the elasticity of the SIPN hydrogels indicates that these systems behave like real containers capable of absorbing different cleaning systems without undergoing any macroscopically meaningful mechanical alteration.

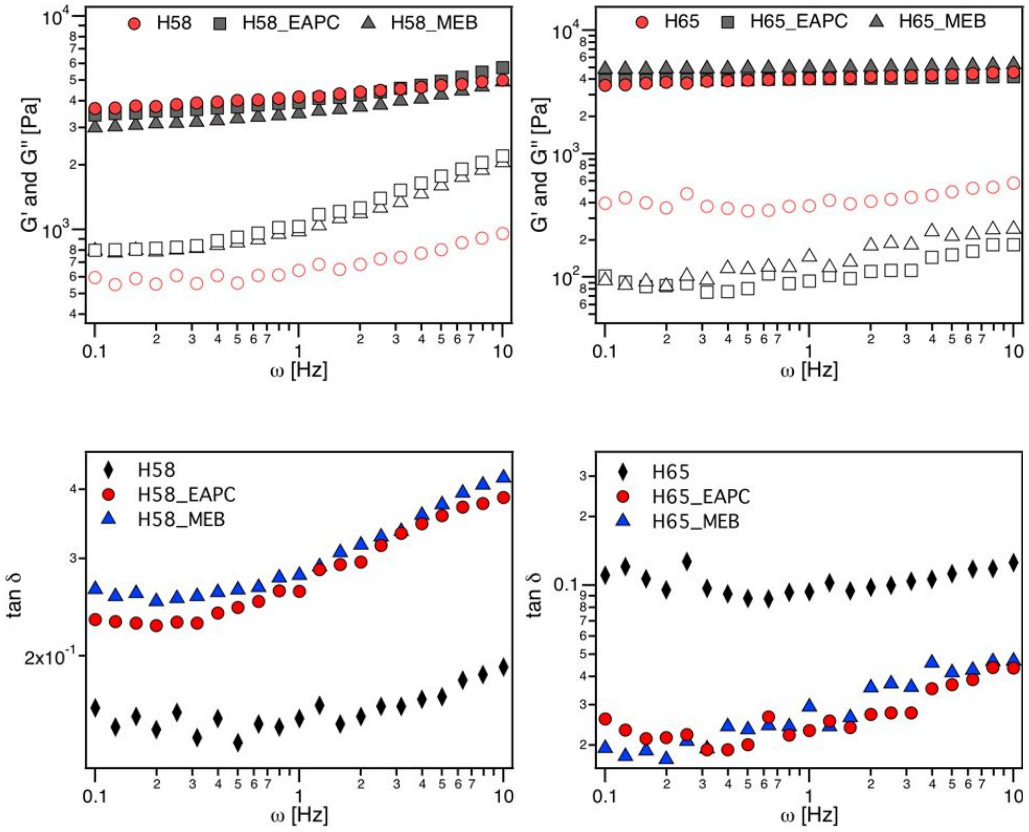

Figure 6.13. Storage *G′* (filled marks) and loss *G″* (empty marks) moduli of the ***H58*** and ***H65*** hydrogels loaded with different liquid systems: water (red marks); EAPC; MEB (top graphics). Tanδ for the same systems (below graphics).

6.5. SIPN microporosity

FEG-SEM images were acquired for the hydrogels with more and less EWC (***H65*** and ***H50***, respectively) to detail the structure and porosity of the lyophilized hydrogels (xerogels). Since xerogel state is required for FEG-SEM image acquisition, EWC_{rehydr} was considered, to evaluate if the freeze-drying process compromises the microstructure of the hydrogel. A decrease of the EWC was observed in both cases: 0.2% and 2.2% for ***H50*** and ***H65***, respectively. In the case of ***H50*** the variation is negligible, while for ***H65*** the difference of EWC is considerable, which means that ca. 2% of microporosity is collapsed during freeze-drying as a consequence of the water to ice expansion associated with the freezing step necessary for the freeze-drying. This difference is, thus, relevant to be considered when dealing with FEG-SEM results.

FEG-SEM images are shown in figure 6.14 for ***H50*** and ***H65*** xerogels. A sponge-like structure is observed for both samples, and pore dimensions are approximately comprised in the range 5-40μm. A more inhomogeneous structure is clearly noted for ***H65*** with respect to ***H50*** xerogel. Pore wall thickness in ***H50*** xerogel presents an average value of ≈2.4±1.3μm. In accordance with the inhomogeneity of the ***H65*** structure, there is a broader distribution of pore wall thickness. In ordinary cross-linked chemical hydrogels, the amount of water in the reaction mixture is the major contributor to final porosity. FEG-SEM images clearly show smaller pores for ***H50*** formulation compared with ***H65***.

To further quantify this aspect, a pore size distribution was extracted from several FEG-SEM images using ImageJ analysis software. The obtained histogram is presented in figure 6.15. ***H65*** hydrogel displays a broader distribution with pore diameters going from 5 to 39μm. As for ***H50***, a more narrow distribution is noted with the main pore diameters comprised between 6 and 11μm. Furthermore, the porosity was estimated to be approximately 10400 pores/mm^2 for ***H50*** and 2600 pores/mm^2 for ***H65*** xerogel. The difference of porosities between the two hydrogels is due to three main factors: the water content in the initial polymerization mixture, which is the main factor responsible for final gel porosity and dimension of pores; the PVP release after polymerization; and the cross-linker content, which contributes, for the same PVP/HEMA/H_2O ratios, to more compact network structures.

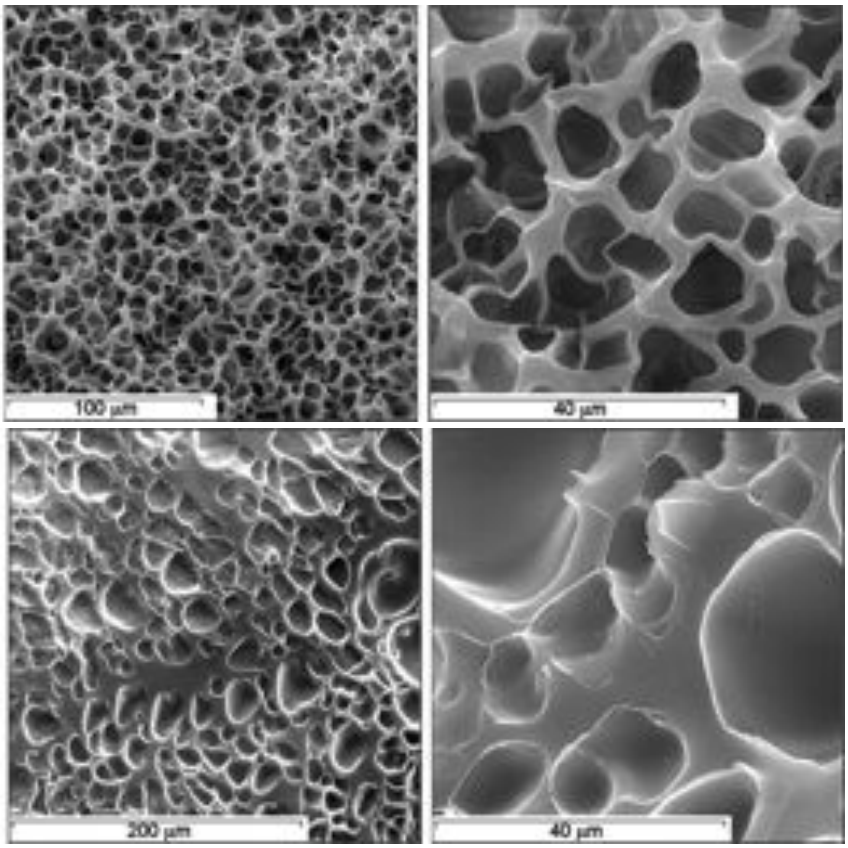

Figure 6.14. FEG-SEM images of ***H50*** (above) and ***H65*** (below) xerogels obtained at two different magnifications.

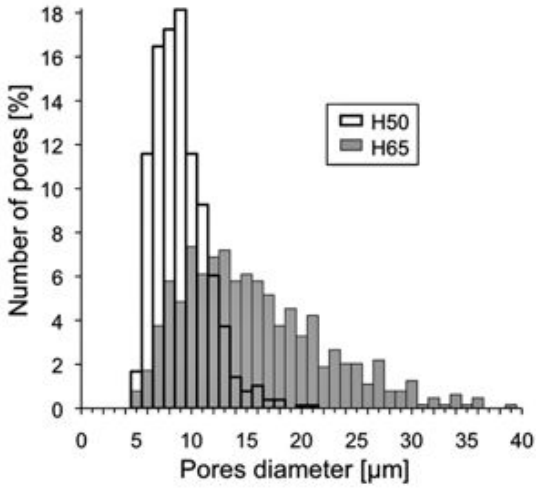

Figure 6.15. Pore size distributions for ***H50*** and ***H65*** SIPN xerogels.

6.6. Network characterization

SAXS investigations were carried out to detail the structural changes imposed at the nanoscale by the PVP addition at the nanoscale. The investigated hydrogel formulations were compared to a cross-linked pHEMA hydrogel as a reference. pHEMA hydrogel is prepared analogously to ***H50*** except for the addition of PVP. Thus, the cross-linked pHEMA network percentage in pHEMA hydrogel is higher than in SIPN formulations (50wt% in the composition of pHEMA compared with a maximum of 25wt% in SIPN compositions), and the water-phase was maintained at 50wt% of the total. This excess of water leads to phase separation during polymerization of pHEMA hydrogel, as demonstrated before. SAXS curves, as shown in figure 6.16, were modeled using the Debye-Bueche approach (see materials and methods). Best fitting curves are reported as solid lines in figure 6.16, while the extracted parameters are listed in table 6.10.

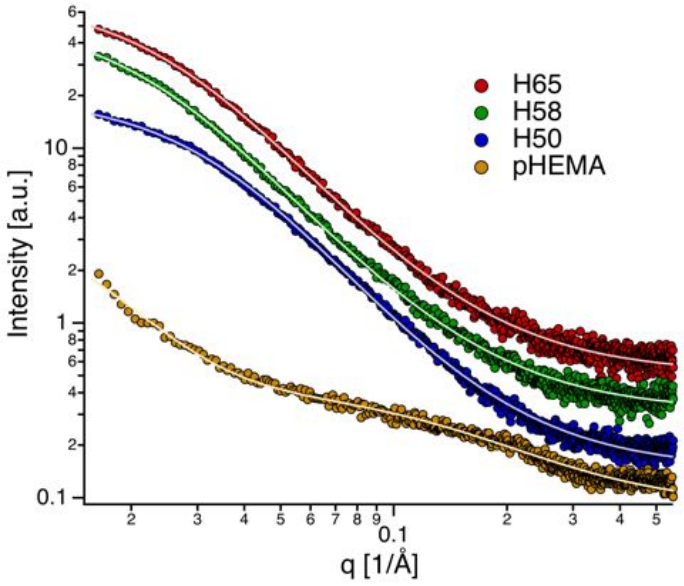

Figure 6.16. SAXS intensity distribution in a log–log scale for all SIPN hydrogels investigated. A cross-linked pHEMA hydrogel is reported as reference. The solid lines are the fits with the Debye-Bueche approach. The curves are shifted upward by an arbitrary factor to avoid overlap.

Table 6.10. Parameters obtained from the SAXS curves of the investigated hydrogels.

Gel	$I_{Lorentz}(0)$	ζ (nm)	$I_{excess}(0)$	Ξ (nm)	bkg	$I_{excess}(0)/I_{Lorentz}(0)$
H50	12.1	2.5	40.2	2.5	0.39	3.3
H58	8.2	2.8	45.3	3.6	0.30	5.5
H65	7.8	3.1	25.1	3.3	0.23	3.2
pHEMA	1.7	0.7	27.4	6.0	0.50	16.1

The SAXS profiles in figure 6.16 show a neat difference between pHEMA and SIPN hydrogels. According to the literature,[30] mesh dimension depends mainly on the equilibrium water content, which in the present case is proportional to the HEMA/PVP ratio in the reaction mixture. ***H50*** SIPN hydrogel has a mesh size of 2.5nm while ***H58*** of 2.8nm and ***H65*** of 3.1nm. In fact, mesh size increase for each SIPN formulation is accompanied by a comparable increase of EWC. Namely, the mesh volume increase over ***H50*** is 41% and 91% in ***H58*** and ***H65***, respectively, which is in agreement to the EWC increase of 11% and of 21% in the same formulations. The increase of average mesh size is also related to the decrease in cross-linker concentration, as reported in the literature.[31] Despite cross-linker content decreases, ***H50*** shows a smaller mesh than ***H65***. This is due to the decreasing percentage of PVP from ***H65*** to ***H50***, which leads to a less swollen network.

As reported in the literature[32–34] less homogeneous structures are likely to form when the syntheses are conducted at higher polymer volume fractions (water-poor systems) and/or higher cross-linker concentration. The variation on inhomogeneity dimension, Ξ, is not clear for the three SIPN formulations since the more water-poor system (***H50***) has the lower number of cross-links, while the formulation with higher EWC (***H65***) is characterized by a higher cross-linker content. So the effect of these two components is disguised. As a matter of fact, ***H50*** has the smallest Ξ dimension in the series, thus resulting in the most homogeneous, both in the nanometer-scale length and in the micrometer-scale length, as already shown by the porosity distribution extracted from the SEM images. The increase of inhomogeneities dimension is clearly noticed in the water-poor pHEMA system.

The $I_{excess}(0) / I_{Lorentz}(0)$ ratio is proportional to inhomogeneity/mesh volume fractions. In this regard, the collected SAXS data agree with the increase of inhomogeneity abundance related to the higher polymer volume fraction. In fact, there is an increase of inhomogeneities of a factor 4 for pHEMA hydrogel with respect to SIPN formulations.

6.6.1. Effects on loading nanofluids

From the rheological investigation emerges that nanofluid-loaded hydrogels do not significantly change the elasticity in comparison to water-loaded hydrogels. Since the mechanical behavior of hydrogels is in direct relationship with hydrogel's structure, it was relevant to investigate the interaction between hydrogels and nanofluids from a structural point of view, using an *in situ* analysis method. SAXS measurements were performed in order to observe whether the structure of either the hydrogel and/or the nanofluid was altered due to interaction phenomena. The following results must be reserved with the consideration that these are based on combined complex systems, in which both hydrogel network and nanofluid structure scatter at small-angles. SAXS profiles were collected on nanofluid systems, nanofluid-loaded SIPN hydrogels and on water-loaded SIPN hydrogels. The nanofluid systems studied are EAPC and MEB systems (introduced in sub-chapter 6.3.4). Figures 6.17 (for the EAPC system) and 6.18 (for the MEB system) show the comparison between scattering curves of the nanofluid, the gel and the nanofluid-loaded gel. Interestingly, for both systems, the contribution coming from the nanofluid is clearly visible in the scattering profile of the nanofluid-loaded gel, indicating that the micellar nature of the liquid phase is preserved.

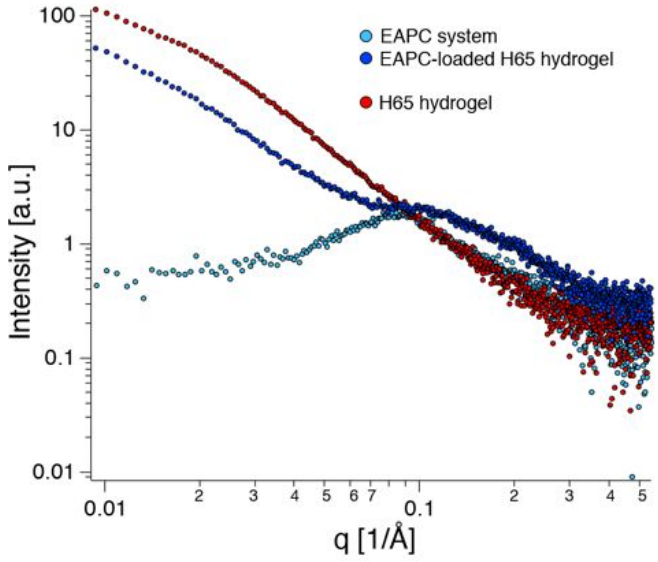

Figure 6.17. Log-log representation of SAXS intensity distribution for water-loaded and EAPC-loaded ***H65*** hydrogel.

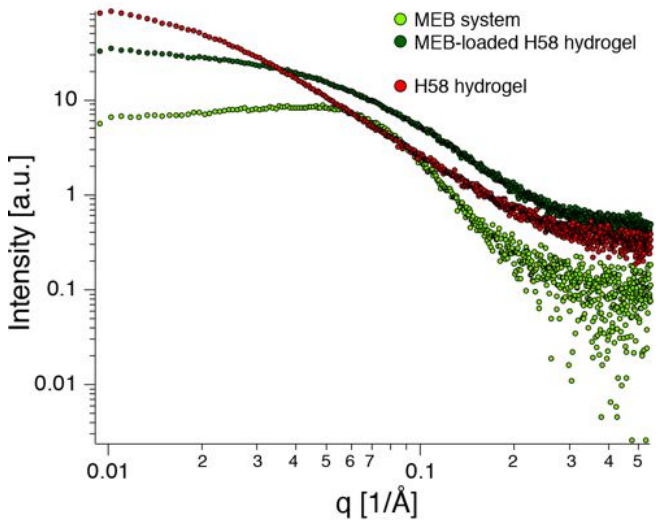

Figure 6.18. Log-log representation of SAXS intensity distribution for water-loaded and MEB-loaded ***H58*** hydrogel.

In order to fit the experimental data, the scattering signals coming respectively from the gel network and from the micelles were considered as purely additive, meaning that the analysis of the loaded gel scattering profile could be performed by combining two fitting models, one for the gel network and one for the micellar phase. Since, according to rheological investigations, the loading of the nanofluid did not alter the gel's elastic behavior, it was hypothesized that also its structure was mostly unaltered. For this reason, the scattering profile of the sole gel (conveniently scaled by a multiplicative factor) was subtracted from the nanofluid-loaded gel scattering curve. The resulting "simulated" curve is an approximation of the scattering profile of the nanofluid when loaded into the gel.

In figure 6.19 the simulated curves of EAPC (obtained from ***H58*** and ***H65*** hydrogels) are compared with the SAXS curve of the extracted EAPC from inside gels (see materials and methods for the extraction procedure). Apart from a slight deviation at low-*q*, the mathematically obtained curves almost perfectly superimpose to the scattering profile of the extracted EAPC. This evidence is a confirmation of the reliability of the hypothesis that the signals coming from the gel network and the micelles are purely additive. Furthermore, the superposition of the simulated curves from ***H58*** and ***H65*** is almost perfect (figure 6.19), which indicates that among different formulations of SIPN hydrogels there is no significant modifications to nanofluids' structure. This could be expected since the chemical moieties involved in the hydrogel architecture do not change along the

Hxx series. The confirmation of the additive character of the obtained SAXS curves gives the possibility to fit the simulated nanofluid systems and compare fitting parameters with the ones obtained from an experimental nanofluid SAXS curve. In figures 6.20 and 6.21 the simulated curves were therefore compared to the respective reference nanofluids, for the EAPC and MEB systems, respectively.

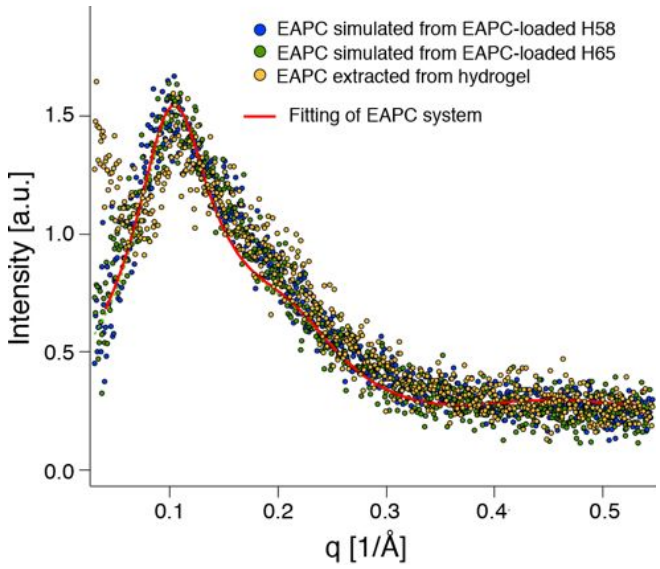

Figure 6.19. SAXS intensity distribution of the extracted nanofluid from the gel (see materials and methods) in comparison with the two simulated SAXS curves obtained from the subtraction of the water-loaded gel from the EAPC-loaded gels for both ***H58*** and ***H65*** hydrogels. The fitting model for the simulated EAPC curves is presented as solid line.

In the loaded-EAPC simulated curves the correlation peak is shifted towards higher *q* values, and also the shape appears to be slightly different with respect to the reference EAPC scattering profile (see figure 6.20). SANS and SAXS fitting of the EAPC system has already been reported.[35,36] However, the fitting of the nanofluid was performed again to account for small possible changes due to composition and measurement variability. Micelles were modeled as monodisperse core/shell charged prolate ellipsoids interacting through a screened Coulomb potential, as reported in previous works. The same model was used to fit the EAPC simulated curve. Fitting parameters of the EAPC and the simulated EAPC systems are reported in table 6.11. The output parameters for the EAPC reference system are in agreement with previously reported data.

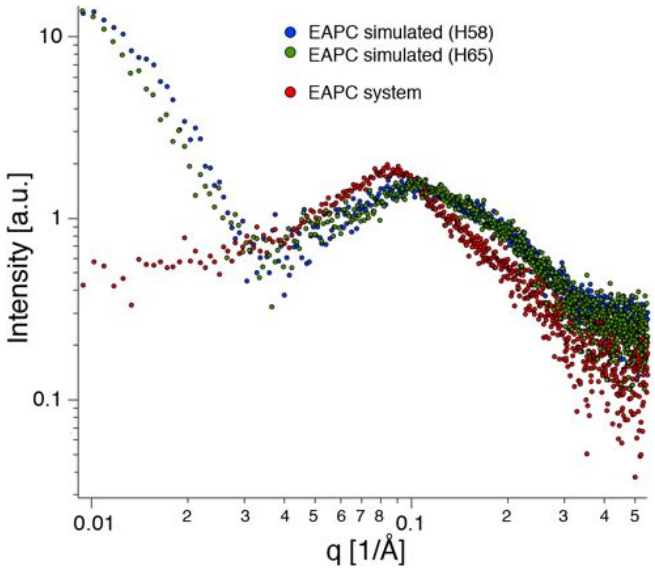

Figure 6.20. Log-log representation of SAXS intensity distribution of the EAPC system and two simulated SAXS curves, obtained from the SAXS curves subtractions of the water-loaded from the EAPC-loaded gels.

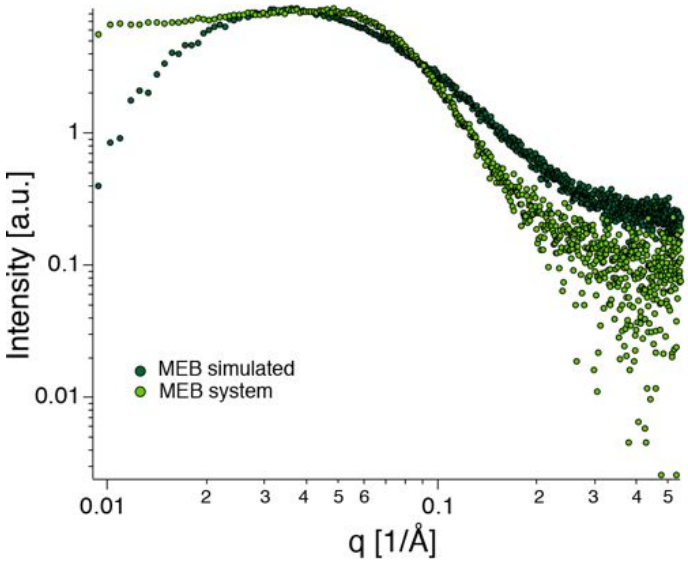

Figure 6.21. Log-log representation of SAXS intensity distribution of the MEB system and the simulated SAXS curves of the MEB system inside the gel, obtained from the SAXS curves subtraction of the water-loaded gel from the MEB-loaded ***H58*** gel.

Table 6.11. Parameters obtained from the fitting equation for the SAXS curve of EAPC systems.

Fitting parameters	EAPC	Simulated EAPC
Φ	0.19	0.18
a (Å)	61.5	41.1
b (Å)	12.7	12.1
t (Å)	2.5	5.5
ρ_{core} (Å^{-2})	7.95 x 10^{-6}	7.96 x 10^{-6}
ρ_{shell} (Å^{-2})	1.07 x 10^{-5}	1.0 x 10^{-5}
ρ_{bulk} (Å^{-2})	9.4 x 10^{-6}	9.4 x 10^{-6}
Z (e^-)	8.0	7.6

The fitting parameters of the simulated nanofluid, on the other hand, show a decrease of micelles size, expressed mostly by the decrease in the core major semi-axis, *a*. This may indicate that, upon loading of the nanofluid into the gel, a certain amount of solvents that were included in the micelles (and possibly some surfactant molecules) leaves the aggregates to interact with the pHEMA/PVP polymeric network. Conversely, the shell thickness, *t*, slightly increases when EAPC is loaded into the hydrogel. This could be due to the insertion of pHEMA moieties or PVP portions between the polar heads of the surfactant. The subsequent reorganization of the polar interface of the micelles would most likely lead to the inclusion of more water molecules into the shell. A similar behavior has already been reported[37–39] In particular, the interaction between SDS and PVP has been extensively studied and their ability to form "pearl necklace"-like structures is known, that is, micelle clusters are found along the polymer chain.[38] In the present case the interaction seems to be less important since the HEMA and PVP are already in intermolecular hydrogen bonding.

However, the presence of PVP/micelles "pearl-necklace" structures seems to be excluded by the result of the following experiment. SAXS profiles of a 20% (w/w) solution of PVP in the EAPC system and of a 20% (w/w) aqueous solution of PVP were collected. Then, the signal of the aqueous solution of PVP was subtracted from the PVP/EAPC mixture signal (in the same way described above) and the resulting simulated curve was compared to the sole EAPC scattering profile. The result is presented in figure 6.22. The superposition of the two SAXS curves is almost perfect, suggesting that no interaction between EAPC and PVP is observable in the measured *q*-range. This suggests that the interaction between micelles and the polymeric network inside the gel could be mainly due to the pHEMA.

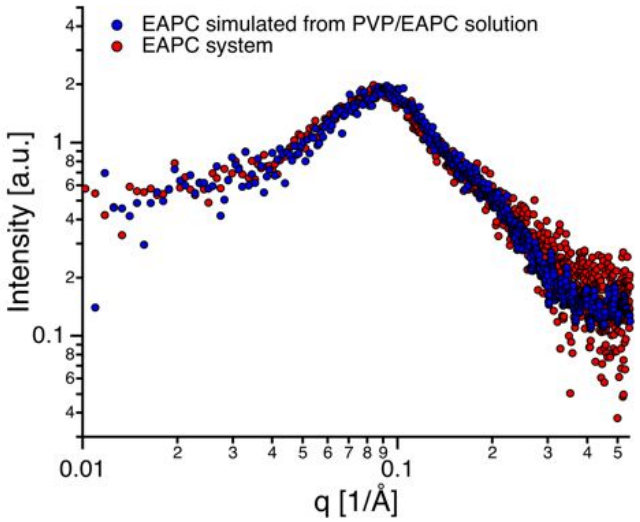

Figure 6.22. SAXS intensity distribution of the EAPC system and a simulated EAPC, obtained by the subtraction of the aqueous solution of PVP (20wt%) with the solution EAPC and PVP (20wt%) SAXS curves.

Table 6.12. Parameters obtained from the fitting equation for the SAXS curve of MEB systems.

Fitting parameters	MEB	Simulated MEB
Φ	0.15	0.13
r (Å)	24.5	11.5
t (Å)	1.5	1.6
Poly	0.39	0.78
ρ_{core} (Å^{-2})	8.0 x 10^{-6}	8.0 x 10^{-6}
ρ_{shell} (Å^{-2})	1.18 x 10^{-5}	1.30 x 10^{-5}
ρ_{bulk} (Å^{-2})	9.32 x 10^{-6}	9.4 x 10^{-6}
Z (e^-)	3.9	2.6

The fitting parameters obtained by the analysis of the simulated MEB curve are shown in table 6.12 and compared to the fitting results for the reference MEB system. Also in this case, a decrease in the size of the aggregates is observed, with the core radius, *r*, which is reduced to almost the half of its starting value (while the shell thickness remains unchanged). The same considerations about solvents' partitioning between micellar and bulk phases made in the case of the EAPC system, apply in this case. On the other hand, the polydispersity of the system significantly increases from 0.39 to 0.78. A higher polydispersity of the

system generally means that smaller and larger micelles coexist. In this case the increase is indeed very high and some concerns about the fitting output were raised. Nevertheless, no better fitting curves could be obtained for this system, thus this value was kept with some regards. It is, however, valid to qualitatively consider an increased polydispersity of micelles' core.

As observed in figures 6.20 and 6.21, the main deviation of the simulated loaded-nanofluids scattering profiles with respect to their reference systems curves, lies in the low-q region. Interestingly, while for the simulated EAPC curve there is a steep raise of the scattering intensity, for the simulated MEB curve the situation is reversed, and a marked decrease in the scattering intensity is observed when compared to the reference system. Since it has been observed that this region does not influence the nanofluid's fitting parameters, it most probably concerns the differences in the hydrogels structure. Low-q region accounts for the hydrogels inhomogeneity domains, Ξ. To confirm this hypothesis, an additional term was added to the nanofluid fitting models, regarding the $I_{excess}(q)$, and the resulted fitting is presented in figure 6.23. In both cases the fitting was accurate and appears to be able to describe the experimental data.

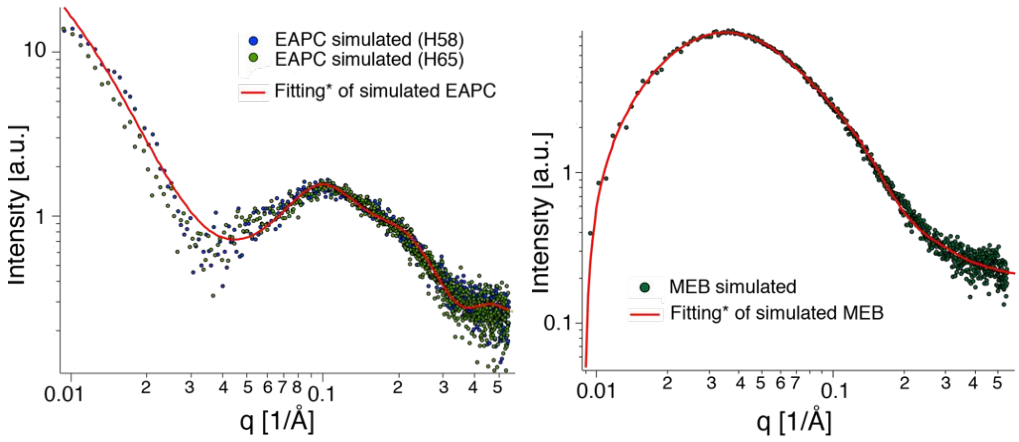

Figure 6.23. Fitting models for the simulated nanofluid systems. The asterisk is for the addition of an extra term accounting for the data points at low-q, related to differences in hydrogel inhomogeneities.

In the case of the EAPC system it results in an increase of the Ξ dimension, which may ulterior confirm the fact that micelles interact with branched sites of the polymer network, which are mostly created in zones of high polymer volume

fraction, leading to the increase of these inhomogeneity regimes. On the other hand, in the MEB system, there is a decrease in the inhomogeneity domains. This may be explained by the obtained values of Equilibrium Solvent Content, which are substantially high for the MEB and water/DDAO systems. The high swelling degree of MEB-loaded hydrogels leads to the expansion of high polymer volume regions and therefore to the decrease of the Ξ value.

6.7. Materials and methods

6.7.1. Gravimetric measurements

Each of the following parameters was calculated from at least three different measurements.

6.7.1.1. Gel content

The gel content (*G*) gives the ratio between the mass of the final SIPN p(HEMA)/PVP hydrogel and the mass of the two components in the initial mixture, which can be calculated as follows:[40]

$$G = \frac{W_d}{W_0} \times 100 \tag{6.2}$$

where W_d is the dry weight of the hydrogel and W_0 is the weight of HEMA and PVP in the initial reaction mixture. The dry weight was obtained by heating at 70°C for 5h and then increasing the temperature to 120°C for 48h. The obtained xerogels were placed in a desiccator to cool down to room temperature before weighing.

6.7.1.2. Swelling kinetics

For the swelling dynamic studies, the hydrogels were immersed after the reaction polymerization in deionized water and after a freeze-drying process (lyophilized xerogels). With a certain time interval, the hydrogels were taken out from the water and weighed after removal of the excess water from the surface of the hydrogel. The swelling ratio (SR) of the hydrogels was calculated according to:

$$SR = \frac{W_i - W_{d^*}}{W_{d^*}} \tag{6.3}$$

where W_i is the hydrogel weight at the specific time *i* and W_{d^*} is the dry weight of the prepared hydrogel (in the case of the hydration phase) or the weight of the lyophilized xerogel (in the case of rehydration phase). The SR of the hydration phase when i=0 is >0 due to the presence of water in the reaction mixture.

To determine the nature of water diffusion into the hydrogels, initial swelling data were fitted to the following exponential equation:[41]

$$F = \frac{M_i}{M_\infty} = ki^n \tag{6.4}$$

where *F* denotes the fraction of water at time *i*, M_t and M_∞ represent the amount of solvent diffused into the hydrogel at time *i* ($W_i - W_d$) and infinite time ($W_w - W_d$), respectively; *k* is a constant related to the structure of the network; and the exponent *n* is a characteristic coefficient of transport. This equation is applied to the initial stages of the swelling ratio, and plots of *lnF* vs *lnt* yield straight lines.[5]

6.7.1.3. Equilibrium Water Content

The equilibrium water content (EWC) of hydrogels gives information on the polymer network hydrophilicity and can be calculated as follows:[42]

$$EWC = \frac{W_w - W_d}{W_w} \times 100 \tag{6.5}$$

where W_w is the weight of the water swollen hydrogel in equilibrium, obtained at least after 7 days of swelling.

6.7.1.4. Dehydration kinetics

To determine the dehydration kinetics, expressed as water decrease over time (WD), swollen hydrogel films were weighted and placed in a humidity chamber at 53% relative humidity (RH) until equilibrium was reached. The weight decrease as a function of time was calculated as follows:

$$WD = \frac{W_i - W_d}{W_w - W_d} \times 100 \tag{6.6}$$

6.7.1.5. Loading of solvents and nanofluids

The swelling capacity of SIPN hydrogels when loading solvents and nanofluids was calculated by immersing the lyophilized ***H58*** hydrogel into the selected systems. The solvents were chosen from those commonly used by conservators.[43] Squared hydrogel films of about 1cm^2 and 2mm of thickness were used. Hydrogel weights were registered before and after immersion in the solvent system to calculate the Equilibrium Solvent Content (ESC):[44]

$$ESC = \frac{W_w - W_d}{W_w} \times 100 \quad (6.7)$$

For all the other experiments using hydrogels loaded with nanofluids (e.g. rheology and SAXS measurements) hydrogels were loaded with the systems by putting water-loaded hydrogels in a Falcon container with excess liquid for 12h.

6.7.2. Preparation of nanostructured fluids

The composition of the EAPC system (wt%) is deionized water, 73.3%; sodium dodecyl sulfate (SDS), 3.7%; 1-pentanol, 7%; ethyl acetate, 8%; propylene carbonate, 8%. The composition of the MEB system (wt%) is deionized water, 81.85%; dodecyl dimethyl amine oxide (DDAO), 6.15%; 2-butanone, 4%; ethyl acetate, 4%; butyl acetate, 4%. The components were added in solution following the given order.

6.7.3. SIPN hydrogel composition

The SIPN hydrogels compositions were semi-quantified by means of ATR-FTIR spectroscopy. A pHEMA homopolymer was prepared without PVP according with the synthesis method described before. A dry sample was obtained at 60ªC for 48h, which was then pulverized with a mortar. Powder mixtures of pHEMA and PVP linear polymer (used as received) were prepared in known proportions of HEMA/PVP (1:9, 1:2.3, 1:1, 1:0.4, 1:0.1), adding a small amount of water in order to have an homogeneous mixing. Dry samples were obtained after 48h at 60ºC, which were then, pulverized with a mortar.

The obtained ATR-FTIR spectra were analyzed with the software MagicPlot in order to carry out multi-peak fitting of the characteristic carbonyl stretching vibration peaks. Assumption of the use of Gaussian curves for the FTIR deconvolved components have already been reported[45] (example given in figure 6.24).

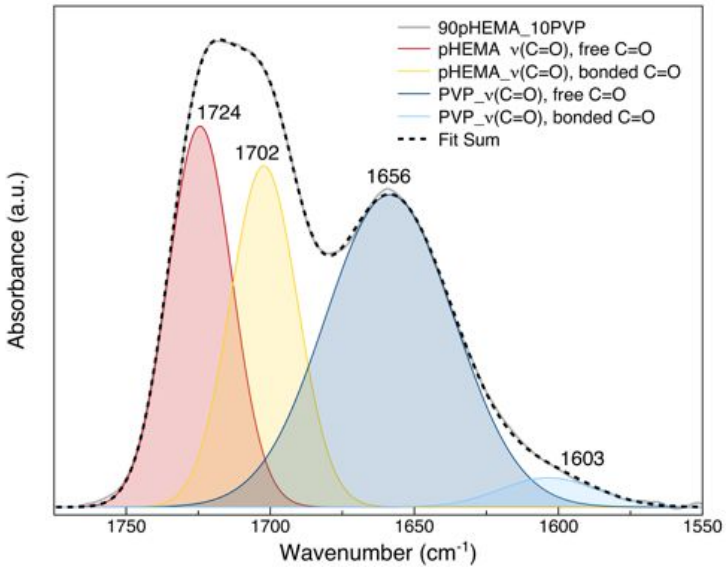

Figure 6.24. Example of the four-Gaussian decomposition of pHEMA and PVP mixtures. HEMA peaks, 1724 and 1702cm^{-1}, are assigned to the C=O stretching vibration of free hydrogen bonded and for hydrogen bonded carbonyl group,[46] respectively. PVP peaks at 1656 and 1603cm^{-1} are assigned to the C=O stretching vibration of free hydrogen bonded and for hydrogen bonded carbonyl group,[47,48] respectively.

Peak areas were obtained and the pHEMA/PVP ratios were presented in function of PVP concentration in the powder mixture. An exponential fitting function was obtained and used to estimate the "real" PVP quantity in the composition of hydrogels, using an exponential function:

$$f(\phi) = A \cdot e^{k\phi} \tag{6.8}$$

where ϕ is PVP weight percentage concentration and A and k are constants.

6.7.3.1. Instrumentation

A FTIR spectrometer (Thermo Nicolet Nexus 870) in attenuated total reflectance FT-infrared mode (ATR-FTIR), equipped with a Golden Gate diamond cell was used to investigate on the cured gel composition. Data were collected with an MCT detector with a sampling area of 150μm^2. The spectra were obtained from 128 scans with 2cm^{-1} of optical resolution.

6.7.4. Quantification of water states

Water in swollen hydrogels can be classified into three different states: bound, interfacial and free, which can be identified by their freezing features: bound water is unfreezable water; interfacial water is bound-freezable and free water have the same properties as bulk water. The determination of the amount of freezable water can be carried out through Thermoanalysis (Differential Scanning Calorimetry - DSC, and Differential Thermogravimetry - DTG).

6.7.4.1. Free Water Index

The Free Water Index (FWI) was calculated as follows:[49]

$$FWI = \frac{\Delta H_{\exp}}{WC \times \Delta H_{theo}} \tag{6.9}$$

where the $\Delta H_{\exp}$ (J/g) represents the melting enthalpy variation for free water and can be determined by integration of the DSC peak around 0°C, WC is the water weight fraction in the fully hydrated hydrogel, and ΔH_{theo} is the theoretical value of the specific enthalpy of fusion for bulk water (333.61 J/g).[50]

6.7.4.2. Freeze-Bound Water Index

Partially rehydrated hydrogels were prepared to determine the freeze-bound water fraction.[51] About 15mg of sample were first equilibrated at 75% and then at 100% relative humidity (RH) for 6 days. The Freeze-Bound Water Index was determined from the relationship:[49]

$$FBWI = \frac{\Delta H_{\exp}}{WC \times \Delta H_{bound}} \tag{6.10}$$

where ΔH_{bound} (J/g) is the theoretical value of the melting enthalpy of water at the specific temperature below 0°C, and it was calculated as described in the literature.[52]

6.7.4.3. Instrumentation

Gel samples of 12–18mg were analyzed in closed aluminum pans to determine both Free Water Index (FWI) and Freeze-Bound Water Index (FBWI).

Melting enthalpies were calculated from DSC thermograms using a Q1000 (TA Instruments) apparatus. It is equipped with an autosampler and a cooling device.

Measurements were carried out at a constant nitrogen flow rate of 50ml/min. The temperature range scan was from –80 to 20°C with 0.5°C/min rate.

The water content expressed as weight fraction in the gel, *A*, was determined by DTG, using a SDT Q600 (TA Instruments) apparatus with balance sensitivity of 0.1μm with respect to weight change. Measurements were performed in a nitrogen atmosphere with a sample purge flow rete of 100ml/min. The temperature scan was from 20 to 450°C with a heating rate of 10°C/min over open aluminum pans after DSC runs.

6.7.5. Mechanical analysis

Oscillatory rheology measurements were performed to investigate on the mechanical features of the selected hydrogels. Water-swollen and nanofluid-loaded hydrogels were used in the film form (≈2mm tick).

6.7.5.1. Instrumentation

Viscoelastic features of hydrogel formulations in flat film form were analyzed with a DHR rheometer from TA Instruments equipped with a parallel plate geometry of 40 mm diameter. All hydrogel samples where cut to plate shape under a trim gap and then equilibrated for 20 min and at 25.00 ± 0.01 ºC (Peltier temperature control system). The plate was lowered to the measuring position in the z-axis force controlled mode; the maximum squeezing force was 2.5 N. This was inspected during a series of rheology measurements on the same sample during time. The rheological behavior was determined by measuring the G' and G'' moduli in an oscillation regime in the linear viscoelastic region of deformations. The storage, *G'*, and the loss, *G''*, moduli were measured over the frequency range 100-10^{-3} Hz at a temperature of 25.00 ± 0.01°C with a strain of 0.1%. The values of the stress amplitude were confirmed through amplitude sweep runs in order to ensure that all measurements were performed within the linear viscoelastic region (see example in figure 6.25). Data was acquired after 10 points/decade. At least 5 measurements were performed on each fully hydrated sample and the results presented are average waves.

6.7.6. SIPN microporosity

Scanning Electron Microscopy (SEM) was used to investigate on gel's microporosity. Since SEM measurements must be carried out in high vacuum conditions, analysis must be performed on dried gels, i.e. xerogels. To obtain xerogels, a freeze-drying process was used (low temperature and pressure), where water inside gels passes first to solid state and then from solid to vapor by

sublimation. It is important to remark that this process may affect the gel structure and the mesoporosity might collapse during the process.

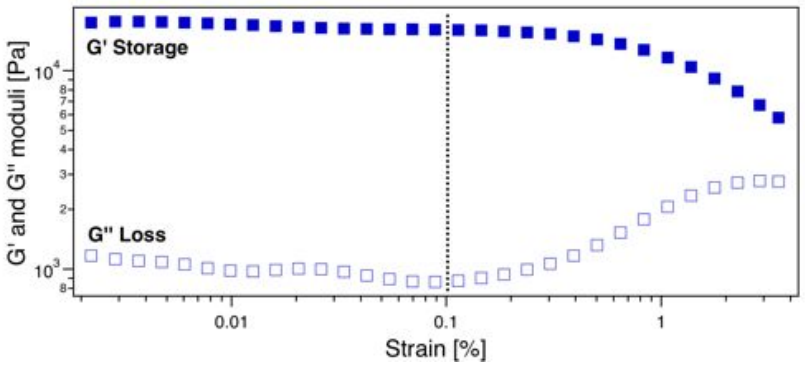

Figure 6.25. Amplitude sweep measurement for ***H65*** hydrogel. The chosen strain (0.1%) is highlighted by the dashed line.

6.7.6.1. Instrumentation

A FEG-SEM ΣIGMA (Carl Zeiss, Germany) was used to acquire the images using an acceleration potential of 1kV and a working distance of 1.4mm. The metallization of the samples was not necessary with these experimental conditions.

6.7.7. Network characterization

Small Angle R-ray Scattering (SAXS) was used to investigate on the polymeric structure of hydrogels. Water-swollen and nanofluid-swollen hydrogels were examined.

For studying the structure features of the SIPN hydrogels water loaded hydrogels were used and SAXS curves were obtained. In this case, SAXS intensity distribution, *I*, as a function of the amplitude of the scattering modulus *q*, can be generally described by the sum of two *q*-dependent contributions and an instrumental flat background:

$$I(q) = I_{Lorentz}(q) + I_{excess}(q) + bkg \qquad (6.11)$$

The first contribution, $I_{Lorentz}(q)$, is a Lorentzian term, that is an Ornstein–Zernike function, accounting for the scattering associated of a tridimensional

network where the correlation length ζ is the average distance between polymer chains. It can be expressed as follows:[53]

$$I_{Lorentz}(q) = \frac{I_{Lorentz}(0)}{1+q^2\zeta^2} \tag{6.12}$$

where $I_{Lorentz}(0)$ is the Lorentzian intensity at q = 0 and ζ is the average mesh dimension of the network. If the correlation length among the inhomogeneous regions is larger than the correlation length of the cross-links ($\Xi > \zeta$), an "excess" structure factor that takes into account of the scattering excess may be considered. This second contribution, $I_{excess}(q)$, is a Debye-Bueche function[54] that concerns the scattering at low q produced by inhomogeneities, as for example, solid-like polymer domains.

$$I_{excess}(q) = \frac{I_{excess}(0)}{(1+q^2\Xi^2)^2} \tag{6.13}$$

where $I_{excess}(0)$ is the excess intensity at q = 0 and Ξ is the average dimension of the inhomogeneity domains accessible by the SAXS experiment.

To study on the possible interactions between hydrogels and nanofluids and how these may affect their structures, nanofluid-swollen hydrogels were exanimated. To obtain a sample of the nanofluid inside hydrogels, an extracting method was used as follows: nanofluid-loaded hydrogels were placed into a syringe, which had a plastic filter (pore size 1.2μm) attached to the syringe end. Hydrogels were squeezed in order to allow the liquid to pass through the filter membrane. The collected liquid was analyzed immediately to obtain SAXS curves.

The scattered intensity for nanofluids is given by:[35]

$$I(q) = N_p V^2 \Delta\rho^2 P(q) S(q) \tag{6.14}$$

where $P(q)$ is the form factor, (ellipsoidal for EAPC system and polydispersed spheres for MEB system), $S(q)$ is the structure factor, N_p is the number density of scattering objects, V is their volume and $\Delta\rho$ is the contrast term, which is the squared difference of the scattering length densities between the micelles and the solvent. The micelles have an effective charge Z and are described by the following geometrical parameters: a (major semi-axis), b (minor semi-axis) and t

(shell thickness), sufficient to identify a prolate ellipsoid, identified for the EAPC system, and *r* (core radius), *t* (shell thickness) and poly (core polydispersity), to identify a spherical particle, identified in MEB system. Other parameters that complete the fitting models are the scattering length densities (SLDs), ρ_{core}, ρ_{shell} and ρ_{bulk}, which describe the contrast between the micelle and the solvent and the volume fraction, Φ, of the scattering objects with respect to the whole system volume.

The fitting of the curve at low-*q* was carried out by adding/subtracting to the previous nanofluid fitting model an additional equation, referred to the inhomogeneities of the hydrogels, thus equal to equation (6.13).

6.7.7.1. Instrumentation

SAXS measurements were carried out with a HECUS S3-MICRO camera (Kratky-type) equipped with a position-sensitive detector (OED 50M) containing 1024 channels of width 54µm. Cu Kα radiation of wavelength λ=1.542Å was provided by an ultrabrilliant point microfocus X-ray source (GENIX-Fox 3D, Xenocs, Grenoble), operating at a maximum power of 50W (50kV and 1mA). The sample-to-detector distance was 269mm. The volume between the sample and the detector was kept under vacuum during the measurements to minimize scattering from the air. The Kratky camera was calibrated in the small angle region using silver behenate (d=58.38Å).[55] Scattering curves were obtained in the *q*-range between 0.01 and 0.54 $Å^{-1}$, assuming that *q* is the scattering vector, $q=4\pi/\lambda \sin\theta$, and 2θ the scattering angle. Hydrogel samples were placed into a 1mm demountable cell having Mylar films as windows, while liquid samples were put in 2mm thick quartz capillary tubes sealed with hot-melting glue. The temperature was set to 25°C and was controlled by a Peltier element, with an accuracy of 0.1°C. All scattering curves were corrected for the empty cell contribution considering the relative transmission factor.

6.8. Bibliography

(1) Mori, S. Determination of Chemical Composition and Molecular Weight Distributions of High-Conversion Styrene-Methyl Methacrylate Copolymers by Liquid Adsorption and Size Exclusion Chromatography. *Anal. Chem.* **1988**, *60*, 1125–1128.

(2) Huang, Y.; Yang, J. Gelation Forming Process for Low Toxicity System. In

Novel Colloidal Forming of Ceramics; Springer: Berlin Heidelberg, 2011; p 124.

(3) Yanez, F.; Concheiro, A.; Alvarez-Lorenzo, C. Macromolecule Release and Smoothness of Semi-Interpenetrating PVP–pHEMA Networks for Comfortable Soft Contact Lenses. *Eur J Pharm Biopharm* **2008**, *69*, 1094–1103.

(4) Korsmeyer, R. W.; Peppas, N. A. Effect of the Morphology of Hydrophilic Polymeric Matrices on the Diffusion and Release of Water Soluble Drugs. *J. Membr. Sci.* **1981**, *9*, 211–227.

(5) Çaykara, T.; Turan, E. Effect of the Amount and Type of the Crosslinker on the Swelling Behavior of Temperature-Sensitive Poly(N-tert-Butylacrylamide-co-Acrylamide) Hydrogels. *Colloid Polym. Sci.* **2006**, *284*, 1038–1048.

(6) Alfrey, T.; Gurnee, E. F.; Lloyd, W. G. Diffusion in Glassy Polymers. *J. Polym. Sci. Part C Polym. Symp.* **2007**, *12*, 249–261.

(7) Bajpai, A. K.; Bajpai, J.; Shukla, S. Water Sorption Through a Semi-Interpenetrating Polymer Network (IPN) with Hydrophilic and Hydrophobic Chains. *React. Funct. Polym.* **2002**, *50*, 9–21.

(8) Paradiso, P.; Galante, R.; Santos, L.; Alves de Matos, A. P.; Colaço, R.; Serro, A. P.; Saramago, B. Comparison of Two Hydrogel Formulations for Drug Release in Ophthalmic Lenses. *J. Biomed. Mater. Res. B Appl. Biomater.* **2014**, *102*, 1170–1180.

(9) Lou, X.; Munro, S.; Wang, S. Drug Release Characteristics of Phase Separation pHEMA Sponge Materials. *Biomaterials* **2004**, *25*, 5071–5080.

(10) Giorgi, R.; Baglioni, M.; Berti, D.; Baglioni, P. New Methodologies for the Conservation of Cultural Heritage: Micellar Solutions, Microemulsions, and Hydroxide Nanoparticles. *Acc. Chem. Res.* **2010**, *43*, 695–704.

(11) Baglioni, M.; Rengstl, D.; Berti, D.; Bonini, M.; Giorgi, R.; Baglioni, P. Removal of Acrylic Coatings from Works of Art by Means of Nanofluids: Understanding the Mechanism at the Nanoscale. *Nanoscale* **2010**, *2*, 1723.

(12) Baglioni, M.; Giorgi, R.; Berti, D.; Baglioni, P. Smart Cleaning of Cultural Heritage: a New Challenge for Soft Nanoscience. *Nanoscale* **2012**, *4*, 42.

(13) Baglioni, M.; Berti, D.; Teixeira, J.; Giorgi, R.; Baglioni, P. Nanostructured Surfactant-Based Systems for the Removal of Polymers from Wall Paintings:

A Small-Angle Neutron Scattering Study. *Langmuir* **2012**, *28*, 15193–15202.

(14) Baglioni, M.; Jàidar Benavides, Y.; Berti, D.; Giorgi, R.; Keiderling, U.; Baglioni, P. An Amine-Oxide Surfactant-Based Microemulsion for the Cleaning of Works of Art. *J. Colloid Interface Sci.* **2015**, *440*, 204–210.

(15) Bouguerra, S.; Letellier, P.; Turmine, M. Acid–Base Equilibrium of Dodecyldimethyl-Amine-N-Oxide Micelles in Water–Butanol Binary at 298 K. *J. Surfactants Deterg.* **2010**, *13*, 217–224.

(16) Soontravanich, S.; Walsh, S.; Scamehorn, J. F.; Harwell, J. H.; Sabatini, D. A. Interaction Between an Anionic and an Amphoteric Surfactant. Part II: Precipitation. *J. Surfactants Deterg.* **2009**, *12*, 145–154.

(17) García, M. T.; Campos, E.; Ribosa, I. Biodegradability and Ecotoxicity of Amine Oxide Based Surfactants. *Chemosphere* **2007**, *69*, 1574–1578.

(18) Gulsen, D.; Chauhan, A. Dispersion of Microemulsion Drops in HEMA Hydrogel: a Potential Ophthalmic Drug Delivery Vehicle. *Int. J. Pharm.* **2005**, *292*, 95–117.

(19) Wolfe, J.; Bryant, G.; Koster, K. L. What is Unfreezable Water, How Unfreezable Is It and How Much is There? *CryoLetters* **2002**, *23*, 157–166.

(20) Li, X.; Cui, Y.; Xiao, J.; Liao, L. Hydrogel–Hydrogel Composites: The Interfacial Structure and Interaction between Water and Polymer Chains. *J Appl Polym Sci* **2008**, *108*, 3713–3719.

(21) Goodwin, W.; Hughes, R. W. *Rheology for Chemists. An Introduction*; Royal Society of Chemistry: Cambridge, 2000.

(22) Almdal, K.; Dyre, J.; Hvidt, S.; Kramer, O. Towards a Phenomenological Definition of the Term “Gel.” *Polym. Gels Netw.* **1993**, *1*, 5–17.

(23) Gottlieb, M.; Macosko, C. W.; Benjamin, G. S.; Meyers, K. O.; Merrill, E. W. Equilibrium Modulus of Model Poly (Dimethylsiloxane) Networks. *Macromolecules* **1981**, *14*, 1039–1046.

(24) Jovaševića, J. S.; Dimitrijevića, S. I.; Filipovića, J. M.; Tomića, S. L.; Mićićb, M. M.; Suljovrujića, E. H. Swelling, Mechanical and Antimicrobial Studies of Ag/P (HEMA/IA)/PVP Semi-IPN Hybrid Hydrogels. *Acta Phys. Pol. A* **2011**, *120*.

(25) MacKintosh, F.; Käs, J.; Janmey, P. Elasticity of Semiflexible Biopolymer Networks. *Phys. Rev. Lett.* **1995**, *75*, 4425–4428.

(26) De Gennes, P. G. Scaling Theory of Polymer Adsorption. *J. Phys.* **1976**, *37*, 1445–1452.

(27) Guenet, J.-M. Structure versus Rheological Properties in Fibrillar Thermoreversible Gels from Polymers and Biopolymers. *J. Rheol.* **2000**, *44*, 947.

(28) Pääkkö, M.; Ankerfors, M.; Kosonen, H.; Nykänen, A.; Ahola, S.; Österberg, M.; Ruokolainen, J.; Laine, J.; Larsson, P. T.; Ikkala, O.; Lindström, T. Enzymatic Hydrolysis Combined with Mechanical Shearing and High-Pressure Homogenization for Nanoscale Cellulose Fibrils and Strong Gels. *Biomacromolecules* **2007**, *8*, 1934–1941.

(29) Domingues, J.; Bonelli, N.; Giorgi, R.; Baglioni, P. Chemical Semi-IPN Hydrogels for the Removal of Adhesives from Canvas Paintings. *Appl. Phys. A* **2014**, *114*, 705–710.

(30) Canal, T.; Peppas, N. A. Correlation between Mesh Size and Equilibrium Degree of Swelling of Polymeric Networks. *J Biomed Mater Res Part A* **1989**, *23*, 1183–1193.

(31) Peppas, N. A.; Hilt, J. Z.; Khademhosseini, A.; Langer, R. Hydrogels in Biology and Medicine: From Molecular Principles to Bionanotechnology. *Adv. Mater.* **2006**, *18*, 1345–1360.

(32) Panyukov, S.; Rabin, Y. Statistical Physics of Polymer Gels. *Phys Rep* **1996**, *269*, 1–131.

(33) Benguigui, L.; Boue, F. Homogeneous and Inhomogenous Polyacrylamide Gels as Observed by Small Angle Neutron Scattering: A Connection with Elastic Properties. *Eur Phys J B* **1999**, *11*, 439–444.

(34) Ikkai, F.; Shibayama, M. Inhomogeneity Control in Polymer Gels. *J Polym Sci Part B Polym Phys* **2005**, *43*, 617–628.

(35) Baglioni, M.; Rengstl, D.; Berti, D.; Bonini, M.; Giorgi, R.; Baglioni, P. Removal of Acrylic Coatings from Works of Art by Means of Nanofluids: Understanding the Mechanism at the Nanoscale. *Nanoscale* **2010**, *2*, 1723.

(36) Baglioni, M.; Berti, D.; Teixeira, J.; Giorgi, R.; Baglioni, P. Nanostructured Surfactant-Based Systems for the Removal of Polymers from Wall Paintings: A Small-Angle Neutron Scattering Study. *Langmuir* **2012**, *28*, 15193–15202.

(37) Goddard, E. D. Polymer–Surfactant Interaction. Part I. Uncharged Water-

Soluble Polymers and Charged Surfactants. *Colloids Surf.* **1986**, *19*, 255–300.

(38) Shirahama, K.; Tsujii, K.; Takagi, T. Free-Boundary Electrophoresis of Sodium Dodecyl Sulfate-Protein Polypeptide Complexes with Special Reference to SDS-Polyacrylamide Gel Electrophoresis. *J. Biochem. (Tokyo)* **1974**, *75*, 309–319.

(39) Carretti, E.; Fratini, E.; Berti, D.; Dei, L.; Baglioni, P. Nanoscience for Art Conservation: Oil-in-Water Microemulsions Embedded in a Polymeric Network for the Cleaning of Works of Art. *Angew Chem Int Ed* **2009**, *48*, 8966–8969.

(40) Ming Kuo, S.; Jen Chang, S.; Jiin Wang, Y. Properties of PVA-AA Cross-Linked HEMA-Based Hydrogels. *J Polym Res* **1999**, *6*, 191–196.

(41) Korsmeyer, R. W.; Gurny, R.; Doelker, E.; Buri, P.; Peppas, N. A. Mechanisms of Solute Release From Porous Hydrophilic Polymers. *Int. J. Pharm.* **1983**, *15*, 25–35.

(42) Liu, Q.; Hedberg, E. L.; Liu, Z.; Bahulekar, R.; Meszlenyi, R. K.; Mikos, A. G. Preparation of Macroporous Poly (2-Hydroxyethyl Methacrylate) Hydrogels by Enhanced Phase Separation. *Biomaterials* **2000**, *21*, 2163–2169.

(43) Smith, G. D.; Johnson, R. Strip “Teas” - Solubility Data for the Removal (and Application) of Low Molecular Weight Synthetic Resins Used as Inpainting Media and Picture Varnishes. *WAAC Newsl.* **2008**, *30*, 11–19.

(44) Fratini, E.; Carretti, E. Chapter 10. Cleaning IV: Gels and Polymeric Dispersions. In *Nanoscience for the Conservation of Works of Art*; Baglioni, P.; Chelazzi, D.; O’Brien, P., Eds.; Royal Society of Chemistry: Cambridge, 2013; pp 252–279.

(45) Byler, D. M.; Susi, H. Examination of the Secondary Structure of Proteins by Deconvolved FTIR Spectra. *Biopolymers* **1986**, *25*, 469–487.

(46) Perova, T. S.; Vij, J. K.; Xu, H. Fourier Transform Infrared Study of Poly (2-Hydroxyethyl Methacrylate) PHEMA. *Colloid Polym. Sci.* **1997**, *275*, 323–332.

(47) Oh, T.-J.; Nam, J.-H.; Jung, Y. M. Molecular Miscible Blend of Poly(2-Cyano-1,4-Phenyleneterephthalamide) and Polyvinylpyrrolidone Characterized by Two-Dimensional Correlation FTIR and Solid State 13C NMR Spectroscopy. *Vib. Spectrosc.* **2009**, *51*, 15–21.

(48) Imamura, K.; Asano, Y.; Maruyama, Y.; Yokoyama, T.; Nomura, M.; Ogawa, S.; Nakanishi, K. Characteristics of Hydrogen Bond Formation between Sugar and Polymer in Freeze-Dried Mixtures under Different Rehumidification Conditions and its Impact on the Glass Transition Temperature. *J. Pharm. Sci.* **2008**, *97*, 1301–1312.

(49) Nakamura, K.; Hatakeyama, T.; Hatakeyama, H. Relationship between Hydrogen Bonding and Bound Water in Polyhydroxystyrene Derivatives. *Polymer* **1983**, *24*, 871–876.

(50) Lide, D. R. *CRC Handbook of Chemistry and Physics*, 79th ed.; CRC Press: Boca Raton, FL, 1998.

(51) Faroongsarng, D.; Sukonrat, P. Thermal Behavior of Water in the Selected Starch- and Cellulose-Based Polymeric Hydrogels. *Int J Pharm* **2008**, *352*, 152–158.

(52) Landry, M. R. Thermoporometry by Differential Scanning Calorimetry: Experimental Considerations and Applications. *Thermochim Acta* **2005**, *433*, 27–50.

(53) D'Errico, G.; De Lellis, M.; Mangiapia, G.; Tedeschi, A.; Ortona, O.; Fusco, S.; Borzacchiello, A.; Ambrosio, L. Structural and Mechanical Properties of UV-Photo-Cross-Linked Poly(N-Vinyl-2-Pyrrolidone) Hydrogels. *Biomacromolecules* **2007**, *9*, 231–240.

(54) Debye, P.; Bueche, A. M. Scattering by an Inhomogeneous Solid. *J Appl Phys* **1949**, *20*, 518–525.

(55) Blanton, T.; Huang, T. C.; Toraya, H.; Hubbard, C. R.; Robie, S. B.; Louer, D.; Gobel, H. E.; Will, G.; Gilles, R.; Raftery, T. JCPDS-International Centre for Diffraction Data Round Robin Study of Silver Behenate. A Possible Low-Angle X-Ray Diffraction Calibration Standard. *Powder Diffr* **1995**, *10*, 91–95.

CHAPTER 7
Application of SIPN p(HEMA)/PVP Hydrogels: Cleaning Tests on Mock-ups

7.1. Introduction

Cleaning of Cultural Heritage artifacts represents one of the most delicate operations of restoration because it is potentially invasive and aggressive for the original materials as well as completely irreversible. As discussed in chapter 1, the list of unwanted materials to be removed from artifacts surface can include a wide group of substances: from deposits of pollutants and grime to aged adhesives and darkened varnish coatings. The unwanted materials can be chemically divided into hydrophilic and hydrophobic materials. The hydrophilic materials are removed with neat water, while the hydrophobic materials (not similar to water) are removed using nanostructured fluids. One of the most serious concerns of restorers and conservation scientists is the removal of these materials without affecting the original painting. Therefore, high performing cleaning systems must be able to ensure a controlled and selective cleaning action.

In this chapter, the application features of the selected SIPN hydrogels, ***H50***, ***H58*** and ***H65*** are evidenced, through the use of some representative mock-ups and of painted objects with no historic value. In all the given examples, a different conservation issue is addressed, accounting for the water-sensitive character of the material or the necessity of a layer-by-layer removal. This is usually extremely difficult to face using conventional methods. In fact, these novel hydrogel systems have exceptional highly retentive features that can potentially solve both conservation issues.

During the course of this research project, several mock-ups were prepared to examine the versatility of using these hydrogels in different cases. Only the most relevant are presented.

7.2. Gel residues investigation

Chemical hydrogels are permanent structures due to the covalent bonds that build the polymer network. In the case of SIPN hydrogels, the linear PVP is bonded by physical forces to the permanent network of pHEMA. To confirm that the selected SIPN hydrogels do not leave residues on the surface after a cleaning treatment, ATR-FTIR spectra were performed on a highly hydroscopic material (cotton canvas) previously in contact with water-loaded SIPN hydrogels. The resulting ATR-FTIR spectra are reported in figure 7.1. Two reference spectra (cotton canvas and ***H50*** hydrogel) are compared with the spectra of two canvas samples where ***H50*** and ***H65*** were previously applied. The characteristic carbonyl stretching vibration peaks of pHEMA and PVP (marked as red asterisks in the figure) are not present in the spectra of the treated canvases, proving that no detectable gel residues are left after the cleaning procedure.

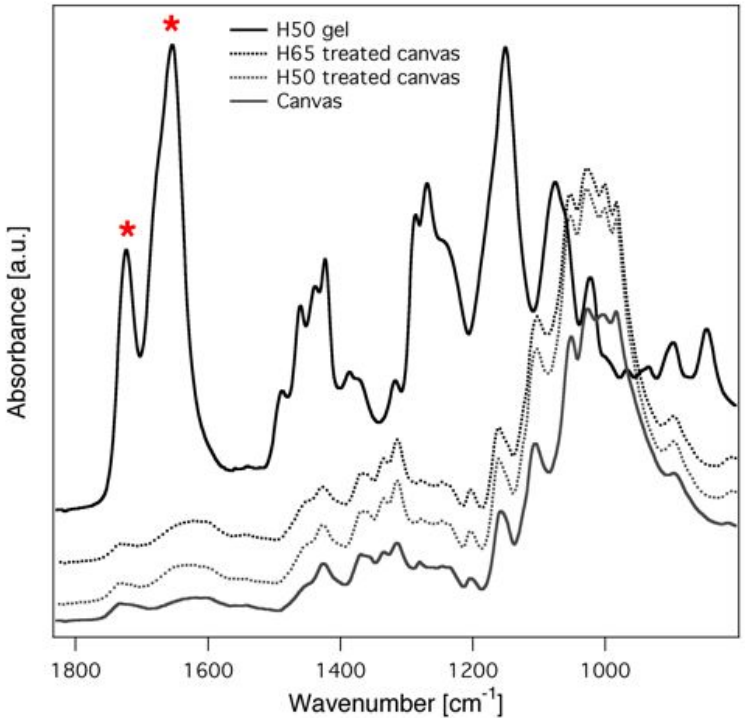

Figure 7.1. ATR-FTIR fingerprint region spectra of a cotton canvas, of ***H50*** hydrogel and of canvases previously in contact with p(HEMA)/PVP hydrogels ***H65*** and ***H50***. Marked peaks (asterisk) correspond to characteristic C=O stretching vibration of pHEMA (1724 cm^{-1}) and PVP (1654 cm^{-1}).

7.3. Removal of hydrophilic materials

The hydrophilic materials to remove from an artifact are majorly represented by the superficial grime formed by natural causes. Even if other kinds of materials are not excluded, in this section only grime removal is assessed. In order to build mock-ups that mimic a real case of natural soil deposition, an artificial grime powder mixture was prepared according to the preparation procedure developed by Wolbers.[1] The powder mixture is composed of organic and inorganic materials: carbon black; iron oxide; gelatin; soluble starch; cement; silica; lime; kaolin; and peat moss. The artificial grime was then applied in a 4.5% (v/v) solution of mineral oil in chloroform using a paintbrush over the mock-ups surface.

SIPN p(HEMA)/PVP hydrogels are highly hydrophilic, therefore, they are able to load materials solubilized by water, as highlighted in figure 7.2. This fact permits to completely eliminate the necessity of any mechanical action in the removal of such materials, strongly reducing the damage caused on the surface. Further on, two examples of the prepared mock-ups for removal of hydrophilic grime from water-sensitive surfaces are presented.

Figure 7.2. Hydrogel's capacity to perform uptake of hydrophilic materials, such as grime, is noticed (the film thickness is ≈6mm).

7.3.1. From a tempera *painting*

An artificially soiled *Thang-Ka* mock-up was considered to assess the efficiency of hydrophilic grime removal from a water-sensitive substrate. A *Thang-Ka* is a Tibetan votive artifact based on *tempera magra* painting on canvas, where the binder is animal glue (see figure 7.3). This painting technique is characterized by a high pigment volume concentration (PVC), equal or slightly higher than

critical PVC, at which there is just sufficient binder to wet the pigment particles. This leads to a rougher surface and a very low cohesive paint layer, where the scarce quantity of binder is water-sensitive.[2] This is a optimal example of a water-sensitive artifact combined with ulterior conservation problems. In fact, the removal of hydrophilic grime, which is in part trapped into the painting porosity, is a challenge for restorers using conventional methods. Because paint layer is water-sensitive and is low cohesive, the traditional use of a water-impregnated cotton swab can cause paint loss. For these reasons it is necessary to achieve a controlled removal through the precise confinement of the solvent. Hence, the *Thang-Ka* represents an appropriate example to test SIPN hydrogel's capability to perform an efficient and highly controlled cleaning action.

Figure 7.3. Detail of a *Thang-Ka* from the 18th century.

The *Thang-Ka* mock-up prepared is composed of a multilayer structure in which a cotton canvas is covered with a preparation layer containing $CaCO_3$ and animal glue. The painting technique is a *tempera magra*, where pigments and colorants are mixed with animal glue dissolved in water. In the prepared mock-up, the white pigment is calcium carbonate; the green pigment is malachite; the blue colorant is indigo; and the golden lines are obtained from shell gold. To carry out cleaning tests, the mock-up surface was previously covered with the artificial grime mixture.

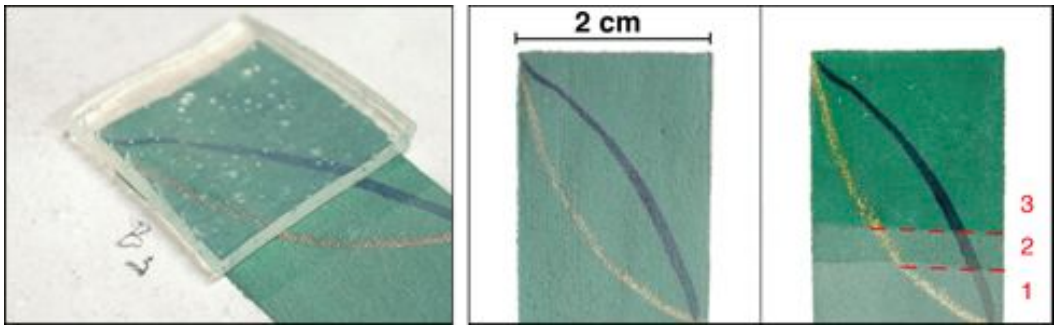

Figure 7.4. Artificial grime removal using water-loaded ***H58*** hydrogel from a *Thank-Ka* mock-up. Right image presents different levels of cleaning: not cleaned (1); after 20min of hydrogel application (2); after further 20min of hydrogel application (3).

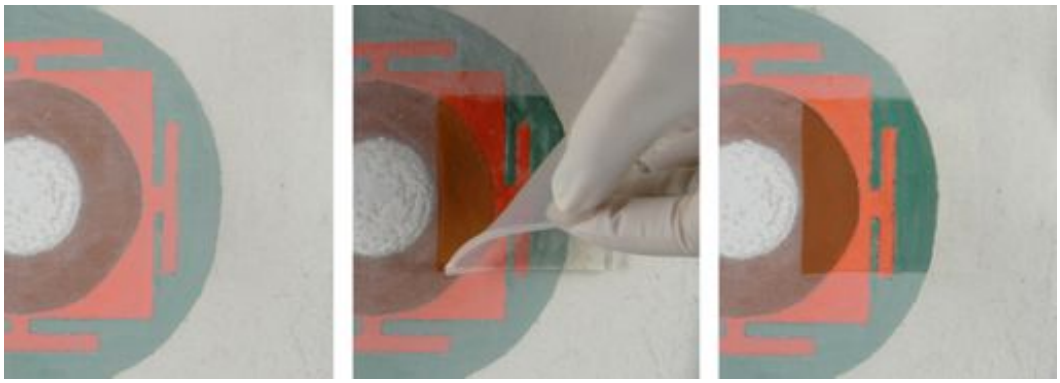

Figure 7.5. The cleaning stages on *Thang-ka* mock-up.

The application features of SIPN hydrogels for the removal of hydrosoluble superficial grime from a *Thang-Ka* mock-up are presented here. Preliminary cleaning tests were performed using ***H50***, ***H58*** and ***H65*** hydrogels. From all the tested hydrogels, ***H58*** showed the best compromise between cleaning efficiency and water-diffusion control. To obtain a gradual and controlled cleaning action, the most efficient procedure was the use of ***H58*** hydrogel in two short applications, each of about 20min (see figure 7.4). The ease of handling of this hydrogel film is evidenced in figure 7.5.

After each hydrogel application, some layers of the grime were loaded inside the hydrogel, which means that no further mechanical action was necessary. In fact, the gentle cleaning process carried out by these hydrogels do not show pigment loss. As seen in chapter 6, hydrogels dehydrate very slow, so they

remain humid for the time necessary to perform cleaning, while avoiding tearing of the painting layers when the hydrogel is removed (see figure 7.5). These cleaning trials have demonstrated the outstanding cleaning control that can be achieved by using SIPN hydrogels, since the superficial grime is gradually removed and the original water-sensitive paint layers are not affected.

7.3.2. From an acrylic-vinyl painting

Water-borne modern paints are known to be water-sensitive. In fact, when in contact with water, they tend to swell (see the modeled example in figure 7.6). This fact can cause color loss during cleaning process by conventional methods, i.e. using liquid impregnated cotton-swabs. Furthermore, most of contemporary paintings are monochromes, or have large monochromatic areas, so every alteration to the paint morphology may be perceptible and inflict alteration to the painting's value in the market.

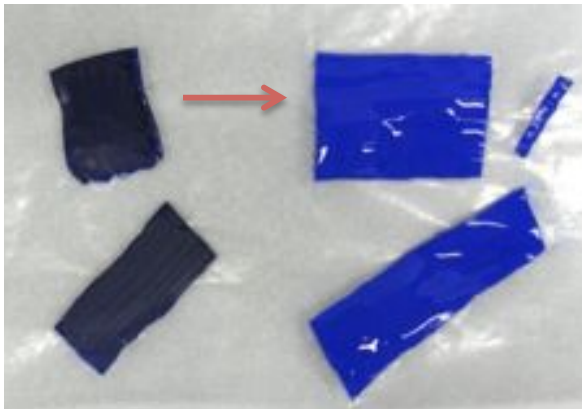

Figure 7.6. Emulsion paint film from Liquitex PB29 acrylic color (p*n*BA/MMA). The swelling effect is evidenced after immersion in deionized water for 12h.

To address the problem of cleaning such paintings a comparison between the application of SIPN hydrogels and an humidified cotton-swab is presented here. A mock-up sample composed of acrylic (Liquitex blue PB29) and vinyl (Polycolor white PW5, PW6) emulsion paints over a canvas was prepared. On the top of the paint layers, the artificial grime mixture was applied as described before. Cleaning tests were carried out using the three selected hydrogel formulations, and compared with the use of a classic humidified cotton-swab. Results are illustrated in figure 7.7. None of the hydrogel formulations led to color removal. The best

cleaning result was achieved with formulation ***H65***. Contrariwise, evident color traces were noted on cotton-swab after its use (see figure 7.7, right), due to the swelling and loss of adhesion of the paint layer favored by both free water and cotton-swab's mechanical action.

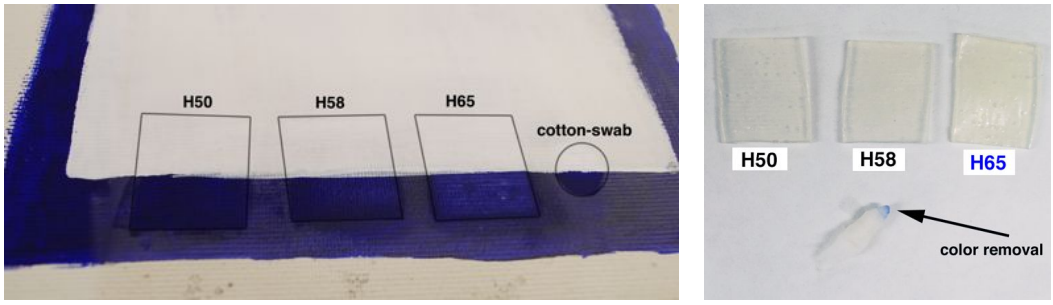

Figure 7.7. Cleaning tests on a canvas painted with modern tempera (acrylic/vinyl resins) and coated with artificial grime. Cleaning was performed with water-loaded SIPN hydrogels applied for 5 minutes. Cotton-swab wetted with water was used for comparison purpose.

7.4. Removal of hydrophobic materials

Hydrophobic materials are solubilized by organic solvents. The use of oil-in-water nanostructured fluids is preferred over neat solvents, for the reasons explained in chapters 1 and 3. Mock-ups were selected to evaluate the applicability of the SIPN hydrogels when combined with nanofluids. In this case, the hydrophobic materials are rather swelled than solubilized by the cleaning system, so mechanical action after hydrogel application is inevitable.

The use of an highly retentive system is extremely necessary to avoid the diffusion of the cleaning fluids into the pictorial layer, which could result in the swelling of the binder. Whereas the painting support is water-sensitive, it is, as well, important to restrict the water-based system penetration, to prevent mechanical competing forces that could lead to paint detachment or material damage. Therefore, SIPN hydrogels loaded with nanofluids were tested on different mock-ups to evaluate the retention capabilities, the cleaning control and the cleaning efficiency of the combined system.

7.4.1. From a canvas

The case study reported is a lining removal. A lining consists of a structural treatment where a new canvas is attached to the backside of the canvas support. Aging of linings leads to an accelerated degradation of the painting caused by acid formation due to molecular decay of the used adhesives, so lining removal is often necessary. Adhesives removal is very stressful for the painting because the use of pure solvents can transport the dissolved polymer into the canvas fibers and, in the worst cases, into the preparation layers. Moreover, canvas can easily absorb water-based systems, leading to the swelling of the hydrophilic layers of the painted artifact, which may lead to paint detachment.

The removal of aged adhesives from the back of canvas paintings can be done using oil-in-water nanofluids. However, in order to ensure a controlled cleaning process, the confinement of this cleaning tool inside hydrogels is important to minimize fibers swelling due to contact with the water phase. It is already reported in the literature that EAPC system (an ethyl acetate/propylene carbonate based oil-in-water nanofluid) can be effectively loaded inside acrylamide hydrogels and provide an efficient removal of lining adhesives.[3]

Figure 7.8. Application of EAPC-loaded ***H50*** hydrogel on the canvas glued with Plextol adhesive, which, after swelling, could be removed by gentle mechanical action (left and center); removal of Mowilith adhesive after application of EAPC-loaded ***H65*** hydrogel (right).

To evaluate the effectiveness of the EAPC-loaded SIPN hydrogels canvas mock-ups were prepared. Linen canvas samples were previously treated with two different polymers widely used in lining procedure, Mowilith DM5 (vinyl acetate/*n*-butyl acrylate copolymer) and Plextol B500 (ethyl acrylate/methyl methacrylate copolymer). To simulate the natural aging process samples were submitted to an

artificial aging as described in the literature.[4] The EAPC-loaded hydrogel was kept in contact with the canvas surface for 4h. In order to avoid excessive liquid evaporation, the hydrogel was covered with a plastic foil. A Whatman filter paper was placed on the backside of the canvas to verify the absence of dissolved polymer or solvent diffusing through the canvas.

The application of EAPC-loaded hydrogels ***H50*** and ***H65*** for the removal of aged adhesives is illustrated in figure 7.8. The artificially aged polymer adhesives, swollen after application of EAPC-loaded p(HEMA)/PVP hydrogels, are easily removed by gentle mechanical action. In figure 7.8 (center and right), the enhanced swelling of these adhesives, after contact with the nanofluid confined inside hydrogels, is clearly detectable. In addition, the Whatman filter paper placed on the backside of the canvas samples did not show traces of diffusing polymer on the backside of the canvas. This confirms the hydrogel's effectiveness in confining the cleaning action only at the interface. The ***H65*** hydrogel showed better efficacy in swelling both polymers making it the most appropriate confining tool for this kind of cleaning procedure under these circumstances. The required application time of 4h allows the swelling and the partial solubilization of the polymer by the nanofluid. In this case, shorter application times result in a non-complete swelling of the polymer leading to an inhomogeneous removal.

The cleaning results are highlighted by optical microscopy images given in figure 7.9. The adhesive removal obtained through the application of ***H50*** shows an incomplete cleaning action (figure 7.9, right), while the canvas cleaned with ***H65*** hydrogel presents a complete removal of the acrylic adhesive, without visible damage of canvas fibers (figure 7.9, center).

Figure 7.9. Optical microscopy images (x100 magnification) of the canvas with Plextol before (left) and after removal of the aged adhesive using EAPC system confined in ***H65*** (center) and ***H50*** (right) hydrogels.

7.4.2. From a resin-based panel painting

This example involves the cleaning of a real painting with no historic value, bought in a local antiquity market. It is an Icon (panel painting) with a representation of the Madonna and Child. An aged brownish resinous coating overlays the pictorial layer, which is constituted by a similar kind of resin. In other words, two different types of varnishes were used: one for binding the pigments and another one for the coating layer. The top varnish was darkened due to ageing, so it needed to be removed to improve the readability of the painting. In this case, the unwanted material is chemically similar to the painting binder so it is a good candidate to test the SIPN capability of performing a controlled layer-by-layer cleaning.

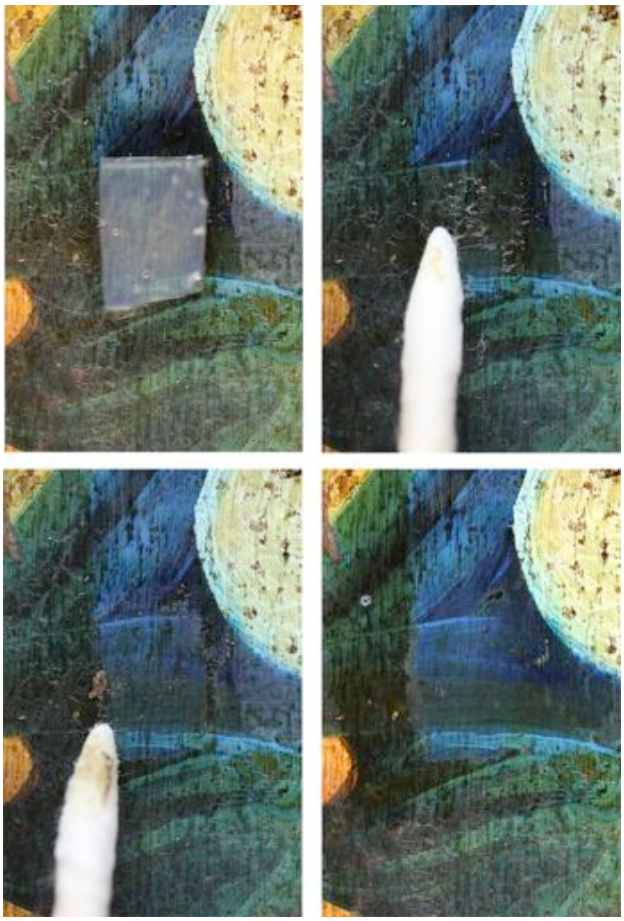

Figure 7.10. Detail of the cleaning process using a SIPN ***H58*** hydrogel loaded with the EAPC system (from top left to bottom right): after 1min of gel application the swollen varnish layer is gently removed with an humidified cotton swab.

Figure 7.11. Detail of the Icon (panel painting), before and after the cleaning tests, under Vis light (left, center). The UV fluorescence photograph (right) highlights the removal of the varnish.

Both ***H65*** and ***H58*** hydrogels loaded with nanofluids were tested, but the ***H58*** hydrogel proved to be the most suitable, owing to the particularly water-sensitive character of the artifacts that required highly retentive confining systems. The nanofluid used was the EAPC system, which gave the best results over other nanofluids. The cleaning procedure consisted in applying the hydrogel foil (0.5x1cm^2, thickness 2mm) for one minute, and then gently removing the swollen resin top layer with a slightly wet cotton swab (figure 7.10). In figure 7.11, the overall result of cleaning with EAPC-loaded ***H58*** gel is shown (under Vis and UV light).

Due to the similarity between top varnish and painting binder, a further examination of the gel cleaning efficiency was necessary by ATR-FTIR (figure 7.12). Natural varnishes commonly found as historic finishes of artworks include terpene-based resins (e.g. sandarac, mastic) and polyhydroxy acid-based resins (e.g. shellac), besides oils, waxes and polysaccharide gums[5]. One of the most characteristic IR peaks is the carbonyl stretching vibration, which ranges from 1695 to 1715cm^{-1} if the varnish is terpene-based, or from 1715 to 1722cm^{-1} for polyhydroxy acid-based varnishes[5]. The spectrum collected on the painting surface before the cleaning intervention shows a strong peak centered at 1716cm^{-1} (C=O str.), and absorptions at approximately 1650cm^{-1} (shoulder, C=C str.), 1461cm^{-1} (CH_2 bend.), 1382cm^{-1} (-C-H bend.), 1257cm^{-1} (C-O str., ester), 1165cm^{-1} (C-O str., acid), 1040cm^{-1} (C-O str., alcohol), 970cm^{-1} and 925cm^{-1} (=C-

H bend.), which suggest the presence of a polyhydroxy acid-based resin.[5] The spectrum of the painted surface after cleaning shows a peak at 1706cm^{-1} with a shoulder at ≈1735cm^{-1}, while the peak at 1716cm^{-1} is strongly decreased and no longer clearly observable (see inset in figure 7.12). The C=O stretching peak at 1706cm^{-1} and the absorptions at 1390, 1240, 1170 and 1041cm^{-1}, suggest the presence of a terpene-based resin.[5] The peaks at 874 and 712cm^{-1} are due to the presence of $CaCO_3$ (CO_3 asymmetric and symmetric deformation[6]), and the strong peak at 2090cm^{-1} (CN str.) is due to the Prussian blue pigment. This confirms that the top layer and the painted layer comprise different types of resins, and indicates that the use of the hydrogel allowed the gradual and controlled release of EAPC cleaning system, leading to the selective removal of the undesired top (brownish) resin layer without removing the binder in the painted layer.

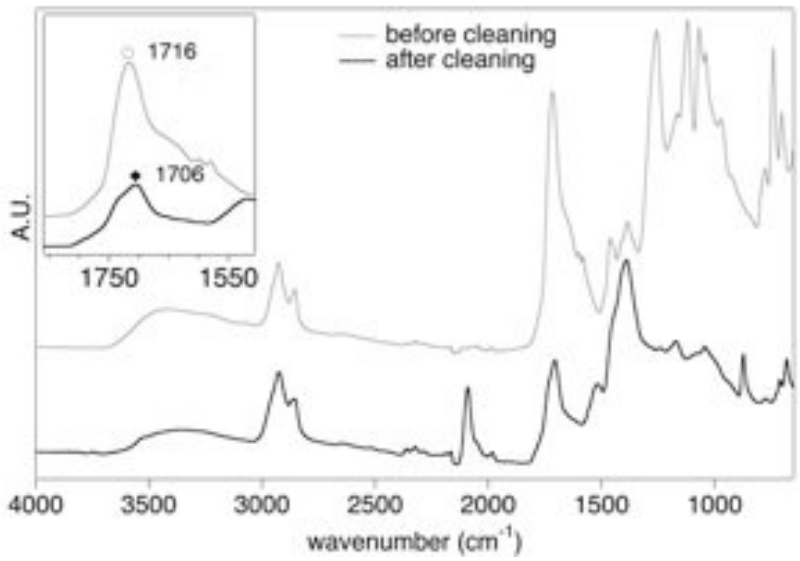

Figure 7.12. ATR-FTIR spectra of Icon (panel painting) surface before and after cleaning. The inset highlights the peaks assigned to the carbonyl stretching vibration of the undesired brownish varnish (1716cm^{-1}) and of the paint binder (1706cm^{-1}).

7.4.3. From a watercolor on paper

This example involves the removal of an aged varnish from a watercolor on paper. The controlled delivery of the cleaning fluid is necessary in order to remove the varnish without leaching of pigments of the watercolor painting or swelling the

paper fibers. It is therefore an optimal example of a critical conservation issue where the use of an highly retentive system is mandatory to avoid irreparable damage during cleaning. Therefore, nanofluid-loaded SIPN hydrogels were tested with the aim of removing the aged yellowish varnish without causing damage to paper fibers or watercolor's painting leaching. The application (1-2min) of the loaded hydrogels resulted in the swelling of the unwanted varnish layer that was then removed by gentle mechanical action using a slightly humidified cotton swab.

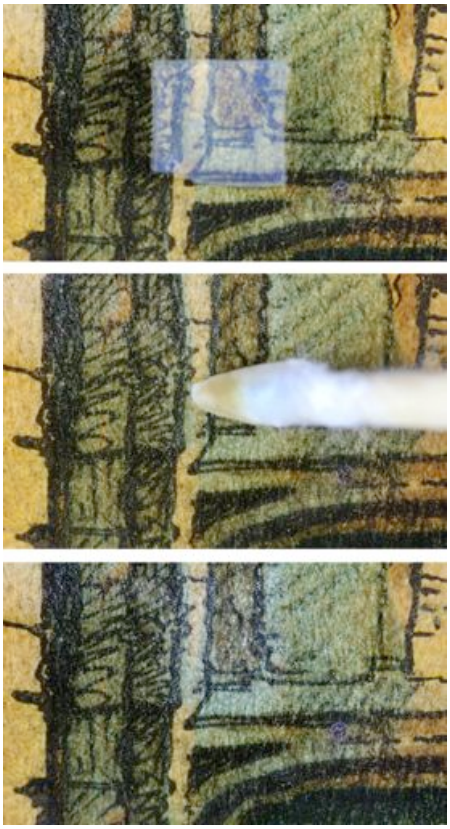

Figure 7.13. Detail of the cleaning process using a SIPN ***H58*** hydrogel loaded with the MEB system: after 2min of gel application the swollen varnish layer is gently removed with a slightly wet cotton swab. The final result (bottom) has been obtained after two successive gel applications.

MEB-loaded ***H58*** hydrogel was the system that provided the best results for the safe removal of the aged yellowed varnish. In this cleaning test it is fundamental to avoid the swelling of the water-sensitive paper fibers while

maintaining the advantages involved in the use of water-based nanofluids in terms of cleaning effectiveness and decreased eco-toxicological impact as compared to the traditional solvents used in the restoration practice.

Figure 7.14. Detail of a watercolor on paper, before (left) and after the cleaning tests (center). The UV fluorescence photograph (right) highlights the removal of the varnish.

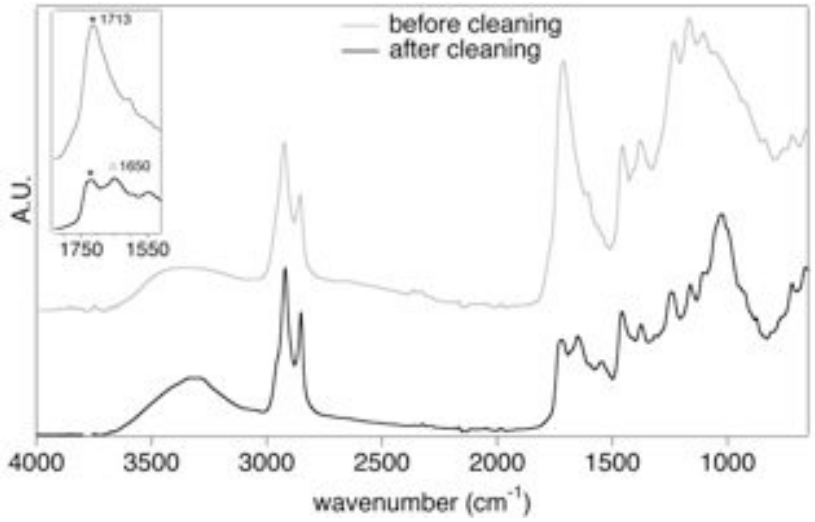

Figure 7.15. ATR-FTIR spectra of the watercolor on paper before and after the cleaning tests. The inset highlights the 1750-1550cm^{-1} region, with the absorptions of the varnish layer (1713cm^{-1}, C=O str.) and of the paper support (1650cm^{-1}, δ(OH) vibration of water absorbed in cellulose fibers).

The ***H58*** hydrogel foil (0.5x1cm^2, thickness of 2mm), loaded with MEB cleaning system, was applied on the artwork surface for two minutes. Then, the swollen and softened varnish was removed with a gentle mechanical action using a swab slightly embedded with the MEB system (see figures 7.13 and 7.14). Two short successive applications over the same area, rather than a single longer application, allowed a more gradual and controlled removal of the unwanted layer. It is important to remark that the mechanical action with the swab has to be minimal to avoid damage to the watercolor, the ink and the paper fibers. In this case the use of MEB-humidified instead of water-humidified cotton-swab was considered to be more efficient and more gentle, since the needed mechanical action was minimized.

ATR-FTIR was carried out on the artwork surface before and after the cleaning tests (figure 7.15). The spectrum collected of the varnish coating shows a strong peak centered at 1713cm^{-1} (C=O str.), and absorptions at approximately 1605cm^{-1} (C=C str.), 1453cm^{-1} (CH_2 bend.), 1376cm^{-1} (-C-H bend.), 1229cm^{-1} (C-O str., ester), 1167cm^{-1} (C-O str., acid), 1105cm^{-1} (C-O str., alcohol), and 926cm^{-1} (=C-H bend.), which suggest the presence of a natural resin, possibly polyhydroxy acid-based.[5] In the spectrum collected after the cleaning tests, the peaks of the varnish are strongly decreased, while the peaks of the cellulosic support (paper) are clearly observable at 1650cm^{-1} (δ(OH) vibration of absorbed water), 1242cm^{-1} (δ(C-OH) out-of-plane), 1160cm^{-1} (ν(C-C) asymm., ring breathing) and 1027cm^{-1} (ν(C-O) alcohol)[7]. This confirms that the coating varnish layer is removed after application of MEB-loaded ***H58*** hydrogel, which is an excellent result considering the undamaged paper's fibers and the unmodified painting.

7.5. Materials and methods

7.5.1. Gel residues and cleaning efficiency investigation

The presence of gel residues over the cleaned surface was checked with Attenuated Total Reflectance-Fourier Transform Infrared Spectroscopy (ATR-FTIR) on canvas or paper samples kept in contact with the hydrogel for 4h. The cleaning efficiency in removing hydrophobic layers was evaluated as well with ATR-FTIR. A Thermo Nicolet Nexus 870 FTIR spectrometer equipped with a Golden Gate diamond cell was used. Data were collected with an MCT detector with a sampling area of 150μm^2. The spectra were obtained from 128 scans with 4cm^{-1} of optical resolution.

7.5.2. Preparation of nanostructured fluids

The composition of the EAPC system (wt%) is deionized water, 73.3%; sodium dodecyl sulfate (SDS), 3.7%; 1-pentanol, 7%; ethyl acetate, 8%; propylene carbonate, 8%. The composition of the MEB system (wt%) is deionized water, 81.85%; dodecyl dimethyl amine oxide (DDAO), 6.15%; 2-butanone, 4%; ethyl acetate, 4%; butyl acetate, 4%. The components were added in solution following the given order. The hydrogels were loaded with nanofluid systems through immersion for at least 12h before the cleaning tests.

7.6. Bibliography

(1) Wolbers, R. The Use of a Synthetic Soiling Mixture as a Means for Evaluating the Efficacity of a Aqueous Cleaning Materials on Painted Surfaces. *Conserv.-Restaur. Biens Cult.* **1992**, *4*, 22–29.

(2) Jackson, D. P.; Jackson, J. A. *Tibetan Thangka Painting: Methods & Materials*, 2nd ed.; Serindia: London, 1988.

(3) Pizzorusso, G.; Fratini, E.; Eiblmeier, J.; Giorgi, R.; Chelazzi, D.; Chevalier, A.; Baglioni, P. Physicochemical Characterization of Acrylamide/Bisacrylamide Hydrogels and their Application for the Conservation of Easel Paintings. *Langmuir* **2012**, *28*, 3952–3961.

(4) Chevalier, A.; Chelazzi, D.; Baglioni, P.; Giorgi, R.; Carretti, E.; Stuke, M.; Menu, M.; Duchamp, R. Extraction d'adhésifs de rentoilage en peinture de chevalet: nouvelle approche. In *ICOM committee for conservation*, Proceedings of 15th Triennial Conference, New Delhi, India, Sept 22-26, 2008; Allied Publishers: New Delhi, 2008; Vol. II, pp 581–589.

(5) Derrick, M. Fourier Transform Infrared Spectral Analysis of Natural Resins Used in Furniture Finishes. *J Am Inst Conserv* **1989**, *28*, 43–56.

(6) Gunasekaran, S.; Anbalagan, G.; Pandi, S. Raman and Infrared Spectra of Carbonates of Calcite Structure. *J. Raman Spectrosc.* **2006**, *37*, 892–899.

(7) Garside, P.; Wyeth, P. Identification of Cellulosic Fibres by FTIR Spectroscopy: Thread and Single Fibre Analysis by Attenuated Total Reflectance. *Stud. Conserv.* **2003**, *48*, 269–275.

CHAPTER 8
Application of SIPN p(HEMA)/PVP Hydrogels: Two Important Case Studies

8.1. Introduction

Testing the developed new materials in real case studies is extremely important to check the impact that these materials might have in the conservation and restoration field. This is due to the fact that each painted artifact has its own degradation history, which is very far from what can be reproduced by mock-ups in laboratory. During this research project, there was the opportunity to test the SIPN hydrogel formulations on two important case studies with inherent complex conservation issues: the contemporary mural painting of *Giuseppe Capogrossi*, located at the ex-cinema Airone, Roma, Italy, and the Terrestrial Globe of *Vincenzo Coronelli*, property of the Angelo Mai Library, Bergamo, Italy.

Both case studies were ideal to test the highly retentive features of the developed system. In fact, in the first case the conservation issue was the removal of several overpainting layers of composition similar to the original underlying *Capogrossi*'s painting, which could be carried out only by a controlled layer-by-layer removal. In the second case, the water-sensitive nature of the paper support that constitutes the Terrestrial Globe makes any attempts of controlled cleaning, without affecting the original materials, a challenging task to perform. Furthermore, in this case-study, other than grime removal, there was also an aged adhesive to remove, which also gave the possibility to evaluate the applicative features of SIPN p(HEMA)/PVP hydrogels when loaded with nanostructured fluids.

8.2. Removal of overpaintings from Capogrossi *mural painting located at the ex-cinema Airone, Rome, Italy*

The overpainting issue in contemporary paintings is gaining attention among restorers and conservation scientists because they can potentially cause irreparable damage to the paintings. In fact, overpaintings are usually done using materials chemically similar to the original paint. Thus, painting retouching in this situation is completely irreversible, which in worst situations can dramatically reduce the work's value. One of the "black paintings" of *Ad Reinhardt* (1960-66) is a famous case where this problem was addressed in a systematic way by different professionals. The painting had been covered over time by various layers of overpainting. This fact led to the complete loss of painting's value, and the painting was donated to research. Various technologies were tested for the controlled removal of these layers, either by rather conventional methods, or by some innovative technologies (such as laser ablation). The conclusions of that research was that the available technologies did not provided satisfactory results.[1]

In the present case study, this conservation problem is once more considered, and efforts to apply an innovative technology with potential applicative features for the controlled removal of overpaintings are here described.

The contemporary work-of-art, here subject of study, is a ceiling mural painting of *Giuseppe Capogrossi*, completed in 1956-57, which is located at the entrance, on the top of the staircase (figure 8.1), of a former cinema (cinema "Airone"), in the city of Rome, in Italy. This ex-cinema was built around 1952-56, by the project of the architect *Libera*.[2] At some point, the cinema lost its function to a discotheque, which led to a complete renewal of the spaces, including the decoration. In fact, the mural painting of *Capogrossi* was completely covered with several layers of industrial paints (figure 8.1). Ever since this place has ceased to function as a discotheque, it has no longer been used and, consequently, the degradation has deteriorated, including the severe water infiltrations.

The project for the intervention on this mural painting started in 2011 and is part of a joint-collaboration with the restorers *Grazia De Cesare*, *Giulia Putaturo* and *Natalia Gurgone*, and two University research groups: the research group leaded by Prof. *Sgamellotti*, from the Chemistry Department of University of Perugia, Italy (CNR-ISTM), for the spectroscopic analysis of the painting layers; and the research group leaded by Prof. *Colombini*, from the Chemistry and Industrial Chemistry Department of University of Pisa (SCIBEC), Italy, for the analytical analysis of the paint components. The project was incentivized by the *Actors Center Roma*, a NPO cultural association that currently manages the space

of the ex-cinema Airone. The project aims the removal of the overpaintings and the retrieval of the original painting underneath.

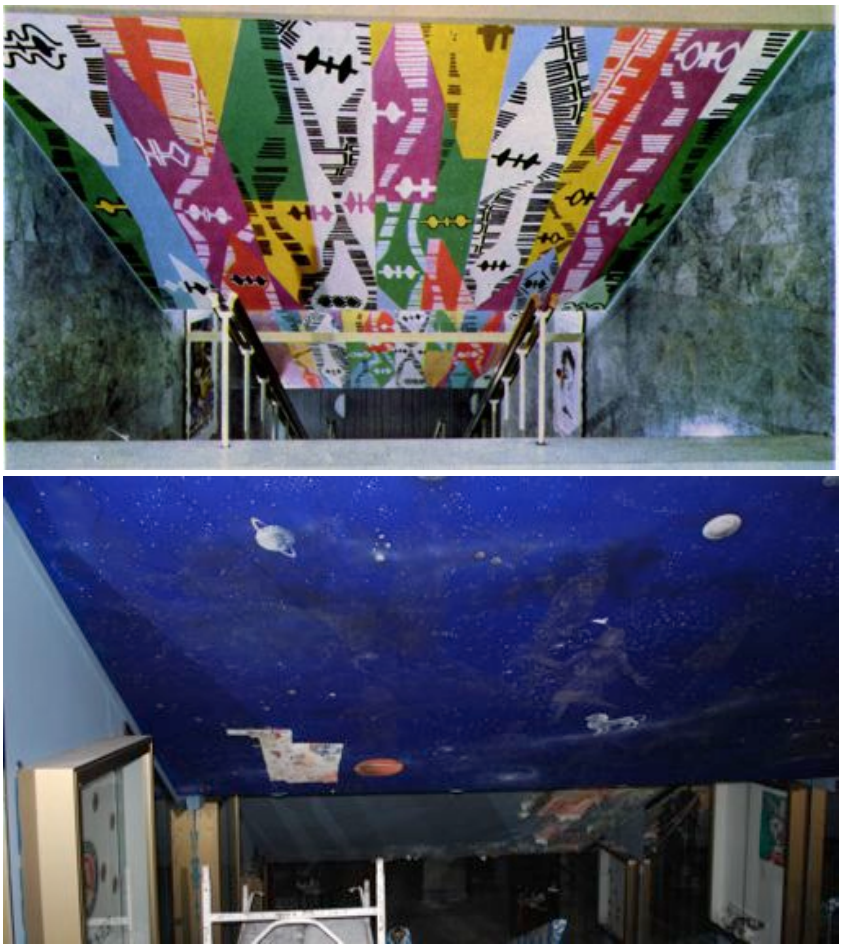

Figure 8.1. The original mural painting of *Capogrossi* painted in 1956-7 (top);[2] the actual condition of the painting (bottom).

8.2.1. Paint material characterization

In order to characterize the components of both overpaintings and original mural painting of *Capogrossi*, analysis were carried out in some samples. The techniques, used to characterize the main binder and pigment materials, were FTIR and Raman spectroscopies (CNR-ISTM, University of Perugia) and Pyrolysis Gas Chromatography Mass Spectrometry (Py-GC/MS) (SCIBEC, University of Pisa).

According to these analyses, all the paint layers (including the original) are constituted in different proportions by mixtures of these binder components:

- PVAc, with VeoVa® (plasticizer) resin;
- Styrene/*n*-butyl acrylate resin;
- Alkyd resin.

Figure 8.2. The water infiltration that caused the detachment of the complete section of overpainting paint film, revealing the original paint of *Capogrossi*. The detached paint fragments were used for the cleaning tests carried out in laboratory.

These results are in concordance with the use of low-cost industrial coatings for covering a large surface, such as this ceiling. The fact that all layers contain traces of all these paint materials is due to the fact that the applied films in liquid form allow the binder to penetrate in the already existent paint film, especially if they have been applied as solvent-borne paints. The different amount proportions indicate that the overpainting layers are based on a PVAc/styrene/*n*BA resin, while the original paint is constituted by an alkyd resin. From these results it becomes clear that the removal of the overpaintings becomes a serious issue, since overpainting and original paint materials have similar chemical nature.

8.2.2. Cleaning tests on fragment pieces

Fragments of the ceiling that have fell down due to water infiltration problems (see figure 8.2), were used to test the efficiency of the developed method for the

removal of hydrophobic layers, i.e. SIPN hydrogels loaded with nanofluids. For the following tests the ***H65*** hydrogel loaded with EAPC system was used to evaluate the controlled layer-by-layer removal of the overpaintings. The choice of the gel formulation is due to the rather rough surface of these samples. In fact, ***H65*** is the gel formulation that is able to combine an appropriate adhesion with suitable retention features for these particularly water-sensitive materials.

8.2.2.1. Description of the fragments

The fragments used for the cleaning trials constitute the complete stratigraphy of the overpaintings that cover the original *Capogrossi*'s mural painting. On the backside of the fragments there are traces of thin paint layers that are most probable from the original painting (for photos and a detailed description of these fragments see table 8.1). In the cross-section of one of the fragment samples (see figure 8.3) there are three major paint layer groups to consider, since they have a considerable thickness in order to be macroscopically distinguishable from the following cleaning tests.

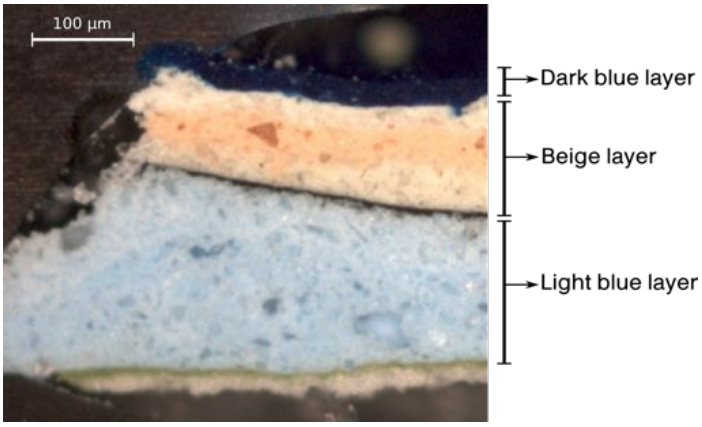

Figure 8.3. Cross-section observation under the microscope of **fragment #1** (with permissions of CNR-ISTM, University of Perugia).

Based on the analysis performed on the constitution of the different layers, the EAPC cleaning system was chosen for the controlled removal of these layers. Nanostructured fluids, as explained before, are the most viable cleaning tools over organic solvents, due to their proven effectiveness, while suppressing the negative factors associated with the use of pure organic solvents, such as the toxicity, and

non-control of the cleaning process. The EAPC system, as described formerly, is an extensively studied cleaning system and its efficiency in the removal of polymeric materials from different supports has been demonstrated.[3–5]

Table 8.1. Description of the mural painting's fragments, on which cleaning tests were performed.

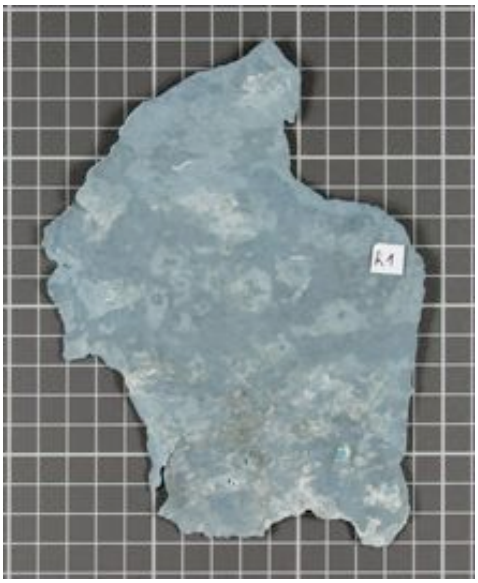

Front (newest layer of overpainting)

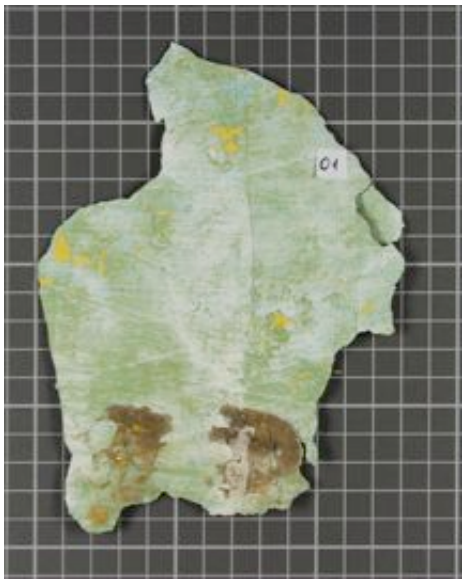

Back (possible oldest layer of overpainting)

Fragment #1
Maximum dimensions: 13x17cm^2
Description: Irregular and extremely rough surface. This sample was also used for the spectroscopic analyses (Perugia) and the analysis of Py-GC/MS (Pisa).

8.2.2.2. Cleaning trials

The cleaning tests were performed taking into account the time and number of applications on the same area. After each application of the gel, the surface of the swollen paint could be removed with a slightly humid cotton swab (humidified with deionized water).

The first cleaning trial was to verify the solubility of the layers using only the EAPC system in a cotton-swab. The first solubilized layer was the dark blue layer (from a macroscopic point of view, this layer appears first as grayish blue), which was removed very effortlessly. The beige layer is thicker and difficult to remove

due to the high pigment volume concentration. This paint layer characteristics implies a more aggressive mechanical action using the cotton-swab. The underlying paint layers, of light blue color, were easily removed.

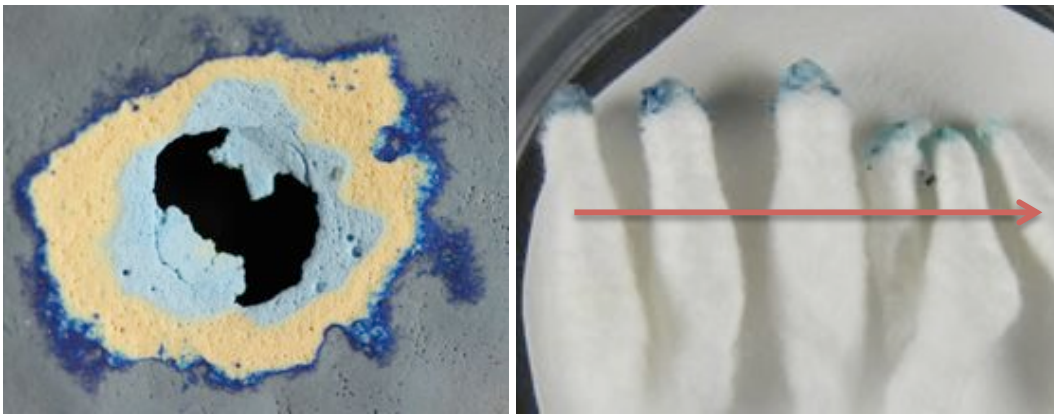

Figure 8.4. Cleaning trial over **fragment #1** with EAPC system in a cotton-swab.

It must be noted, however, that after reaching the beige paint layers, the free liquid system had already penetrated throughout the overpainting stratigraphy, reaching the backside of the fragment, with a visible broad spreading of the liquid. It was confirmed that all layers are solubilized or swelled using this cleaning system (see figure 8.4) and might be removed in a gradual manner when loaded inside retentive hydrogels.

The following removal tests were carried out using ***H65*** hydrogel loaded with the EAPC system, to evaluate the best time of application and number of applications over the same area. This cleaning test took place in a single area with the following trials (see figure 8.5):

1 - Removal of surface grime using water-swollen ***H65*** and cotton swab.
2 - 2 minutes of gel application loaded with the EAPC system.
3 - Application of further 5 minutes.
4 - Application of further 5 minutes.
5 - Application of further 10 minutes.
6 - Application of further 20 minutes.

Table 8.1. (cont.) Description of the mural painting's fragments, on which cleaning tests were performed.

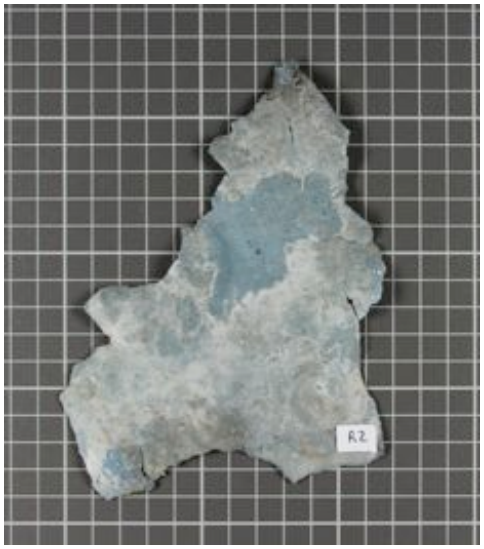

Front (newest layer of overpainting)

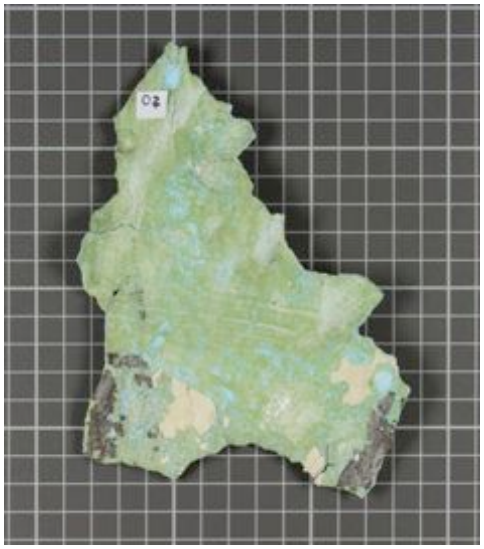

Back (possible oldest layer of overpainting)

Fragment #2

Maximum dimensions: 12x16cm^2

Description: Extremely irregular surface, with whitish spots due to infiltration complications.

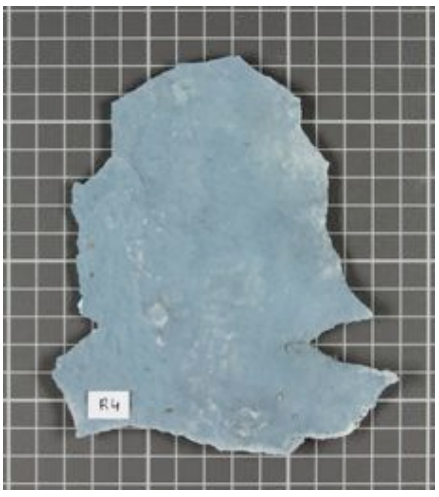

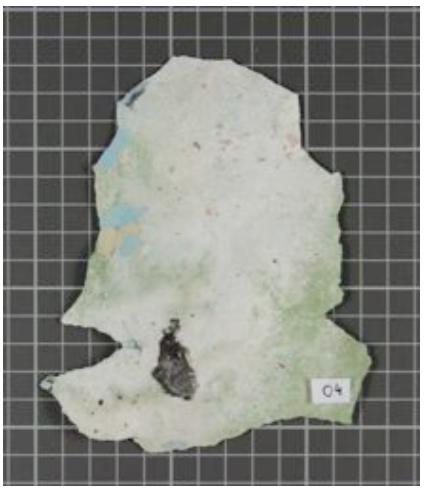

Fragment #4

Maximum dimensions: 12x14cm^2

Description: Rather homogeneous and regular surface.

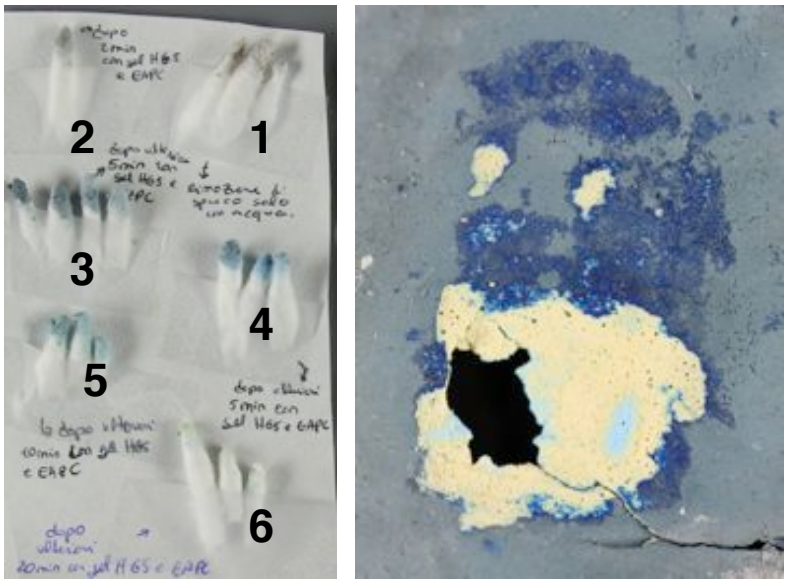

Figure 8.5. Cotton-swabs after each hydrogel application as described in the text (left) and **fragment #2** surface after the cleaning trials (right). The upper cleaning area of the fragment contains only the results of 1-3 cleaning trials.

This cleaning trial gave the best results with short application times (2-5min), combined with a high number of repeated applications. The comparison between the summed application time and a one-application of that same time highlights that the last is more aggressive, since it permits the penetration of more liquid (from 3-5 the removal was controlled, while test #6 was not controlled). With this trial it was also confirmed that paint layers are swollen rather than dissolved and absorbed within the gel, so the mechanical action using humidified cotton swab is required for the removal of the swollen paint layers.

The following cleaning trial was the best result in attaining a controlled and gradual removal of the paint layers of the fragment. The removal was carried out using this procedure (see figure 8.6 and 8.7):

1 - (A-E). Application of 2 minutes.
2 - (A-D). Application of further 2 minutes.
3 - (A-C). Application of further 5 minutes.
4 - (A-B). Application of further 5 minutes.
5 - (A). Application of further 5 minutes.
6 - (A). Application of further 10 minutes.

The conclusions from the cleaning trials carried out over the overpainting fragments were that shorter application times are preferred, in order to allow the nanofluid to wet the surface enough to swell only the first microns of painting layers; the successive use of the slightly humidified cotton swab allows the removal of the swollen material by mechanical action and the removal of nanofluid's residues off the surface.

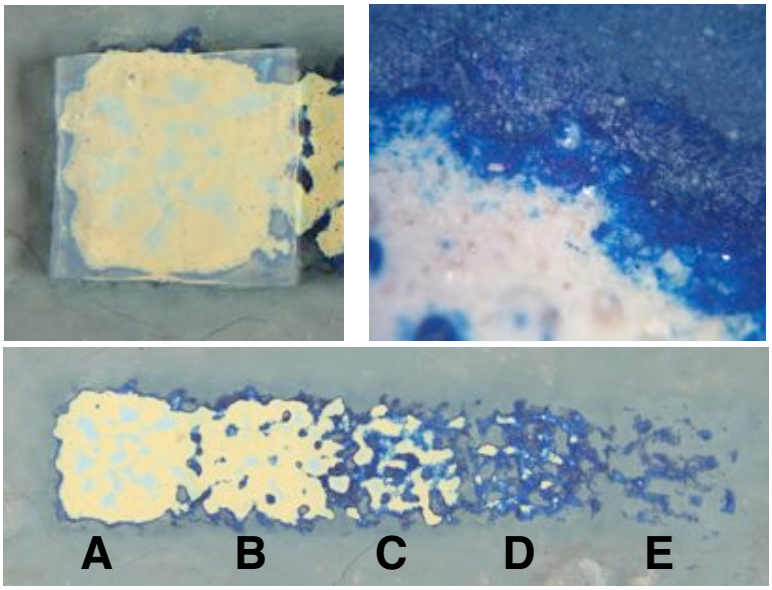

Figure 8.6. Cleaning trial with ***H65*** hydrogel and EAPC system over **fragment #4**, using various times of application and different numbers of applications. The hydrogel applied over the surface (top, left); the edge of gel contact observed under the microscope (top, right). The cleaning trials progress, as explained in the text (bottom).

8.2.3. Cleaning tests in situ

The cleaning tests performed *in situ* provided an important opportunity to test the possible limits of SIPN hydrogel application in downward position. The results were very encouraging since during the overall application time the hydrogels remained perfectly attached to the surface. Moreover, after a 20min application of ***H65*** hydrogel loaded with EAPC system it was possible to swell and remove the last overpainting layer and reveal the original painting of *Capogrossi* (figure 8.8).

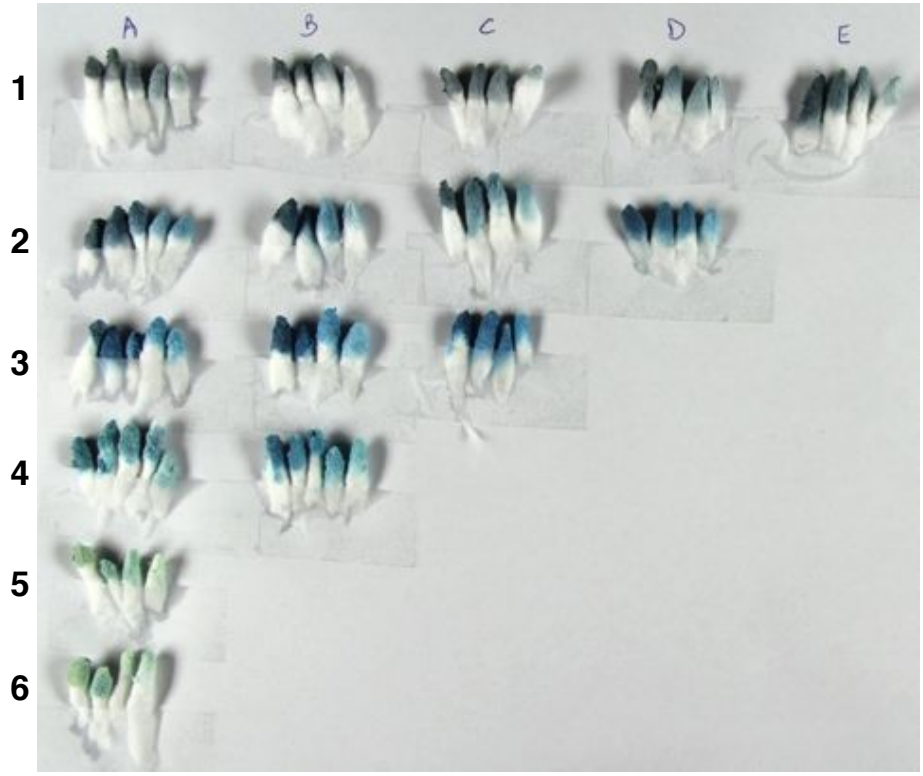

Figure 8.7. Cotton-swab after each hydrogel application as described in the text.

8.2.4.Considerations for further outcomes

With the combination of both cleaning results from the painting fragments and from the test performed *in situ*, in alliance with the paint material characterization, it is possible to propose a more performative intervention for the *in situ* removal of overpaintings from *Capogrossi* mural painting. It was considered appropriate to load EAPC within a highly retentive SIPN hydrogel, since the cleaning action revealed to be more controlled; the evaporation of the cleaning system was reduced; and the swelling of the painting's surface was minimized and reduced to the gel contact area. Hydrogel application time in the order of few minutes is preferred, because it allows a suitable amount of liquid diffusion from the hydrogel to the surface able to swell just some microns of polymeric layers, and thus perform a controlled layer-by-layer removal.

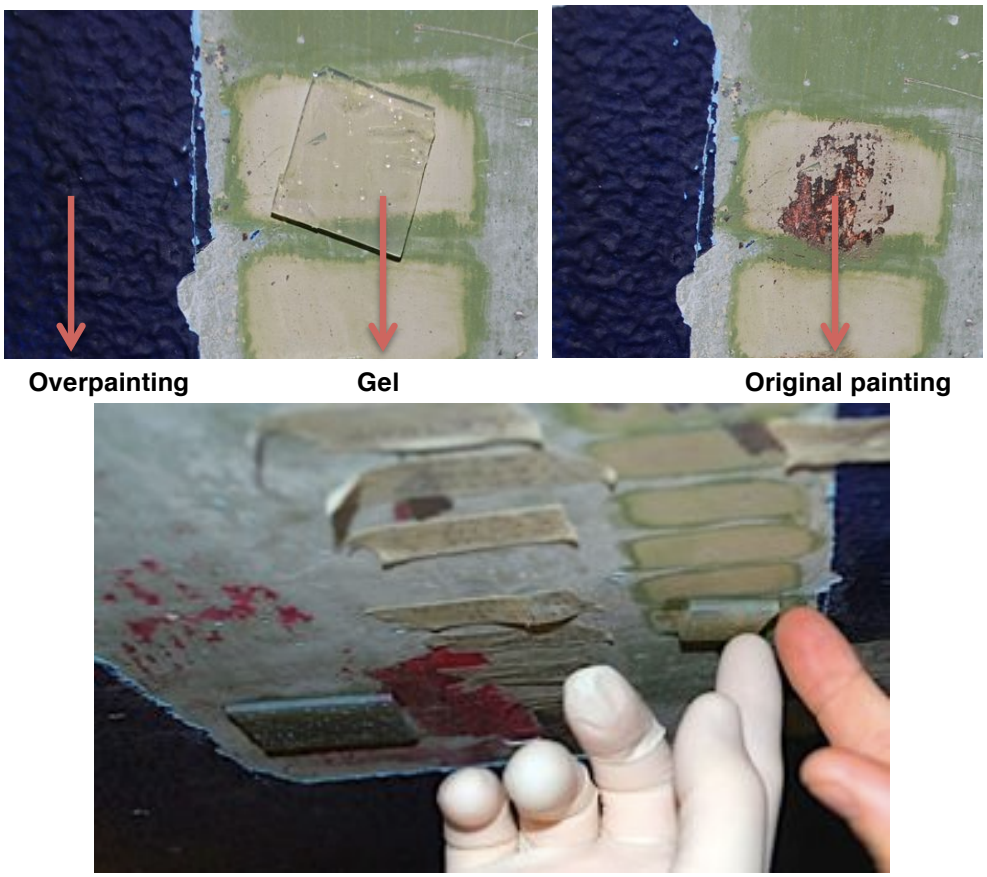

Figure 8.8. Cleaning tests carried out *in situ*. Application of 20min of ***H65*** gel loaded with EAPC system. After this time, a cotton-swab was used to remove the swollen overpainting layer. Hydrogels remained attached to the surface during the application time.

8.3. Removal of grime and an aged adhesive from a Coronelli*'s Terrestrial Globe, property of Angelo Mai Library, Bergamo, Italy*

The removal of unwanted hydrophilic and hydrophobic layers using water-based systems from a highly water-sensitive material such as paper, is a challenging conservation issue. More recently, a class of physical gels, known as "rigid gels", has been considered among restorers as an innovative new confining tool for the cleaning of water-sensitive materials.[6–8] They are polysaccharide-based gels (e.g. agar-agar and gellan gum), which are constituted by polymeric chains bounded by weak interactions. In water-swollen physical gels the competition of water-polymer with polymer-polymer interactions may reflect in the

decrease of hydrogel mechanical stability. Moreover, from a practical point of view, these characteristics can be responsible for an excessive wetting and for left gel residues on the painted surface.

Figure 8.9. The Terrestrial Globe of *Coronelli*, during the restoration intervention.

For these reasons, the present case study was an excellent opportunity to test the highly retentive features of SIPN hydrogels. The implementation of a new diffusion controlled method for the cleaning of conventional materials such as grime and aged adhesives from a paper-based artifact is here presented. The work-of-art, here subject of study, is a Terrestrial Globe made by *Vincenzo Coronelli*, an important Italian cartographer, which lived in the second half of the 17th century. This Terrestrial Globe, along with its "twin" Celestial Globe, is property of the Civic Library *Angelo Mai* in Bergamo, Italy. This artifact, with a

diameter of 107.5cm, is composed by 24 stripes of paper over a canvas covered wooden internal structure. The paper is mainly draw with black ink and painted with watercolors (see figure 8.9).

The collaboration for performing some cleaning tests on this Terrestrial Globe using nanotechnology methods initiated in 2012, thanks to the project *Bergamo! Save the Globes*, supported by both the FAI (Fondo Ambiente Italiano) delegation of Bergamo, and the Civic Library *Angelo Mai*. Cleaning tests were performed under the guidance of restorers *Lucia Dori*, *Andrea Dori*, *Maurizio Boni* and *Sergio Boni*.

Before the restoration intervention, this Terrestrial Globe showed two types of superficial unwanted layers, which altered significantly its appearance: a deposit of hydrophilic grime, mostly evident in the upper area of the globe; and glossy tick spots, related to the presence of an aged adhesive used in a previous restoration intervention. This last was considerably damaging the paper material.

Because of paper's highly water-sensitive nature, the use of water-based systems for the removal of water-soluble materials, such as grime, and hydrophobic layers, such as the adhesive employed (using nanostructured fluids), must be confined in an highly retentive container, able to provide a controlled release of the cleaning agent. Furthermore, the removal of water-soluble materials using conventional methods implies the mechanical action of a cotton-swab, which can severely damage the paper fibers. For these reasons the cleaning tests were performed using SIPN hydrogels, which do not foresee any mechanical action in the case of grime removal.

8.3.1. Characterization of the aged adhesive

ATR-FTIR analyzes were carried out to individuate the nature of the aged adhesive. The obtained spectrum is presented in figure 8.10, which confirmed the presence of a poly(vinyl acetate)-based adhesive, by the presence of intense peaks related to the stretching vibrations of the carbonyl group at 1736cm^{-1} and of the C–O, from the acetate group, at 1239cm^{-1}.

8.3.2. Cleaning tests in situ

All the three selected SIPN hydrogel formulations (***H50***, ***H58*** and ***H65***) were tested over the Globe's surface for the grime removal trial. The water-swollen systems were tested over a drawing-free area to evaluate the efficiency related to the varying of application time and to the number of applications, in order to assess the best operating conditions (figure 8.11, top). The most satisfactory

result obtained from this trial was the use of ***H58*** hydrogel combined to a short application time (≈2min), which can be eventually repeated over the same area.

To confirm the retention characteristics of this hydrogel, the same application procedure was repeated over an area containing both black ink and red watercolor. After 2min of the water-swollen ***H58*** application, the area was cleaned and the drawing remained undamaged (see figure 8.11, bottom).

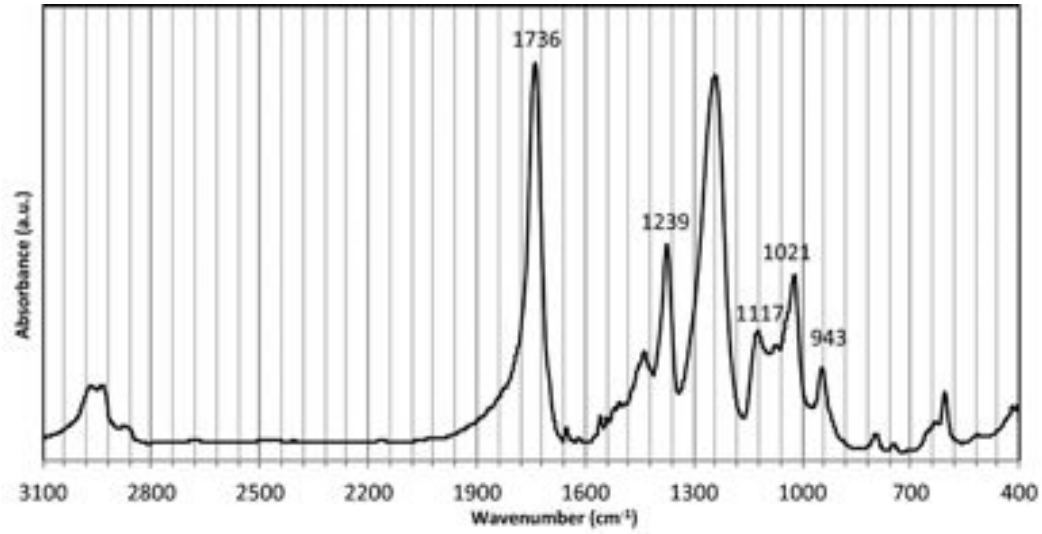

Figure 8.10. ATR-FTIR spectrum of the aged adhesive from the Terrestrial Globe, which is present in the joint of two paper stripes. The stretching vibrations of C=O at 1736cm^{-1} and of C–O of the acetate group at 1239cm^{-1} identifies the vinyl acetate nature of the adhesive used in the course of a previous restoration.

The removal of an PVAc based polymer can be carried out through the use of nanostructured fluids and, in particular the EAPC system showed to be an efficient cleaning agent for the removal of this class of materials.[9] A cleaning test was performed to evaluate the efficiency of the combined system of ***H58*** SIPN hydrogel loaded with the EAPC system, for the removal of the aged varnish. Once again the best cleaning result was obtained with ***H58*** hydrogel applied for 2min. One single application of the EAPC-loaded hydrogel was enough to induce the needed swelling of the polymer, for its removal with a slightly humidified cotton-swab. The results of this cleaning procedure are shown in figure 8.12.

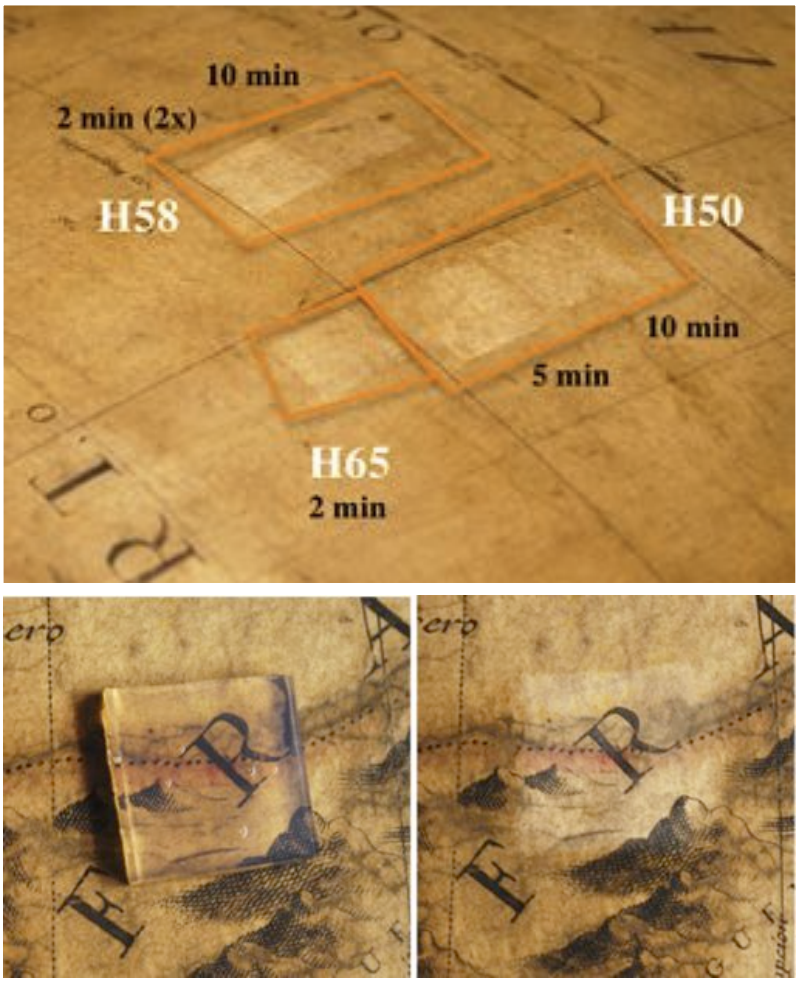

Figure 8.11. Cleaning test for grime removal, using the three water-swollen SIPN hydrogel formulations: ***H50***, ***H58*** and ***H65***, and evaluation of application times (top). Application of ***H58*** hydrogel over an area with black and red inks, to test the retention features of the method (bottom).

8.3.3. Conclusions

The results obtained from the cleaning tests carried out in this case study are an excellent example of how colloid and materials' science may significantly contribute to extend the range of possible solutions for a specific conservation issue. In this case, SIPN hydrogels have contributed with an efficient and controlled cleaning of the undesirable materials (grime and aged adhesive). Furthermore, SIPN hydrogels are chemical gels, which means that they are high cohesive systems, so gel residues over the surface are completely avoided after a

cleaning treatment. The fact that SIPN hydrogels can be loaded with different cleaning agents makes them very versatile systems, suitable for many types of interventions in the cleaning of Cultural Heritage artifacts.

Figure 8.11. Removal of an aged Vinavil adhesive from the paper surface, in the joint of two paper pieces. ***H58*** loaded with EAPC system was used (2min single application). The cleaned area can be easily identified because is less glossy of the surrounding area (top). From left to right: before, during and after gel application (bottom).

8.4. Bibliography

(1) The AXA Reinhardt Project. http://www.guggenheim.org/new-york/collections/conservation/conservation-projects/axa-reinhardt (accessed Dec 9, 2014).

(2) De Cesare, G.; Gurgone, N.; Putaturo, G.; Miliani, C.; Rosi, F. Murals and Architecture: the Case of Capogrossi in Rome. In *Conference of Modern and Contemporary Mural Paintings: Technique, Value and Conservation*, 4-5 May, 2012; Universidad Politécnica de Valencia.

(3) Giorgi, R.; Baglioni, M.; Berti, D.; Baglioni, P. New Methodologies for the Conservation of Cultural Heritage: Micellar Solutions, Microemulsions, and Hydroxide Nanoparticles. *Acc. Chem. Res.* **2010**, *43*, 695–704.

(4) Baglioni, P.; Chelazzi, D.; Giorgi, R.; Poggi, G. Colloid and Materials Science for the Conservation of Cultural Heritage: Cleaning, Consolidation, and Deacidification. *Langmuir* **2013**, *29*, 5110–5122.

(5) Baglioni, P.; Berti, D.; Bonini, M.; Carretti, E.; Dei, L.; Fratini, E.; Giorgi, R. Micelle, Microemulsions, and Gels for the Conservation of Cultural Heritage. *Adv. Colloid Interface Sci.* **2014**, *205*, 361–371.

(6) Campani, E.; Casoli, A.; Cremonesi, P.; Saccani, I.; Signorini, E. *Quaderni del Cesmar7: L'Uso di Agarosio e Agar per la Preparazione di "Gel Rigidi" – Use of Agarose and Agar for Preparing "Rigid Gels,"* n°4; Il Prato: Padua, 2007.

(7) Mazzuca, C.; Micheli, L.; Cervelli, E.; Basoli, F.; Cencetti, C.; Coviello, T.; Iannuccelli, S.; Sotgiu, S.; Palleschi, A. Cleaning of Paper Artworks: Development of an Efficient Gel-Based Material Able to Remove Starch Paste. *ACS Appl. Mater. Interfaces* **2014**, *6*, 16519–16528.

(8) Micheli, L.; Mazzuca, C.; Cervelli, E.; Palleschi, A. New Strategy for the Cleaning of Paper Artworks: A Smart Combination of Gels and Biosensors. *Adv. Chem.* **2014**, *2014*, 1–10.

(9) Baglioni, M.; Giorgi, R.; Berti, D.; Baglioni, P. Smart Cleaning of Cultural Heritage: a New Challenge for Soft Nanoscience. *Nanoscale* **2012**, *4*, 42.

CONCLUSIONS

CONCLUSIONS

This dissertation presents the synthesis and characterization of highly retentive SIPN hydrogels, specifically developed for applications in art conservation. SIPN hydrogels were prepared by free radical polymerization of HEMA monomer in the presence of linear PVP, which remains embedded into the hydrogel network. It has been shown that by varying the SIPN composition (water, PVP, HEMA and MBAm quantities) it is possible to tune the hydrogels characteristics, which are directly related to the desirable application features, i.e. retention/release balance, softness, transparency, and elasticity. The preliminary assessment carried out on SIPN hydrogels (reported in chapter 5) has shown that these polymeric networks have most of the desired properties to achieve a high-controlled cleaning action, that is, the appropriate equilibrium between release and retention properties. These features allow a real confinement of the cleaning system, and thus permit to use water-based systems also on water-sensitive substrates. The direct comparison with polysaccharide-based hydrogels has highlighted that by using SIPN hydrogels it is possible to obtain an enhanced control of the liquid medium penetration and to limit the interaction between cleaning system and artifact surface.

The physicochemical characterization of the selected SIPN formulations, presented in chapter 6, was fundamental to study each gel characteristic related to the required application features. The SIPN chemical composition was assessed by the gel content parameter and by pHEMA/PVP ratios obtained from ATR-FTIR spectra. It has been observed that the initially added PVP in SIPN composition is not completely embedded in the hydrogel network. However, the function of PVP is not only to provide high hydrophilicity to the hydrogel, through its interpenetration, but also during the polymerization reaction, where its hydrophilic chains increase the water affinity, and therefore increase the water content of the reaction mixture. Added volumes of water fraction and non-embedded PVP lead to an higher porosity and, thus, to an higher EWC.

The interaction with the liquid fraction of the gel was evaluated with hydration/rehydration cycles, which shown that the liquid diffusion follows a diffusion controlled mechanism (Fickian diffusion). Thermoanalysis permitted to

investigate the water inside swollen hydrogels and to classify it as unfreezable, bound-freezable, and free water, depending on the extent of interactions with the polar part of the polymer chains. This was carried out through the calculation of Free Water Index and Freeze-Bound Water Index. The results show that more than ≈70wt% of the water content acts as bulk water, thus participating in the cleaning procedure.

The capacity of SIPNs of loading organic solvents and nanofluids was also evaluated. In particular, SIPN hydrogels are able to load high amounts of two selected nanofluids (EAPC and MEB systems) that have improved detergency capacity towards polymers used in restoration (e.g. adhesives, varnishes, consolidants).

The mechanical features of SIPN hydrogels were evaluated through rheological measurements. All SIPN formulations show gel-like-behavior, which means that they can be applied over a surface and maintain its form, or in vertical position without showing flowing behavior for a long time. Moreover, the influence on the hydrogel's mechanical features regarding the increasing of the MBAm and HEMA amounts in the composition was exanimated. The increasing of both components reflects in an increase of the hydrogel elasticity. The SIPN formulation without cross-linker produces a gel, having solid-like behavior, which is possibly due to the inter-entanglements of long chains of HEMA. The addition of PVP into the composition reflects in decreasing of elasticity, which is related to an increasing of flexibility. It was observed that small amounts of HEMA (down to ≈3wt%) produces as well cross-linked polymer structures with gel-like behavior, which is probably due to the additional hydrogen bonds between HEMA and PVP. A power law was observed with increasing in polymer concentration, which seems to follow the percolation model for the gelation process. The mechanical features of water-loaded and nanofluid-loaded hydrogels were as well compared and no significant change in the elasticity of the SIPNs were observed, even when loaded with two completely different nanofluids (EAPC and MEB systems), which means that these hydrogels act as real nanocontainers.

The hydrogel's microporosity was observed using a FEG-SEM, which allowed graphing a pore size distribution for the selected hydrogels. From the less hydrophilic (***H50***) to the more hydrophilic (***H65***) selected SIPN formulations an increase of the pore size dimension is observed, as expected. Moreover, ***H50*** displays a narrow pore size distribution, which is related to a relatively high homogeneity, reflecting in the homogenous loading of cleaning systems.

Hydrogel's network was investigated with SAXS, accounting for average mesh size and inhomogeneities domains. A comparison with a pHEMA homopolymer

hydrogels was carried out, for accounting the influence of PVP in the SIPN structure. It was observed and confirmed in the literature that the mesh size increases with the increase of the EWC. Moreover, the increased distance between topological sites is as well, related to the decrease in the HEMA/PVP ratio in the reaction mixture, which means that the higher amounts of PVP, with respect to HEMA monomer, act as obstacles for the cross-links formation during polymerization, thus, distancing them, which reflects in the increase of the correlation length. Contrariwise, the pHEMA homopolymer, being poorer in water content (thermodynamically limited up to ≈40wt%) show a considerably smaller mesh size with respect to the selected SIPNs.

It was important to compare water-loaded with nanofluid-loaded hydrogels using SAXS measurements accounting for possible changes in the gel's network and/or in the nanostructured fluid system, when they are combined in the same system. For this purpose the EAPC and MEB systems were considered. The first considerable result is that no difference is observed between different SIPN compositions. This means that, from a practical point of view, no matter the hydrogel formulation used, the nanofluid detergency behavior remains invariant. For both EAPC and MEB-loaded hydrogels it was observed that the micelle size decreases in size when loaded inside SIPNs, which may be explained by the fact that upon loading of the nanofluid into the gel, a certain amount of the oil fraction and some surfactant molecules constituting the micelles, leave the aggregates attracted by the pHEMA/PVP polymeric network. Furthermore, for what concerns the EAPC-loaded hydrogel, a slight decrease of the micelle shell thickness was observed, which could be due to the presence of the polymer network moieties or PVP end chains between the polar heads in the micelles, which reorganization could lead the inclusion of more water molecules into the shell. On the other hand, the EAPC-loaded hydrogel shows an increase in the inhomogeneity domains, which ulterior confirms the interaction of the micelles with the polymer branched sites. This can result in the formation of agglomerates near the more compact zones of the polymeric network, thus, increasing the hydrogel inhomogeneity domains. As for the MEB-loaded hydrogel, a substantial increase of the micelle core polydispersity was observed, while the hydrogel shown a decrease in the inhomogeneity domains. This could be explained by the observed values of ESC for the MEB and DDAO-loaded hydrogels, which are substantially higher compared with the water and the EAPC-loaded hydrogels. This means that the higher swelling degree in the MEB-loaded hydrogel is responsible for the expansion of the more compact regions in the polymeric network, leading, thus, to a decrease in the inhomogeneity domains.

Cleaning tests performed on mock-ups and on old paintings with no artistic or historic value, shown in chapter 7, were relevant to qualitatively evaluate the benefits and assets, as well as the limits of the application procedure. The gel residue-free feature, characteristic of chemical gels, was confirmed by ATR-FTIR. The cleaning tests were divided by the nature of the material to remove, because it was governed by the cleaning system used: water for the hydrophilic materials and nanofluids for the hydrophobic materials, thus, using on all situations water-based system. The SIPN hydrogels possess suitable water release and retention properties for a controlled and efficient cleaning of water-sensitive artifacts or whereas the cleaning requires a layer-by-layer removal, due to the similarity of the materials constituting the painting layers. Moreover, due to the fact that the hydrogel's mechanical properties and the water retention/release features can be tailored for the required characteristics to address specific conservation issues by changing gels composition, it was possible to choose for each case the most suitable SIPN formulation. This straightforward versatility makes these new polymeric hydrogels the up-to-date most advanced systems for the cleaning of water-sensitive artifacts. The efficient combination of hydrogels and cleaning systems confined into the chemical gel network is a step forward in the conservation of Cultural Heritage and could be potentially applicable to different case studies.

The possibility to test the application features of the selected SIPN hydrogels on real case studies was extremely important to evaluate the real impact that these cleaning system can have in the restoration practice. In particular, the case study of the mural painting of the contemporary artist *Capogrossi*, was extremely challenging, since it required the removal of painted layers (overpaintings) chemically similar to the original painting. This case study highlighted the SIPNs highly retentive capacity, which provides with the possibility of performing a controlled layer-by-layer removal using the EAPC nanofluid for the detergency process. On the other hand, the case study of the Terrestrial Globe of *Vicenzo Coronelli* was an optimal example of a water-sensitive artifact that requires gentle methods using water-based cleaning tools for the removal of hydrophilic grime and an aged adhesive. In this case, SIPN hydrogels showed the possibility of removing these unwanted materials in a controlled process, and, at the same time, reducing drastically the need of mechanical action with a cotton-swab, used in conventional restoration practice.

Acknowledgements

I would like to extend my gratitude first and foremost to my thesis advisor Piero Baglioni for mentoring me over the course of my graduate studies. His insight led to the original proposal of developing a highly retentive tool based on chemical gels. He provided me with support over the course of the research project and the writing of the dissertation and for that I sincerely thank him for his confidence. I would additionally like to thank Rodorico Giorgi for his support during the course of this research. His expertize and understanding of the materials for the conservation of Cultural Heritage has allowed me to fully express the concepts in this dissertation.

The research included in this dissertation would not have been possible if not for the assistance, patience, and support of many colleagues. In particular, my colleagues of the CSGI group have contributed immensely to my personal and professional experience. Moreover, the CSGI group has been a source of friendships as well as good advices and collaborations. There are some individuals that have collaborated with me actively and that helped me to attain my research goals, to whom I would like to express my sincere thanks: Emiliano Fratini, for the SAXS experiments, for the helpful advices in the hydrogel synthesis and for reading and rectifying the results chapter of this dissertation; Emiliano Carretti, for the rheological experiments, for introducing me to the fascinating rheology world and for the endless constructive discussions about rheological data; Nicola Toccafondi, for assisting me with my laptop issues, for teaching me how to use Igor Pro and for many other stimulating debates; Giovanna Poggi, for the endless advices and interesting discussions, for having me involved in the case study of Coronelli and for the help in the synthesis and packaging of high quantities of hydrogels; Michele Baglioni, for the collaboration for the preparation of nanofluids, for the assistance during some of the cleaning trials and for reading and controlling the SAXS results related to nanofluids in this dissertation; David Chelazzi, for assisting me in the cleaning trials and in the evaluation of the cleaning efficiency with ATR-FTIR; Giacomo Pizzorusso for conveying to me his know-how on chemical gels synthesis and characterization; Francesca Ridi, for the support during Themoanalysis measurements; Marcia Arroyo for the laboratory assistance in the initial period and Yareli Jaidar for helping me in the preparation of some of the mock-ups.

I would particularly like to express my gratitude to my “gel girls”: Nicole Bonelli for her true friendship and for the endless inspirational discussions that not only

made me grow, but also enriched my work; and Erica Parisi, for the important exchange of advices and for bringing me immense joy in the free time.

In regards to the application of the developed SIPN hydrogels and to the preparation of several mock-ups for the cleaning trials, I would like to thank: Aurélia Chevalier, Florence Gorel, Morgane Martin and Maria Castañeda Delgato.

Furthermore, I would like to acknowledge the professional restorers that made the cleaning tests on real case studies possible: Grazia De Cesare, Giulia Putaturo and Natalia Gurgone for the Capogrossi mural painting and Lucia Dori, Andrea Dori, Maurizio Boni and Sergio Boni for the Coronelli's Terrestrial Globe.

The case study of Capogrossi was incentivized by the Actors Center Roma, and in particular by Roberto Zibetti, to whom I acknowledge for this opportunity.

The work done on the Terrestrial Globe would have not been possible without the financial support of Fondo Ambiente Italiano (FAI), delegation of Bergamo and of the Civic Library Angelo Mai of Bergamo. In particular, I would like to thank Lucia Pacati Patt (head of the FAI Bergamo delegation), Riccardo Fogaroli (head of the FAI youth delegation) and Maria Elisabetta Manca (director of the Bergamo Civic Library)

I also would like to express my gratitude to who encouraged me to initiate this pathway 4 years ago: my former professors Antonio Sgamellotti, Bruno Brunetti and Costanza Miliani, and my friend and former colleague Vanessa Otero.

I gratefully acknowledge the funding source that made my Ph.D. work possible. I was funded by the Fundação para a Ciência e a Tecnologia (FCT) grant for my 4 years of doctoral program (SFRH/BD/73817/2010).

From a personal aspect, I would also like to thank my family for their endless love and support in all my pursuits and my friends for the cheerful moments.

Finally, I would like to thank Giuseppe, whose faithful support during the final stages of this Ph.D. is so appreciated, for both keeping me peaceful and helping me putting the pieces together. Thank you.

Joana Domingues
University of Florence
December 2014

ANNEX

List of Publications

Domingues, J. A. L., Bonelli, N., Giorgi, R., Fratini, E., Gorel, F., Baglioni, P., Innovative Hydrogels Based on Semi-Interpenetrating p(HEMA)/PVP Networks for the Cleaning of Water-Sensitive Cultural Heritage Artifacts, *Langmuir*, **29 (8)**, 2013, pp. 2746-2755.

Giorgi, R., Domingues, J. A. L., Bonelli, N., Baglioni, P., Semi-Interpenetrating p(HEMA)/PVP Hydrogels for the Cleaning of Water-Sensitive Painted Artifacts: Assessment on Release and Retention Properties. In *Science and Technology for the Conservation of Cultural Heritage*, Proceedings of the International Congress on Science and Technology for the conservation of Cultural Heritage, Santiago de Compostela, Spain, October 2-5, 2012; Rogerio-Candelera, M. A.; Lazzari, M.; Cano, E., Eds.; CRC Press: Boca Raton, FL, 2013; pp. 291-294.

Domingues, J., Bonelli, N., Giorgi, R., Fratini, E., Baglioni, P., Innovative Method for the Cleaning of Water-Sensitive Artifacts: Synthesis and Application of Highly Retentive Chemical Hydrogels, *International Journal of Conservation Science*, **4**, 2013, pp. 715-722.

Domingues, J., Bonelli, N., Giorgi, R., Baglioni, P., Chemical Semi-IPN Hydrogels for the Removal of Adhesives from Canvas Paintings, *Applied Physics A*, **114 (3)**, 2014, pp.705-710.

Poggi, G., Domingues, J. Bonelli, N., Giorgi, R., Baglioni, P., Nanomateriali Innovativi per la Conservazione dei Beni Culturali. Idrogel ad Alta ritenzione per la Pulitura di Opere d'Arte: l'Intervento sul Globo Terrestre della Biblioteca Civica Angelo Mai di Bergamo, *Bergomum* 2013, Bollettino della Civica Biblioteca Angelo Mai di Bergamo. 2014.

Domingues, J., Carretti, E., Baglioni, M., Fratini, E., Chelazzi, D., Giorgi, R., Baglioni, P. Removal of Varnishes from Old Paintings using Nanofluids Confined in SIPN p(HEMA)/PVP hydrogels. Paper in preparation.

Langmuir

Article

pubs.acs.org/Langmuir

Innovative Hydrogels Based on Semi-Interpenetrating p(HEMA)/PVP Networks for the Cleaning of Water-Sensitive Cultural Heritage Artifacts

Joana A. L. Domingues,[†] Nicole Bonelli,[†] Rodorico Giorgi,[†] Emiliano Fratini,[†] Florence Gorel,[†,‡] and Piero Baglioni*[,†]

[†]Department of Chemistry "Ugo Schiff" and CSGI, University of Florence, Via della Lastruccia 3−50019 Sesto Fiorentino, Florence, Italy

[‡]Florence Gorel, Restauratice du patrimoine, 21, rue E. Goudchaux−57000 Metz, France

Supporting Information

ABSTRACT: Water-based detergent systems offer several advantages, over organic solvents, for the cleaning of cultural heritage artifacts in terms of selectivity and gentle removal of grime materials or aged varnish, which are known to alter the readability of the painting. Unfortunately, easel paintings present specific characteristics that make the usage of water-based systems invasive. The interaction of water with wood or canvas support favors mechanical stresses between the substrate and the paint layers leading to the detachment of the pictorial layer. In order to avoid painting loss and to ensure a fine control (layer by layer) of grime removal, water-based cleaning systems have been confined into innovative chemical hydrogels, specifically designed for cleaning water-sensitive cultural heritage artifacts. The synthesized hydrogels are based on semi-interpenetrating chemical poly(2-hydroxyethyl methacrylate)/poly(vinylpyrrolidone) networks with suitable hydrophilicity, water retention properties, and required mechanical strength to avoid residues after the cleaning treatment. Three different compositions were selected. Water retention and release properties have been studied by quantifying the amount of free and bound water (from differential scanning calorimetry); mesoporosity was obtained from scanning electron microscopy; microstructure from small angle X-ray scattering. To demonstrate both the efficiency and versatility of the selected hydrogels in confining and modulating the properties of cleaning systems, a representative case study is presented.

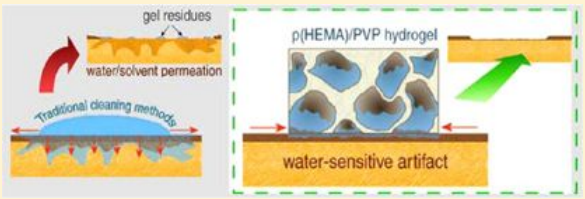

INTRODUCTION

Cleaning of cultural heritage artifacts represents one of the most delicate operations of restoration because it is potentially invasive and aggressive for the original materials as well as completely irreversible. The list of undesired materials to be removed from artifacts surface can include a wide group of substances: from deposits of pollutants and grime due to natural aging process, to aged and darkened varnish coatings. One of the most important issues for conservators and conservation scientists is the removal of materials that do not belong to the artwork, without affecting the original ones. In other words, high performing cleaning systems must be able to ensure a controlled and selective cleaning action.

In traditional conservation procedures, the removal of undesired materials is generally carried out through mechanical action or solubilization processes, mainly achieved with organic solvents. The main problems connected to the use of organic solvents concern their scarce environmental safety and their poor selectivity. The more similar are the characteristics (e.g., polarity) of the painting's original materials to those to be removed, the greater is the risk connected to the use of pure organic solvents. The confinement of solvent action is important to avoid diffusion processes of the dissolved substances into deeper and broader areas of the artifact. Furthermore, the uncontrolled penetration of pure solvents into the artifact's porous structure may cause swelling or leaching of binders and varnishes, with unknown long-term effects.[1,2]

In the past decades conservators devised several methods for the confinement of solvents, with the aim of increasing the control over the cleaning process. Penetration of the solvent via capillary action may be decreased using thickeners like cellulose ethers (e.g., hydroxypropyl cellulose—Klucel, ethyl cellulose) and polyacrylic acids (e.g., Carbopol). Unfortunately, the retention features of those systems are often unsatisfactory, and high evaporation rates of the solvents themselves can lead to formation of dry films of solid material on the treated surface.[3] Solvent gels (solvents in their thickened state) introduced by R. Wolbers,[4,5] are one of the most used cleaning tools. The capillary penetration of the solvent into the artifact is

Received: December 11, 2012
Revised: January 16, 2013
Published: January 18, 2013

dx.doi.org/10.1021/la3048664 | Langmuir 2013, 29, 2746−2755

reduced through immobilization of the solvent within the polymer network forming the solvent gel, characterized by weak intermolecular bonds that are responsible for the viscosity of the dispersion. The most important drawback concerning the use of solvent gels is related to the residues that might remain on the works of art after the cleaning. Following the treatment with a solvent gel system, it is always necessary to perform an appropriate cleaning procedure, which is usually carried out through organic solvent blends.[3] Furthermore, after mechanical removal and solubilization of the solvent gel system, residues of surfactant may remain on artifacts surface.[6]

A solution to the gel residue has been pursued by formulating completely innovative gel systems. Hence, some new confining systems such as highly viscous polymer solutions and physical gels (e.g., rheoreversible polyallylamine based organogels,[7] viscoelastic polyvinyl alcohol-borate based gels[8]) and chemical gels (e.g., polyacrylamide networks, which can be functionalized with magnetic nanoparticles) have been recently developed in our research group.[9−11] In the latter class of gelled systems (chemical gels), the polymeric network is characterized by the presence of covalent bonds. With respect to physical gels, chemical gels exhibit improved mechanical properties; they can be shaped in a well-defined form and can swell in a liquid medium without gel solubilization.

The present study was focused on designing low environmental toxicity hydrogels that fulfill all the mentioned desired characteristics. These gels can be loaded with water or water-based detergent systems (micellar systems, microemulsions), which allow replacing the traditional pure organic solvents.

Because of its high biocompatibility, poly(2-hydroxyethyl methacrylate)—p(HEMA)—hydrogels have been extensively studied in medical and pharmaceutical areas.[12,13] However, hydrophilicity of p(HEMA) is not sufficient for loading water-based cleaning systems for application to cultural heritage conservation. Poly(vinylpyrrolidone)—PVP—is a high hydrophilic polymer, widely used in the pharmaceutical, cosmetic, and food industries,[14] whose cross-linked hydrogels have scarce mechanical features.[15] In this paper we describe how the features of these two polymers can be combined to improve the capability of p(HEMA) to form stable networks with high hydrophilicity, assisted by the presence of hydrophilic PVP chains.

To benefit from both mechanical strength and hydrophilicity, the polymerization reaction was carried out to obtain semi-interpenetrating polymer network (semi-IPN) hydrogels. In fact, the synthesis of classical "copolymer hydrogels" leads to compounds with characteristics usually quite different from those resulting from the sum of single homopolymer properties. Semi-IPNs are based on polymer blends in which linear or branched polymers are embedded into one or more polymer networks during the polymerization reaction, without any chemical reaction occurring between them;[16,17] thus, the obtained hydrogel presents properties similar to the average of the single homopolymer properties. Linear polymers incorporated into a cross-linked network can act as dangling chains, producing softer gel systems, as expressed by the reduction of the friction coefficient.[18] We developed a semi-interpenetrating p(HEMA)/PVP network hydrogel where free chains of PVP macromolecules are embedded into a p(HEMA) network. We tuned the p(HEMA)/PVP ratio and the amount of water added to the reaction mixture to achieve the ideal properties for applications in cleaning of cultural heritage artifacts, i.e., good adhesion with the artifacts surface, high retention of the detergent system combined with efficient cleaning, cleaning action confined exclusively on gel contact area, no gel residues, and capacity of swell in different aqueous cleaning systems (e.g., mixed solvent systems, micellar solutions, microemulsions, etc.). Three semi-IPN hydrogels, differing from each other in the mechanical properties and release/retention capability, are presented in this paper. In order to evaluate the effectiveness of the investigated gel systems, the removal of hydrophilic layers was performed on a water-sensitive substrate. These gels can be also used to remove hydrophobic layers (such as adhesives, polymers, etc.) from water-sensitive materials. For this purpose, semi-IPN p(HEMA)/PVP hydrogels can be loaded with micellar systems or microemulsions, which have shown to be highly performing aqueous systems for the cleaning of cultural heritage artifacts[19−25] and can be efficiently confined in the chemical hydrogels.[9−11]

We show that these novel systems have outstanding cleaning capacity for water-sensitive works of art, and in particular for watercolor paintings that are extremely difficult to clean with conventional methods.

EXPERIMENTAL SECTION

Materials. 2-Hydroxyethyl methacrylate (HEMA) (assay 97%) and poly(vinylpyrrolidone) (PVP) (average $M_w \approx 1300$ kDa) were obtained from Sigma-Aldrich. α,α'-Azoisobutyronitrile (AIBN) (assay 98%) and *N*,*N*-methylene-bis(acrylamide) (MBA) (assay 99%) were obtained from Fluka, AIBN was recrystallized twice from methanol prior to use. All the other chemicals were used as received. Water was purified by a Millipore MilliRO-6 Milli-Q gradient system (resistivity >18 MΩ cm).

Hydrogels Synthesis. The semi-IPN hydrogels were prepared by physically embedding linear PVP into the hydrogel network. This was achieved by free radical polymerization of HEMA monomer and the cross-linker MBA in a water solution containing linear PVP. Series of different hydrogels were designed by varying the proportions of monomer/cross-linker ratio with PVP and water percentages. The composition of the best systems selected for the cleaning trials is presented in Table 1. In particular, these semi-IPN hydrogels can be designed by varying their component ratios (water, PVP, HEMA, and cross-linker quantities) in order to tune their characteristics in terms of mechanical behavior (softness, elasticity, and resistance to tensile strength) and affinity to water.

Table 1. Compositions (w/w) of the Selected Semi-IPN Hydrogels; Monomer/Cross-Linker and HEMA/PVP Ratio[a]

	H50	H58	H65
HEMA	25.0%	16.8%	10.5%
MBA	0.20%	0.20%	0.21%
PVP	24.9%	25.1%	24.5%
water	49.9%	57.9%	64.9%
monomer/cross-linker ratio	$1:1 \times 10^{-2}$	$1:1.5 \times 10^{-2}$	$1:2 \times 10^{-2}$
HEMA/PVP ratio	50/50	40/60	30/70

[a]H58 formulation was specifically designed for the cleaning of the Thang-Ka model samples. The acronym H*XX* refers to the percentage of water (*XX*) in the reaction mixture.

Hydrogels synthesis was carried out in two different types of molds to obtain (i) hydrogels with 2.5 × 2.5 × 1 cm parallelepiped shape used for the physicochemical analyses and (ii) flat hydrogel films having 2 mm thickness used for the cleaning tests. All the products (see Table 1) and radical initiator AIBN (1:0.01 monomer/initiator molar ratio) were mixed together, and the solution was bubbled with nitrogen for 5 min to remove dissolved oxygen that could inhibit the radical polymerization of HEMA. The solutions were gently sonicated for 30 min in pulsed mode to eliminate the formed gas bubbles.

dx.doi.org/10.1021/la3048664 | *Langmuir* 2013, 29, 2746−2755

The polymerization reaction, initiated by thermal homolysis of AIBN, occurred at 60 °C for 4 h. After polymerization, hydrogels were washed and placed in containers filled with distilled water. The water was renewed twice a day for 7 days to remove any residue of unreacted monomer and the free PVP.

Physicochemical Characterization of Hydrogel. Each of the following parameters was calculated from at least three different measurements.

The gel content (G) gives the ratio between the mass of the final semi-IPN p(HEMA)/PVP hydrogel and the mass of the two components in the initial mixture, which can be calculated as follows[26]

$$G(\%) = \frac{W_d}{W_0} \times 100 \tag{1}$$

where W_d is the dry weight of the hydrogel and W_0 is the weight of HEMA and PVP in the initial reaction mixture. The dry weight was obtained by heating at 70 °C for 5 h and then increasing the temperature to 120 °C for 48 h. The obtained xerogels were placed in a desiccator to cool down to room temperature before weighing.

The equilibrium water content (EWC) of hydrogels gives information on the polymer network hydrophilicity and can be calculated as follows[27]

$$\mathrm{EWC} = \frac{W_W - W_d}{W_W} \times 100 \tag{2}$$

where W_W is the weight of the water swollen hydrogel in equilibrium, obtained at least 7 days after polymerization reaction.

Gel samples of 12−18 mg were analyzed in closed aluminum pans to determine both free water index (FWI) and freeze-bound water index (FBWI). The water content expressed as weight fraction in the gel, A, was determined by differential thermogravimetry (DTG), using a SDT Q600 (TA Instruments) apparatus. The temperature scan was from 20 to 450 °C with a heating rate of 10 °C/min. Melting enthalpies were calculated from differential scanning calorimetry (DSC) thermograms using a Q1000 (TA Instruments) apparatus. The temperature range scan was from −80 to 20 °C with 0.5 °C/min rate. The FWI was calculated as follows[28]

$$\mathrm{FWI} = \frac{\Delta H_{exp}}{\mathrm{WC} \times \Delta H_{theo}} \tag{3}$$

where the ΔH_{exp} (J/g) represents the melting enthalpy variation for free water and can be determined by integration of the DSC peak around 0 °C, WC is the water weight fraction in the fully hydrated hydrogel, and ΔH_{theo} is the theoretical value of the specific enthalpy of fusion for bulk water (333.61 J/g).[29]

Since the FWI gives the fraction of free water with respect to the total amount of water in the hydrogel, it is relevant to calculate the amount of free (R_{fx}) and total bound (R_{bx}) water per gram of dry hydrogel. These parameters can be determined according to the following equations:[11]

$$R_{fx} = \frac{W_W \times \mathrm{WC} \times \mathrm{FWI}}{W_d} \tag{4}$$

$$R_{bx} = \frac{W_W \times \mathrm{WC} \times (1 - \mathrm{FWI})}{W_d} \tag{5}$$

Partially rehydrated hydrogels were prepared to determine the freeze-bound water fraction. About 15 mg of sample were first equilibrated at 75% and then at 100% relative humidity (RH) for 6 days.[30] The freeze-bound water amount was determined from the relationship[28]

$$\mathrm{FBWI} = \frac{\Delta H_{exp}}{\mathrm{WC} \times \Delta H_{bound}} \tag{6}$$

where ΔH_{bound} (J/g) is the theoretical value of the melting enthalpy of water at the specific temperature below 0 °C, and it was calculated as described in the literature.[31]

The amounts of freeze-bound, R_{fbx}, and nonfreezable water, R_{nfx}, per gram of dry hydrogel are obtained from

$$R_{fbx} = \frac{W_W \times \mathrm{WC} \times \mathrm{FBWI}}{W_d} \tag{7}$$

$$R_{nfx} = \frac{W_W \times \mathrm{WC} \times (1 - \mathrm{FWI} - \mathrm{FBWI})}{W_d} \tag{8}$$

Xerogels, obtained through a freeze-drying process, were used to determine mesoporosity. A FEG-SEM ΣIGMA (Carl Zeiss, Germany) was used to acquire the images using an acceleration potential of 1 kV and a working distance of 1.4 mm. The metallization of the samples was not necessary with these experimental conditions.

SAXS measurements were carried out with a HECUS S3-MICRO camera (Kratky-type) equipped with a position-sensitive detector (OED 50M) containing 1024 channels of width 54 μm. Cu Kα radiation of wavelength λ = 1.542 Å was provided by an ultrabrilliant point microfocus X-ray source (GENIX-Fox 3D, Xenocs, Grenoble), operating at a maximum power of 50 W (50 kV and 1 mA). The sample-to-detector distance was 269 mm. The volume between the sample and the detector was kept under vacuum during the measurements to minimize scattering from the air. The Kratky camera was calibrated in the small angle region using silver behenate (d = 58.38 Å).[32] Scattering curves were obtained in the q-range between 0.01 and 0.54 Å^{-1}, assuming that q is the scattering vector, $q = 4\pi/\lambda \sin\theta$, and 2θ the scattering angle. Gel samples were placed into a 1 mm demountable cell having Mylar films as windows. The temperature was set to 25 °C and was controlled by a Peltier element, with an accuracy of 0.1 °C. All scattering curves were corrected for the empty cell contribution considering the relative transmission factor.

The presence of gel residues over the cleaned surface was checked with attenuated total reflectance Fourier transform infrared spectroscopy (ATR-FTIR) on canvas or paper samples kept in contact with the hydrogel for 4 h. A Thermo Nicolet Nexus 870 FTIR spectrometer equipped with a Golden Gate diamond cell was used. Data were collected with an MCT detector with a sampling area of 150 μm^2. The spectra were obtained from 128 scans with 4 cm^{-1} of optical resolution.

Gel Retention Capability. Dehydration kinetics and water release provide a better understanding of the retention capability of each gel. To determine the dehydration kinetics, expressed as water decrease over time (WD), swollen hydrogel films were weighted and placed in a humidity chamber at 53% RH until equilibrium was reached. The weight decrease as a function of time was calculated as follows

$$\mathrm{WD} = \frac{W_i - W_d}{W_W - W_d} \times 100 \tag{9}$$

where W_i is the hydrogel weight at the specific time i.

For the evaluation of water release properties, fully swollen hydrogels were gently surface dried and then positioned on four sheets of Whatman filter paper and covered with a lid to avoid water evaporation. The sheets of filter paper were weighted before and after 30 min of gel application. The released water is normalized by unit area.

Removal of Hydrophilic Surface Grime. To assess the gel performance, a Thang-Ka mock-up was prepared. A Thang-Ka consists of a multilayer structure in which a cotton canvas is covered with a preparation layer containing $CaCO_3$ and animal glue. The painting technique is a tempera magra; i.e., pigments and colorants are mixed with animal glue dissolved in water. In the prepared model, calcium carbonate was used as the white pigment; malachite was used to obtain the green color; the blue colorant is indigo; the golden lines are obtained from shell gold. To carry out cleaning tests, the mock-up surface was previously covered with an artificial grime mixture. The grime was applied in a 4.5% v/v solution of mineral oil in chloroform using a paintbrush. The synthetic grime mixture has a hydrophilic composition and was designed by R. Wolbers.[33] The progress of the cleaning process was determined using a spectrophotocolorimetric analysis. The light reflected from the sample was collected by a fiber-

dx.doi.org/10.1021/la3048664 | Langmuir 2013, 29, 2746−2755

optic cable (FRP series) connected to a high sensitivity CCD camera (−10 °C TE cooled Prime X back-thinned) in a 350−1000 nm range. The light spot was around 1 mm in diameter. Reflectance spectra were acquired at a distance of 3 mm from the surface. Colorimetric data were collected using standard illuminant C and standard observer CIE 1931 (2°) in a λ range of 400−700 nm (with 10 nm of resolution) and with a 0°/0° geometry. The degree of cleaning was evaluated through color difference from the ΔE^* parameter

$$\Delta E^* = [(\Delta L^*)^2 + (\Delta a^*)^2 + (\Delta b^*)^2]^{1/2} \quad (10)$$

where ΔE^* is the color difference in the colorimetric space CIELAB 1976 and L^*, a^*, and b^* are the related colorimetric coordinates.[34,35]

RESULTS AND DISCUSSION

The innovative application of a chemical gel for the cleaning of the front of a canvas painting is presented here, as far as we know, for the first time. An artificially soiled Thang-Ka mock-up was considered to assess the efficiency of hydrophilic grime removal from a water-sensitive substrate. A Thang-Ka is a Tibetan votive artifact based on tempera magra painting on canvas, where the binder is animal glue (see Figure 1). This

Figure 1. Detail of a Thang-Ka from the 18th century.

painting technique is characterized by a high pigment volume concentration (PVC), equal or slightly higher than critical PVC, at which there is just sufficient binder to wet the pigment particles. This leads to a very low cohesive paint layer, where the scarce quantity of binder is water-sensitive,[36] making the removal of hydrophilic surface grime, which is trapped into the painting "porosity", a challenge for conservators. Because paint layer is water-soluble, the traditional use of a water-impregnated cotton swab has a nonselective action for hydrophilic grime removal. So it is necessary to achieve a layer by layer removal through the precise confinement of the solvent. Hence, the Thang-Ka represents an appropriate case study to test semi-IPN hydrogel capability to perform an efficient and high-controlled cleaning action.

All the semi-IPN hydrogel formulations were found to have interesting macroscopic characteristics and improved mechanical properties with respect to a p(VP) homopolymer hydrogel. The semi-IPN p(HEMA)/PVP hydrogels properties are strictly dependent on the quantitative ratios of their components. Two formulations having different hydrophilicity, H65 and H50, were investigated. The acronym H*XX* refers to the *XX* percentage of water in the reaction mixture, which is proportional to the hydrophilic character of the hydrogel, enhanced by the addition of linear PVP chains.

The investigated hydrogels are transparent or translucent and easy to manipulate. Specifically, the H50 is the most rigid, homogeneous, and completely transparent, while the H65 hydrogel is opalescent, translucent, pliable and exhibits a reversible enhanced deformability when some mechanical stress is applied. This feature is important to attain better adhesion to rough surfaces. In addition, both hydrogels are to some extent softer than ordinary chemical gels and maintain high water retention capability.

Semi-IPN hydrogels are polymer blends, and during synthesis there is no chemical reaction between monomer and linear polymer. Therefore linear PVP could be separated from the constituent polymer network of HEMA without breaking chemical bonds.[16] Formation of hydrogen bonds between the carbonyl group of PVP and the hydroxyl group of HEMA has already been reported in the literature.[37] This kind of interaction leads to an efficient embedding of linear PVP into the network of p(HEMA). The gel content (G) is 90% for H50 and 74% for H65. Even if the p(HEMA)/PVP ratio in H50 is 50/50, its gel content is substantially high. Increasing linear PVP content lowers G values. This means that the available area of the HEMA network, which interacts with PVP chains, at a specific HEMA/PVP ratio will not be enough to contain further PVP. Hence, besides water, PVP in excess is a further component that contributes to the final porosity of the hydrogel and to a more heterogeneous microporosity, as confirmed by FEG-SEM images.

The EWC in semi-IPN hydrogels is due to both porosity and hydrophilic character of the final polymer network. The water content of H50 and H65 hydrogels increased from the initial 50% to 72% and from 65% to 87%, respectively, without any loss of transparency. This is a noteworthy feature considering that there is a water content limit for the reaction mixture: larger amounts of water produce phase separation during polymerization leading to a totally white opaque hydrogel.[17,38] In fact, p(HEMA) hydrogels have an EWC approximately of 39%.[39] Therefore, to obtain transparent p(HEMA) hydrogels, the maximum water content in the reaction mixture must be lower than this value. By adding highly hydrophilic linear PVP into the reaction mixture, it is possible to increase both the water content and the network hydrophilicity with the result of an increase in the final porosity.

Water inside swollen hydrogels can be classified into three different states: free, bound-freezable, and unfreezable water. This classification takes into account the extent of interactions of water molecules with the polar part of the polymer chains: free water is defined as the water with the same thermodynamic properties of bulk water; freeze-bound water interacts weakly with the polymer chains of the hydrogels so that its freezing point is lower than 0 °C; unfreezable water is strongly hydrogen bonded, and no phase transition is observed from −70 to 50 °C.[40,41] Because only free water is contributing to the cleaning process, the knowledge of the bound-freezable and free water fractions inside hydrogels is important to quantify the hydrogel capability to exchange the solvent at the surface and thus to prevent any excessive wetting. The distribution of "water states" inside hydrogels can be estimated through the calculation of freezable water, from the free water index (FWI) and freeze-bound water index (FBWI) parameters, both determined via DSC. In the DSC thermograms, free water shows a freezing point equal to that of bulk water, while the freezing point of bound-freezable water is lower than 0 °C, due

to the water interactions with polymer chains or the confinement in the mesoporosity.[41]

The DSC thermograms, obtained from the swollen H50 and H65 hydrogels, are shown in Figure 2. Two distinct protocols

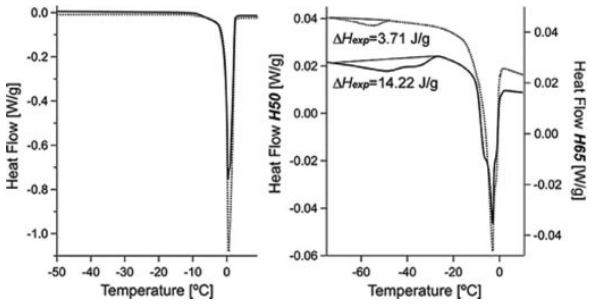

Figure 2. DSC thermograms for the fully swollen hydrogels (left) and partially rehydrated hydrogels (right) for H50 (solid line) and H65 (dotted line). Both thermograms were normalized to sample weight.

were used to determine both FWI and FBWI parameters as described in the Experimental Section. The DSC thermograms in Figure 2 (left panel) show a shoulder below 0 °C, which is associated with a minor fraction of free water that has indirect interactions with the polymer network and, therefore, has a behavior close to freeze-bound water.

The FWI results are reported in Table 2. Freeze-bound water is evidenced by the broad freezing peak visible between −70 and −20 °C in Figure 2 (right panel), in addition to the more intense freezing peak for free water. It is evident that the area associated with the freeze-bound water peak is larger for H50.

The FWI values obtained highlight that free water inside swollen hydrogels is to a large extent higher than bound water. Therefore, aqueous systems inside hydrogels behave mostly as free water. In fact, the free water content is around 73% in H50 and 77% in H65 with respect to the total water inside the swollen hydrogels. In order to point out the evident difference between hydrogels hydrophilicity, it was relevant to analyze both R_{fx} and R_{bx} parameters. From these parameters it is possible to assess the real amount of free water available per each gram of dry hydrogel. As expected, both parameters are higher for H65 (4.72 of R_{fx} and 1.41 of R_{bx}) than for H50 (2.30 of R_{fx} and 0.85 of R_{bx}). This feature is due to the higher amount of PVP in the H65 hydrogel. In fact, higher content of PVP contributes to a more swollen hydrogel that recalls more water molecules per unit mass of polymer, increasing both R_{fx} and R_{bx} parameters.

On the other hand, to better understand the freeze-bound water behavior in hydrogels, FBWI was calculated from the freeze-bound water fusion peak presented in Figure 2 B. The results are listed in Table 2.

H50 has a higher FBWI than H65 as a consequence of a greater number of water molecules in contact with pore walls due to smaller pore dimensions and the higher surface to volume ratio. Furthermore, since the R_{bx} parameter gives the amount of total bound water per gram of xerogel, it was important to split it into the amount of freeze-bound and nonfreezable water per gram of xerogel inside partially rehydrated hydrogels (R_{fbx} and R_{nfx}, respectively). It is evident that the more hydrophilic hydrogel H65 shows a higher R_{nfx} value, while the amount of freeze-bound water is significantly lower.

Table 2. Free Water Index (FWI), Freeze-Bound Water Index (FBWI), and Correlated Parameters for Fully Swollen (HXX) and Partially Rehydrated Hydrogels (HXX*)[a]

	FWI					FBWI			
	A	ΔH_{exp} (J/g)	FWI	R_{fx} (g/g)	R_{bx} (g/g)	ΔH_{exp} (J/g)	FBWI	R_{fbx}	R_{nfx}
H50	0.758 ± 20 × 10^{-3}	184.7 ± 5.9	0.730 ± 4 × 10^{-3}	2.30 ± 0.26	0.85 ± 0.08	–	–	–	–
H65	0.859 ± 13 × 10^{-3}	220.8 ± 0.6	0.770 ± 9 × 10^{-3}	4.72 ± 0.44	1.41 ± 0.20	–	–	–	–
H50*	0.396 ± 22 × 10^{-3}	40.7 ± 5.8	0.309 ± 63 × 10^{-3}	0.20 ± 0.02	0.46 ± 0.08	13.7 ± 1.7	0.161 ± 18 × 10^{-3}	0.10 ± 0.02	0.36 ± 0.06
H65*	0.475 ± 33 × 10^{-3}	47.1 ± 2.6	0.304 ± 6 × 10^{-3}	0.27 ± 0.03	0.61 ± 0.09	4.1 ± 0.6	0.045 ± 4 × 10^{-3}	0.04 ± 0.01	0.57 ± 0.08

[a] A is the weight fraction of water. FBWI was calculated using the partially rehydrated hydrogels as reported in the Experimental Section.

dx.doi.org/10.1021/la3048664 | Langmuir 2013, 29, 2746−2755

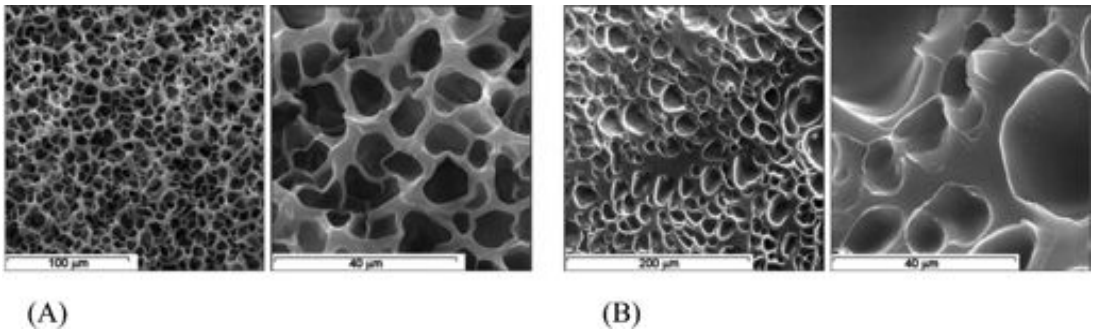

Figure 3. SEM images of H50 (A) and H65 (B) xerogels obtained at two different magnifications.

FEG-SEM images were acquired to detail the structure and porosity of the lyophilized hydrogel (xerogel). Since xerogel state is required for FEG-SEM image acquisition, EWC was determined in the fully rehydrated xerogels as well, to evaluate if the freeze-drying process compromises the microstructure of the hydrogel. A decrease of the EWC was observed in both cases: 0.16% and 8.28% for H50 and H65, respectively. In the case of H50 the variation is almost negligible, while for H65 the difference of EWC is considerable, which means that ca. 8% of microporosity is collapsed during freeze-drying as a consequence of the water to ice expansion associated with the freezing step necessary for the lyophilization. This difference is, thus, relevant to be considered when dealing with FEG-SEM results.

FEG-SEM images are shown in Figure 3 for H50 and H65 xerogels. A spongelike structure is observed for both samples, and pore dimensions are approximately comprised in the range from 5 to 40 μm. A more heterogeneous structure is clearly noted for H65 with respect to H50 xerogel. Pore wall thickness in H50 xerogel presents an average value of $\approx 2.4 \pm 1.3$ μm. In accordance with the heterogeneity of the H65 structure, there is a broader distribution of pore wall thickness.

In ordinary cross-linked chemical hydrogels, the amount of water in the reaction mixture is the major contributor to final porosity. FEG-SEM images clearly show smaller pores for H50 formulation compared with H65. To further quantify this aspect, a pore size distribution was extracted from several FEG-SEM images using ImageJ analysis software. The obtained histogram is presented in Figure 4.

H65 hydrogel displays a broader distribution with pore diameters going from 5 to 39 μm. As for H50, a more homogeneous distribution is noted with the main pore diameters comprised between 6 and 11 μm. Furthermore, the porosity was estimated to be approximately 10375 pores/mm^2 for H50 and 2600 pores/mm^2 for H65 xerogel. The difference of porosities between the two hydrogels is due to three main factors: the water content in the initial polymerization mixture, which is the main factor responsible for final gel porosity and dimension of pores; the PVP release after polymerization; and the cross-linker content, which contributes, for the same PVP/HEMA/H_2O ratios, to more compact network structures.

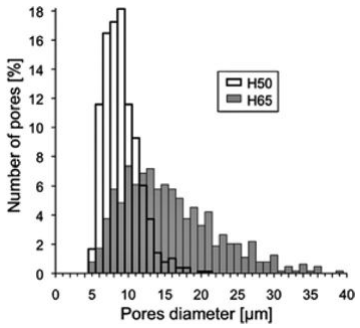

Figure 4. Pore size distributions for H50 and H65 semi-IPN xerogels.

SAXS investigations were carried out to detail the structural changes imposed at the nanoscale by the PVP addition. The investigated hydrogel formulations were compared to a cross-linked p(HEMA) hydrogel as a reference. p(HEMA) hydrogel is prepared analogously to H50 except for the addition of PVP. Thus, the cross-linked p(HEMA) network percentage in p(HEMA) hydrogel is higher than in semi-IPN formulations (50% w/w in the composition of p(HEMA) compared with a maximum of 25% w/w in semi-IPN compositions), and the water-phase was maintained at 50% w/w of the total. This excess of water leads to phase separation during polymerization of p(HEMA) hydrogel, as reported in the literature.[38]

SAXS curves, as shown in Figure 5, were modeled using the Debye−Bueche approach.[42] In this model, SAXS intensity distribution is split in two q-dependent contributions and an instrumental flat background:

$$I(q) = I_{\text{Lorentz}}(q) + I_{\text{excess}}(q) + \text{bkg} \tag{11}$$

The first contribution, $I_{\text{Lorentz}}(q)$, is a Lorentzian term accounting for the scattering associated with a tridimensional network with a characteristic mesh size. It can be expressed as follows

$$I_{\text{Lorentz}}(q) = \frac{I_{\text{Lorentz}}(0)}{1 + q^2\zeta^2} \tag{12}$$

where $I_{\text{Lorentz}}(0)$ is the Lorentzian intensity at $q = 0$ and ζ is the average mesh dimension of the network. The second contribution, I_{excess}, the excess scattering, concerns the scattering at low q produced by inhomogeneities, as for example, solidlike polymer domains.

$$I_{\text{excess}}(q) = \frac{I_{\text{excess}}(0)}{(1 + q^2a^2)^2} \tag{13}$$

where $I_{\text{excess}}(0)$ is the excess intensity at $q = 0$ and a is the average dimension of the inhomogeneity domains accessible by the SAXS experiment.

dx.doi.org/10.1021/la3048664 | Langmuir 2013, 29, 2746−2755

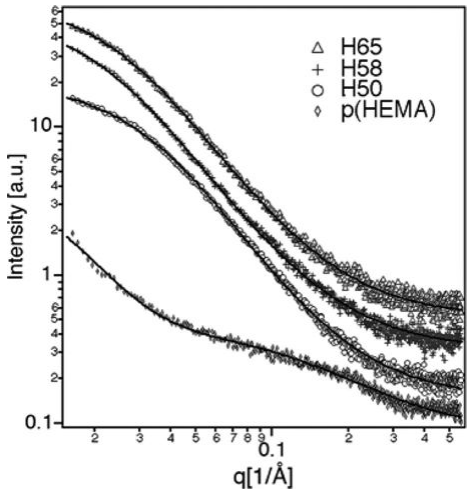

Figure 5. SAXS intensity distribution in a log−log scale for all semi-IPN hydrogels investigated. A cross-linked p(HEMA) hydrogel is reported as a reference. The solid lines are the fits with the Debye−Bueche model. The curves are shifted upward by an arbitrary factor to avoid overlap.

Best fitting curves are reported as solid lines in Figure 5, while the extracted parameters from the Debye−Bueche model are listed in Table 3.

Table 3. Debye−Bueche Parameters Obtained from the SAXS Curves of the Investigated Hydrogels

	p(HEMA)	H50	H58	H65
$I_{Lorentz}(0)$	1.7	12.1	8.2	7.8
ζ (nm)	0.7	2.5	2.8	3.1
$I_{excess}(0)$	27.4	40.2	45.3	25.1
a (nm)	6.0	2.5	3.6	3.3
bkg	0.50	0.39	0.30	0.23
$I_{excess}(0)/I_{Lorentz}(0)$	16.1	3.3	5.5	3.2

The SAXS profiles in Figure 5 show a neat difference between p(HEMA) and semi-IPN hydrogels. According to the literature,[43] mesh dimension depends mainly on the equilibrium water content, which in the present case is proportional to the p(HEMA)/PVP ratio in the reaction mixture. H50 semi-IPN hydrogel has a mesh size of 2.5 nm while the H58 of 2.8 nm and H65 of 3.1 nm. In fact, mesh size increase for each semi-IPN formulation is accompanied by a comparable increase of EWC. Namely, the mesh volume increase over H50 is 41% and 91% in H58 and H65, respectively, which is in agreement to the EWC increase of 11% and of 21% in the same formulations.

The increase of average mesh size is also related to the decrease in cross-linker concentration, as reported in the literature.[44] Despite cross-linker content decreases, H50 shows a smaller ζ than H65. This is due to the decreasing percentage of PVP from H65 to H50, which leads to a less swollen network.

As reported in the literature[45−47] less homogeneous structures are likely to form when the syntheses are conducted at higher polymer volume fractions (water-poor systems) and/or at higher cross-linker concentration. The variation on inhomogeneity dimension, a, is not clear for the three semi-IPN formulations since the more water-poor system (H50) has the lower number of cross-links, while the formulation with higher EWC (H65) is characterized by a higher cross-linker content. So the effect of these two components is disguised. As a matter of fact, H50 has the smallest a dimension in the series thus resulting in the most homogeneous both in the nanometer-scale length and in the micrometer-scale length as already shown by the porosity distribution extracted from the SEM images. The increase of inhomogeneities dimension is clearly noticed in the water-poor p(HEMA) system.

The $I_{excess}(0)/I_{Lorentz}(0)$ ratio is proportional to inhomogeneity/mesh volume fractions. In this regard, the collected SAXS data agree with the increase of inhomogeneity abundance related to the higher polymer volume fraction. In fact, there is an increase of inhomogeneities of a factor 4 for p(HEMA) hydrogel with respect to semi-IPN formulations.

Application of Hydrogels. Due to higher transparency and ease of handling, hydrogels shaped as a film were preferred for carrying out the cleaning tests on model samples. The dehydration kinetics of the hydrogels was evaluated at 55% RH and 20 °C to verify if during the time required for the cleaning process, the amount of water is enough.

Dehydration curves of H50 and H65 hydrogel films are presented in Figure 6. The same amount of water contained in the hydrogel was put in a beaker inside the dehydration chamber to have a comparison with the evaporation kinetics of bulk water.

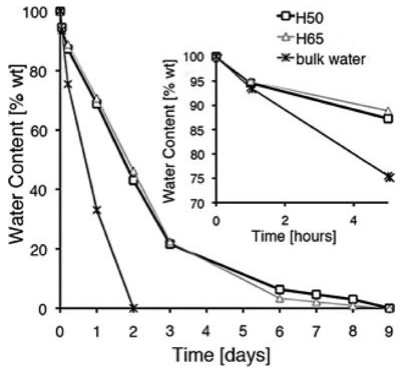

Figure 6. Dehydration curves for H50 and H65 semi-IPN hydrogels and for bulk water. Inset: dehydration curves within the first 5 h.

The dehydration kinetics confirmed that for some hours the amount of water inside hydrogels is still above 95% of the initial value (see inset of Figure 6), while the dehydration equilibrium was reached after 6 days.

A release test was performed using two hydrogel formulations (H50 and H65) to assess the real amount of water released to a highly hydrophilic surface such as paper. Both hydrogels performed a homogeneous release of water restricted to the paper contact area. After 30 min of contact, H50 released 16 ± 1 mg/cm^2 while H65 released 33 ± 3 mg/cm^2. The evident difference of water release between both hydrogels is in accordance with the results of DSC analysis.

To confirm that no gel residues are left after cleaning with semi-IPN hydrogels, ATR-FTIR spectra from a highly hydrophilic material such as cotton canvas were collected.

In Figure 7 the characteristic intense bands assigned to the carbonyl stretching vibration of both HEMA and PVP

dx.doi.org/10.1021/la3048664 | Langmuir 2013, 29, 2746−2755

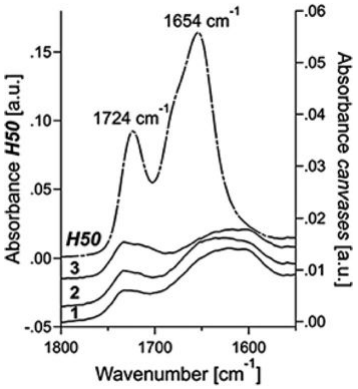

Figure 7. ATR-FTIR spectra of H50 hydrogel (slash-dotted line), of canvases previously in contact with H65 (1) and H50 (2) hydrogels and of canvas as it is (3).

(respectively 1724 and 1654 cm^{-1}) are clearly not present in the other spectra (1 and 2), which confirmed that no residues were left on canvas after treatment.

The application of semi-IPN hydrogels for the removal of hydrosoluble surface grime from a Thang-Ka mock-up is presented below. Cleaning tests were performed using H50 and H65 hydrogels. Since the first gel was not efficient enough and the latter showed an excessive wetting action, water-loaded H58 hydrogel (tailored for this case study; for chemical composition see Table 1) was chosen because it presents retention/release characteristics in between H50 and H65.

To obtain a gradual and controlled cleaning action, the most efficient procedure was the use of water-loaded hydrogel H58 in two short applications, each of about 20 min. Furthermore, the application procedure does not include any mechanical action, while in traditional cleaning methods this is a mandatory step. The ease of handling of this hydrogel film is shown in Figure 8. To evaluate the ability of semi-IPN hydrogels to

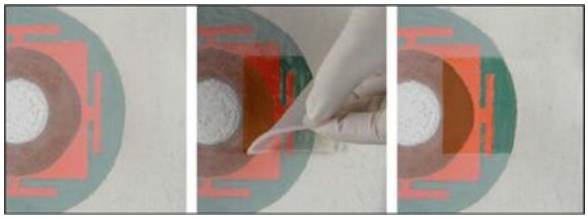

Figure 8. Stages of cleaning on Thang-Ka mock-up (see video in the Supporting Information).

restrain cleaning action while offering an efficient treatment, a comparison with a recently used material for art conservation, i.e., agar–agar gel,[48] was carried out. Semi-IPN p(HEMA)/PVP and agar–agar hydrogels were left in contact for 5 min with paper painted with a water-soluble ink (brazilwood ink). Color leaching, due to an excessive wetting of the treated surface, is highlighted by the diffusion of the colorant that is clearly visible after contact with agar–agar gel, while the color front is still sharp in the case of semi-IPN p(HEMA)/PVP hydrogels (Figure 9).

Figure 10 shows the homogeneous and confined cleaning obtained using H58 hydrogel, resulting in a gradual depletion of the grime coating without any color leaching.

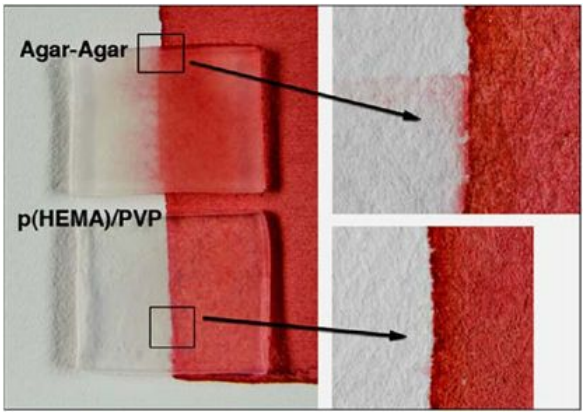

Figure 9. Five minutes application of agar–agar (2% w/w) and semi-IPN p(HEMA)/PVP hydrogels on paper painted with brazilwood ink.

UV–vis reflectance spectra further provide qualitative confirmation of the cleaning results (see Figure 11). Reflectance spectra of artificial soiled areas show enhanced reflectance values in the whole investigated range. This is due to the scattering of incident light caused by grime particles, resulting in a whitish, and thus more reflective, surface. In fact, the reflectance spectra from the cleaned areas show a progressive approximation to the reflectance values of reference areas (not soiled color).

To quantify this approximation, the color difference ΔE^* was calculated for soiled and cleaned surface areas with respect to reference area. Table 4 presents colorimetric data concerning the indigo colorant, the most sensitive paint layer of the Thang-Ka mock-up. The calculated values of ΔE^* show a significant reduction in the treated areas with respect to the artificially soiled area. The same trend is observed for the single colorimetric coordinates. This demonstrates that improved cleaning control can be achieved by using semi-IPN hydrogels based on p(HEMA) and linear PVP. The surface grime is gradually removed, and the original water-sensitive paint layers are not affected.

CONCLUSIONS

In this paper the synthesis and characterization of high retentive semi-IPN hydrogels developed specifically for application in art conservation is presented. Semi-IPN hydrogels have been prepared by free radical polymerization of HEMA monomer embedding linear PVP into the hydrogel network and varying the components ratios (water, PVP, HEMA, and cross-linker quantities) to tune their characteristics in terms of mechanical behavior (softness, elasticity, and resistance to tensile strength) and affinity to water. The water inside swollen hydrogels was characterized by differential scanning calorimetry and classified as unfreezable, bound-freezable, and free water, depending on the extent of interactions with the polar part of the polymer chains. The hydrogels possess suitable water release and retention properties for a controlled and efficient cleaning of water-sensitive artifacts. Moreover, the gels' mechanical properties and the water "mobility" can be tailored to the required characteristics for specific conservation issues by changing gels' composition, making these new polymeric hydrogels the most advanced systems for the cleaning of water-sensitive artifacts.

dx.doi.org/10.1021/la3048664 | *Langmuir* 2013, 29, 2746–2755

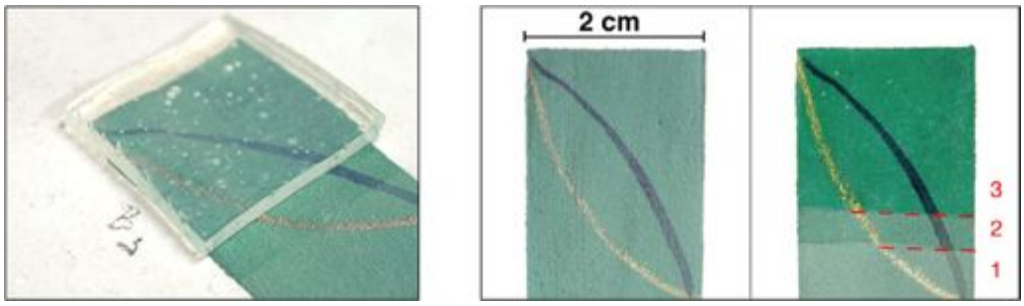

Figure 10. Artificial grime removal using water-loaded H58 hydrogel from a Thank-Ka mock-up. Right image presents different levels of cleaning: not cleaned (1); after 20 min of hydrogel application (2); after further 20 min of hydrogel application (3).

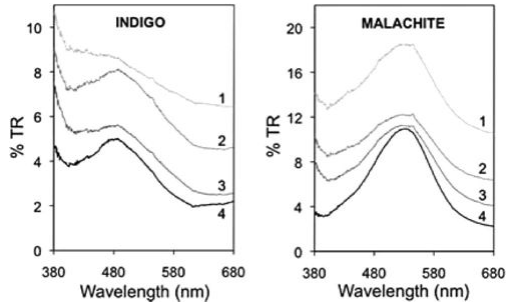

Figure 11. UV−vis reflectance spectra acquired from indigo and malachite painted areas: (1) artificial soiled surface; (2) after 20 min cleaning; (3) after ulterior 20 min cleaning; (4) reference painted area.

Table 4. Colorimetric Coordinates L^*, a^*, b^*, and ΔE^* Values for the Reference Area, Not Cleaned Area, and Different Applications of H58 Hydrogel[a]

indigo	L^*	a^*	b^*	ΔE^*
reference area (not soiled)	21.5 ± 1.9	−7.2 ± 0.4	−7.0 ± 0.4	0
before cleaning	32.8 ± 0.6	−2.6 ± 0.8	−3.7 ± 0.7	12.6
20 min H58 hydrogel application	31.7 ± 1.3	−5.0 ± 0.4	−4.7 ± 0.8	10.6
further 20 min H58 hydrogel application	21.8 ± 1.4	−5.2 ± 0.3	−6.9 ± 0.6	2.1

[a]Each of the colorimetric coordinates presented is the average value of at least 10 measurements.

■ ASSOCIATED CONTENT

Ⓢ Supporting Information

Movie on the cleaning of water-sensitive surface. This material is available free of charge via the Internet at http://pubs.acs.org.

■ AUTHOR INFORMATION

Corresponding Author

*Phone: +39 055 457 3033. Fax: +39 055 457 3032. E-mail: baglioni@csgi.unifi.it. URL: www.csgi.unifi.it.

Author Contributions

The manuscript was written through contributions of all authors. All authors have given approval to the final version of the manuscript.

Notes

The authors declare no competing financial interest.

■ ACKNOWLEDGMENTS

The authors acknowledge Dr. F. Ridi for the thermal analysis experiments and Dr. M. Potenza for the spectrophotocolorimetric measurements. J.A.L.D. acknowledges financial support provided by *Fundação para a Ciência e a Tecnologia* (FCT) through a Ph.D. research grant (SFRH/BD/73817/2010). This work was partly supported by CSGI and the European Union, Project NANOFORART (FP7-ENV-NMP-2011/282816).

■ REFERENCES

(1) Stolow, N. Application of Science to Cleaning Methods: Solvent Action Studies on Pigmented and Unpigmented Linseed Oil Films. In *Recent Advances in Conservation*, Proceedings of the IIC Rome Conference, Rome, Italy, 1961; Butterworths: London, U.K., 1963; pp 84−88.

(2) Phenix, A.; Sutherland, K. The Cleaning of Paintings: Effects of Organic Solvents on Oil Paint Films. *Rev. Conserv.* **2001**, *2*, 47−60.

(3) Cremonesi, P. *L'Uso di Tensioattivi e Chelanti nella Pulitura di Opere Policrome*; Il Prato: Padua, Italy, 2004.

(4) Wolbers, R.; Sterman, N.; Stavroudis, C. *Notes for the Workshop on New Methods in the Cleaning of Paintings*; The Getty Conservation Institute: Marina del Rey, CA, 1988.

(5) Wolbers, R. *Cleaning Painted Surfaces: Aqueous Methods*; Archetype: London, U.K., 2000.

(6) Burnstock, A.; Kieslich, T. A Study of the Clearance of Solvent Gels Used for Varnish Removal from Paintings. In *ICOM Committee for cConservation*, Proceedings of the 11th Triennial Conference, Edinburgh, Scotland, Sept 1−6, 1996; James & James: London, U.K., 1996; pp 253−262.

(7) Carretti, E.; Bonini, M.; Dei, L.; Berrie, B. H.; Angelova, L. V.; Baglioni, P.; Weiss, R. G. New Frontiers in Materials Science for Art Conservation: Responsive Gels and Beyond. *Acc. Chem. Res.* **2010**, *43*, 751−760.

(8) Carretti, E.; Grassi, S.; Cossalter, M.; Natali, I.; Caminati, G.; Weiss, R. G.; Baglioni, P.; Dei, L. Poly(vinyl alcohol)−Borate Hydro/Cosolvent Gels: Viscoelastic Properties, Solubilizing Power, and Application to Art Conservation. *Langmuir* **2009**, *25*, 8656−8662.

(9) Bonini, M.; Lenz, S.; Giorgi, R.; Baglioni, P. Nanomagnetic Sponges for the Cleaning of Works of Art. *Langmuir* **2007**, *23*, 8681−8685.

(10) Bonini, M.; Lenz, S.; Falletta, E.; Ridi, F.; Carretti, E.; Fratini, E.; Wiedenmann, A.; Baglioni, P. Acrylamide-Based Magnetic Nanosponges: A New Smart Nanocomposite Material. *Langmuir* **2008**, *24*, 12644−12650.

(11) Pizzorusso, G.; Fratini, E.; Eiblmeier, J.; Giorgi, R.; Chelazzi, D.; Chevalier, A.; Baglioni, P. Physicochemical Characterization of Acrylamide/Bisacrylamide Hydrogels and Their Application for the Conservation of Easel Paintings. *Langmuir* **2012**, *28*, 3952−3961.

(12) Tighe, B. J. Hydrogels as Contact Lens Materials. In *Hydrogels in Medicine and Pharmacy*; Peppas, N. A., Ed.; CRC Press: Boca Raton, FL, 1987; Vol. *III*, Properties and Applications, pp 53−82.

(13) Mack, E. J.; Okano, T.; Kim, S. W. Biomedical Applications of Poly(2-Hydroxyethyl Methacrylate) and its Copolymers. In *Hydrogels in Medicine and Pharmacy*; Peppas, N. A., Ed.; CRC Press: Boca Raton, FL, 1987; Vol. *II*, Polymers, pp 65−93.
(14) Haaf, F.; Sanner, A.; Straub, F. Polymers of N-Vinylpyrrolidone: Synthesis, Characterization and Uses. *Polym. J.* **1985**, *17*, 143−152.
(15) Wang, J.; Sun, F.; Li, X. Preparation and Antidehydration of Interpenetrating Polymer Network Hydrogels Based on 2-Hydroxyethyl Methacrylate and N-Vinyl-2-Pyrrolidone. *J. Appl. Polym. Sci.* **2010**, *117*, 1851−1858.
(16) McNaught, M.; Wilkinson, A. Definitions of Terms Relating to the Structure and Processing of Sols, Gels, Networks, and Inorganic-Organic Hybrid Materials. In *IUPAC Compendium of Chemical Terminology* [Online]; Blackwell Scientific Publications: Oxford, U.K., 1997; p 1815. http://goldbook.iupac.org/PDF/goldbook.pdf (accessed Oct 10, 2012).
(17) Yanez, F.; Concheiro, A.; Alvarez-Lorenzo, C. Macromolecule Release and Smoothness of Semi-Interpenetrating PVP−pHEMA Networks for Comfortable Soft Contact Lenses. *Eur. J. Pharm. Biopharm.* **2008**, *69*, 1094−1103.
(18) Gong, J. P.; Osada, Y. Surface Friction of Polymer Gels. *Prog. Polym. Sci.* **2002**, *27*, 3−38.
(19) Carretti, E.; Dei, L.; Baglioni, P. Solubilization of Acrylic and Vinyl Polymers in Nanocontainer Solutions. Application of Microemulsions and Micelles to Cultural Heritage Conservation. *Langmuir* **2003**, *19*, 7867−7872.
(20) Carretti, E.; Giorgi, R.; Berti, D.; Baglioni, P. Oil-in-Water Nanocontainers as Low Environmental Impact Cleaning Tools for Works of Art: Two Case Studies. *Langmuir* **2007**, *23*, 6396−6403.
(21) Carretti, E.; Fratini, E.; Berti, D.; Dei, L.; Baglioni, P. Nanoscience for Art Conservation: Oil-in-Water Microemulsions Embedded in a Polymeric Network for the Cleaning of Works of Art. *Angew. Chem., Int. Ed.* **2009**, *48*, 8966−8969.
(22) Giorgi, R.; Baglioni, M.; Berti, D.; Baglioni, P. New Methodologies for the Conservation of Cultural Heritage: Micellar Solutions, Microemulsions, and Hydroxide Nanoparticles. *Acc. Chem. Res.* **2010**, *43*, 695−704.
(23) Baglioni, M.; Rengstl, D.; Berti, D.; Bonini, M.; Giorgi, R.; Baglioni, P. Removal of Acrylic Coatings from Works of Art by Means of Nanofluids: Understanding the Mechanism at the Nanoscale. *Nanoscale* **2010**, *2*, 1723−1732.
(24) Baglioni, M.; Giorgi, R.; Berti, D.; Baglioni, P. Smart Cleaning of Cultural Heritage: A New Challenge for Soft Nanoscience. *Nanoscale* **2012**, *4*, 42−53.
(25) Baglioni, M.; Berti, D.; Teixeira, J.; Giorgi, R.; Baglioni, P. Nanostructured Surfactant-Based Systems for the Removal of Polymers from Wall Paintings: A Small-Angle Neutron Scattering Study. *Langmuir* **2012**, *28*, 15193−15202.
(26) Ming Kuo, S.; Jen Chang, S.; Jiin Wang, Y. Properties of PVA-AA Cross-Linked HEMA-Based Hydrogels. *J. Polym. Res.* **1999**, *6*, 191−196.
(27) Liu, Q.; Hedberg, E. L.; Liu, Z.; Bahulekar, R.; Meszlenyi, R. K.; Mikos, A. G. Preparation of Macroporous Poly(2-Hydroxyethyl Methacrylate) Hydrogels by Enhanced Phase Separation. *Biomaterials* **2000**, *21*, 2163−2169.
(28) Nakamura, K.; Hatakeyama, T.; Hatakeyama, H. Relationship between Hydrogen Bonding and Bound Water in Polyhydroxystyrene Derivatives. *Polymer* **1983**, *24*, 871−876.
(29) Lide, D. R. *CRC Handbook of Chemistry and Physics*, 79th ed.; CRC Press: Boca Raton, FL, 1998.
(30) Faroongsarng, D.; Sukonrat, P. Thermal Behavior of Water in the Selected Starch- and Cellulose-Based Polymeric Hydrogels. *Int. J. Pharm.* **2008**, *352*, 152−158.
(31) Landry, M. R. Thermoporometry by Differential Scanning Calorimetry: Experimental Considerations and Applications. *Thermochim. Acta* **2005**, *433*, 27−50.
(32) Blanton, T.; Huang, T. C.; Toraya, H.; Hubbard, C. R.; Robie, S. B.; Louer, D.; Gobel, H. E.; Will, G.; Gilles, R.; Raftery, T. JCPDS—International Centre for Diffraction Data Round Robin Study of Silver Behenate. A Possible Low-Angle X-Ray Diffraction Calibration Standard. *Powder Diffr.* **1995**, *10*, 91−95.
(33) Wolbers, R. The Use of a Synthetic Soiling Mixture as a Means for Evaluating the Efficacity of a Aqueous Cleaning Materials on Painted Surfaces. *Conservation−Restauration Biens Culturels* **1992**, *4*, 22−29.
(34) Wyszecki, G.; Stiles, W. S. *Color Science: Concepts and Methods, Quantitative Data and Formulae*, 2nd ed.; John Wiley & Sons: New York, 2000.
(35) Kolar, J.; Strlic, M.; Marincek, M. IR Pulsed Laser Light Interaction with Soiled Cellulose and Paper. *Appl. Phys. A: Mater. Sci. Process.* **2002**, *75*, 673−676.
(36) Jackson, D. P.; Jackson, J. A. *Tibetan Thangka Painting: Methods & Materials*, 2nd ed.; Serindia: London, U.K., 1988.
(37) Huang, Y.; Yang, J. *Novel Colloidal Forming of Ceramics*; Springer: Berlin Heidelberg, Germany, 2011.
(38) Lou, X.; Munro, S.; Wang, S. Drug Release Characteristics of Phase Separation pHEMA Sponge Materials. *Biomaterials* **2004**, *25*, 5071−5080.
(39) Okay, O. Macroporous Copolymer Networks. *Prog. Polym. Sci.* **2000**, *25*, 711−779.
(40) Wolfe, J.; Bryant, G.; Koster, K. L. What is Unfreezable Water, How Unfreezable Is It and How Much is There? *CryoLetters* **2002**, *23*, 157−166.
(41) Li, X.; Cui, Y.; Xiao, J.; Liao, L. Hydrogel−Hydrogel Composites: The Interfacial Structure and Interaction between Water and Polymer Chains. *J. Appl. Polym. Sci.* **2008**, *108*, 3713−3719.
(42) Debye, P.; Bueche, A. M. Scattering by an Inhomogeneous Solid. *J. Appl. Phys.* **1949**, *20*, 518−525.
(43) Canal, T.; Peppas, N. A. Correlation between Mesh Size and Equilibrium Degree of Swelling of Polymeric Networks. *J. Biomed. Mater. Res., Part A* **1989**, *23*, 1183−1193.
(44) Peppas, N. A.; Hilt, J. Z.; Khademhosseini, A.; Langer, R. Hydrogels in Biology and Medicine: From Molecular Principles to Bionanotechnology. *Adv. Mater.* **2006**, *18*, 1345−1360.
(45) Panyukov, S.; Rabin, Y. Statistical Physics of Polymer Gels. *Phys. Rep.* **1996**, *269*, 1−131.
(46) Benguigui, L.; Boue, F. Homogeneous and Inhomogenous Polyacrylamide Gels As Observed by Small Angle Neutron Scattering: A Connection with Elastic Properties. *Eur. Phys. J. B* **1999**, *11*, 439−444.
(47) Ikkai, F.; Shibayama, M. Inhomogeneity Control in Polymer Gels. *J. Polym. Sci., Part B* **2005**, *43*, 617−628.
(48) Campani, E.; Casoli, A.; Cremonesi, P.; Saccani, I.; Signorini, E. *Quaderni del Cesmar7: L'Uso di Agarosio e Agar per la Preparazione di "Gel Rigidi"−Use of Agarose and Agar for Preparing "Rigid Gels"*, n°o.4; Il Prato: Padua, Italy, 2007.

Science and Technology for the Conservation of Cultural Heritage, Edited by Miguel Angel Rogerio-Candelera, Massimo Lazzari, Emilio Cano, CRC Press, 2013

Semi-interpenetrating p(HEMA)/PVP hydrogels for the cleaning of water-sensitive painted artifacts: assessment on release and retention properties

R. Giorgi, J.A.L. Domingues, N. Bonelli & P. Baglioni
Department of Chemistry and CSGI, University of Florence, Florence, Italy

Nowadays, aqueous cleaning systems are preferred for the cleaning of painted artifacts because they are environmental friendly and offer several advantages in terms of selectivity and gentle removal of undesired materials. However, materials interaction with water can lead to mechanical stress between the substrate and the paint layers. The confinement of water cleaning systems in a hydrogel with high retention capability can limit this disadvantage. Hence, the aim of this work was to develop novel chemical hydrogels, specifically designed for the cleaning of water-sensitive painted artifacts. These are based on highly hydrophilic semi-interpenetrating p(HEMA)/PVP networks with suitable mechanical strength to avoid gel residues after cleaning treatment. To assess on the potential of these novel hydrogels their release and retention properties were compared with the widely used agar-agar hydrogel.

1 INTRODUCTION

The usage of neat or blended organic solvents for painting cleaning presents several drawbacks due to the poor selectivity and environmental impact. The uncontrolled penetration of solvents into the painted layers may cause swelling or leaching of binders and varnishes (Phenix, A. & Sutherland, K. 2001, The cleaning of paintings: effects of organic solvents on oil paint films. *Reviews in Conservation*. 2: 47–60). To overcome these issues, water-based cleaning systems, such as microemulsions, have recently received much attention (Giorgi, R., Baglioni, M., Berti, D., Baglioni, P., 2010, New Methodologies for the Conservation of Cultural Heritage: Micellar Solutions, Microemulsions, and Hydroxide Nanoparticles. *Accounts of Chemical Research*. 43(6): 695-704 (references therein)), because the amount of organic solvents is very low and it is confined in a stable way. This ensures a bigger control of the cleaning process and a very low environmental impact. Obviously, this approach can be followed on artifacts that are not water-sensitive, i.e. wall paintings and stones. In fact, easel paintings in contact with water are prone to swelling of the hydrophilic layers, which often leads to painting detachment (Pizzorusso, G., Fratini, E., Eiblmeier, J., Giorgi, R., Chelazzi, D., Chevalier, A., Baglioni, P., 2012, Physicochemical characterization of acrylamide/bisacrylamide hydrogels and their application for the conservation of easel paintings. *Langmuir*. 28(8): 3952−3961).

In the last decades, conservators devised several methods to limit solvents action through the use of thickeners (e.g. cellulose ethers; polyacrylic acids, etc.).

More recently, a new class of gels, known as “rigid gels”, has been applied for restoration purposes. Namely, polysaccharide-based gels (e.g. agar-agar and gellan gum) have been used as a container for the controlled release of water solution (Campani, E., Casoli, A., Cremonesi, P., Saccani, I., Signorini, E., 2007. L’uso di Agarosio e Agar per la preparazione di “Gel Rigidi”. *Quaderni del Cesmar7 n.4*. Padova: Il Prato.). These gels can be described as ‘physical gel’, because the gelled state depends on the intermolecular and intramolecular interactions of polymer chains, which are weak (Van der Waals forces and hydrogen bonds) in terms of bond energy. In water-swollen physical gels the competition of water-polymer and polymer-polymer hydrogen bonds may reflect in the decrease of hydrogel mechanical stability. Thus, a small mechanical stress is enough for hydrogel deformation. Hence, from a practical point of view, these characteristics make the hydrogel hard to be handled, when the water content is high, and usually these gels leave residues on the painted surface because the interactions with the support are competitive with the gel cohesion forces.

Studies have been carried out in order to reduce the risk of gel residues and to enhance the hydrogel retention characteristics, as well as their exchange capability with the surface to be treated. As a result, some innovative confining systems have been developed, as described in literature (Baglioni, P., Dei, L., Carretti, E., Giorgi, R. 2009, Gels for the Conservation of Cultural Heritage. *Langmuir*. 25(15): 8373–8374; Carretti, E., Bonini, M., Dei, L., Berrie, B.H., Angelova, L.V., Baglioni, P., Weiss, R.G., 2010, New Frontiers in Materials Science for Art Conservation: Responsive Gels and Beyond. *Accounts of Chemical Research*. 43(6): 751-760 (references therein); Pizzorusso, G., Fratini, E., Eiblmeier, J., Giorgi, R., Chelazzi, D., Chevalier, A., Baglioni, P., 2012, Physicochemical characterization of acrylamide/bisacrylamide hydrogels and their application for the conservation of easel paintings. *Langmuir*. 28(8): 3952−3961).

The current study was focused on designing a new class of chemical hydrogels (i.e. able to load aqueous systems) that fulfill the right equilibrium between retention and release properties in order to ensure an efficient and controlled cleaning. Gelled state depends on the building of a polymer network that is characterized by the presence of covalent bonds, which are stronger than the weak intermolecular forces involved in physical gels. Chemical gels exhibit improved mechanical properties that avoid any left residues and can swell in a liquid medium without gel solubilization.

2 SEMI-IPN P(HEMA)/PVP HYDROGELS

The ideal hydrogel properties for application in cleaning of paintings are achieved if two important features are combined: mechanical strength and hydrophilicity. These two characteristics allow, on one hand, simple manipulation of gel and absence of gel residues after cleaning treatment and, on the other hand, an efficient exchange process between the cleaning system and the artifacts surface. In this contribution, the combination of these two properties is obtained through the synthesis of semi-interpenetrating polymer networks (semi-IPN).

Semi-IPNs are polymer blends in which linear or branched polymers are embedded into one or more polymer networks during polymerization. To obtain the semi-IPN hydrogels, the linear polymer polyvinylpyrrolidone – PVP – was embedded into the forming network of poly(2-hydroxyethyl methacrylate) – p(HEMA). P(HEMA) and p(VP) are extensively used and studied polymers. P(HEMA) forms very resistant hydrogels, however, their hydrophilicity is not sufficient for loading water-based cleaning systems. P(VP), on the other hand, is an high hydrophilic polymer. The semi-IPN hydrogels can be designed by varying their component ratios (water, PVP, HEMA and cross-linker quantities) in order to tune their characteristics in terms of mechanical behavior (softness, elasticity, and resistance to tensile strength) and affinity to water (Domingues, J.A.L., Bonelli, N., Giorgi, R., Fratini, E., Gorel, F., Baglioni, P., Innovative hydrogels based on semi-interpenetrating p(HEMA)/PVP networks for the cleaning of water-sensitive cultural heritage artifacts. *Langmuir* - paper submitted).

Hydrogel synthesis was carried out by free radical polymerization of 2-hydroxyethyl methacrylate (HEMA) monomer and a cross-linker, N,N'-methylene-bisacrylamide (MBA), in a water solution with linear PVP (~1300 KDa). A series of different hydrogels was designed by varying the proportions of monomer/cross-linker ratio with PVP and water percentages. Physico-chemical characterization was carried out by thermal analysis that allowed to calculate the free/bound water ratios and by a Field Emission Gun - Scanning Electron Microscopy (FEG-SEM) Sigma, from Carl Zeiss (Germany), for the study of micro-structure and porosity.

3 HYDROGEL CHARACTERIZATION

All the semi-IPN hydrogels formulations were found to have interesting macroscopic characteristics and satisfactory mechanical properties. Specifically, these hydrogels exhibit a wide range of features: from semi-rigid and completely transparent to pliable and translucent. In fact, they are to some extent softer than ordinary chemical gels, which is an important feature to obtain better adhesion to rougher surfaces. Moreover, the achieved mechanical strength permits to synthesize hydrogels that are film-shaped, with a thickness of ca. 2mm.

These gels are able to load big amount of water solutions or aqueous detergent systems; the equilibrium water content (EWC) value provides an estimation of the amount of cleaning systems can be kept in contact with the artworks surfaces. EWC is calculated as follows:

$$EWC = 100(W_w - W_d)/W_w \quad (1)$$

where W_w and W_d are respectively the weights of fully water swollen and dry hydrogels.

The EWC values for the studied formulations vary from ca. 70% to 90% without any loss of transparency. High EWCs are strictly dependent on hydrogel porosity and hydrophilicity of the network. The obtained results highlight that the addition of linear chains of PVP into the reaction mixture permits to increase water affinity, porosity and, consequently, the EWC of the hydrogels.

Water inside swollen hydrogels can be classified into three different states, depending on the interactions with the polar part of the polymer chains: unfreezable, bound-freezable and free water (Li et al. 2008) Free Water Index (FWI) parameter can be determined by thermal analysis (differential scanning calorimetry – DSC). The FWI can be obtained by the given formula:

$$FWI = \Delta H_{exp}/WC\Delta H_{theo} \quad (2)$$

where the ΔH_{exp} [J/g] represents the melting enthalpy variation for free water, *WC* is the water weight fraction in the hydrogel and ΔH_{theo} is the theoretical value of the specific enthalpy of fusion for bulk water. The FWI values obtained highlight that the free water amount inside the swollen hydrogels is much higher than bound water. Therefore, aqueous system loaded into the hydrogels will behave mostly as free water. The free water content varies from ca. 70% to 80% in respect of the total water quantity in swollen hydrogels.

In order to obtain some information about the structure and porosity of the lyophilized hydrogel (xerogel), FEG-SEM images were acquired. FEG-SEM image of one of the formulations is shown in figure 1. In general, sponge-like network morphology is observed and pore dimensions are approximately in the range of 5 to 40 μm. The difference of porosities between different hydrogel formulations is due to three main factors: the first is the water content in the initial polymerization mixture, which is the main responsible for the final gel porosity and the pore dimension; the second is due to the PVP loss during first washing steps after polymerization; and the third, the cross-linker amount, which contributes, at constant PVP/HEMA/H_2O ratios, to a more compact network structure. Although a compact network is present these hydrogels are highly flexible (see figure 1 right). It should be noted that SEM images refer to xerogels, so hydrogels are expected to have much larger pores in the swollen state.

4 ASSESSMENT ON RELEASE AND RETENTION PROPERTIES

In order to evaluate the effectiveness and versatility of the investigated hydrogel systems, some assessment tests were carried out. The hydrogels dehydration kinetics (recorded at 55% RH and 20ºC) was evaluated to verify if during the time required for the cleaning process the amount of detergent solution is enough. This assessment confirmed that for the first hour the amount of water inside hydrogels is still above 95% of the initial water content. Additionally, water release tests were performed to quantify the water amount flowing into a high hydrophilic support during cleaning process. For this purpose, water-loaded hydrogels were gently dried on the surface, then put on 4 sheets of Whatman® filter paper and covered with a lid to avoid water evaporation. The filter paper sheets were weighted before and after 30 minutes of application. All hydrogels performed a homogenous release of water restricted to the paper contact area. After 30 minutes of contact, released water ranges from 16±1 mg/cm^2 to 33±3 mg/cm^2, depending on the hydrophilicity of the formulation, while the same test performed using an agar-agar hydrogel released 166±8 mg/cm^2. It was important to compare semi-IPN hydrogel action with the widely used agar-agar hydrogel system. Agar-agar hydrogels were chosen because, like semi-IPN p(HEMA)/PVP hydrogels, they are used in conservation treatments in film shaped form and with water based solvent systems. In order to highlight the effective confinement of the cleaning process, some release tests on paper painted with a water-soluble colorant were performed. Few minutes of application are enough to evidence the difference between the two systems. In fact, while the area treated with agar-agar gel (figure 2) shows color leaching, semi-IPN p(HEMA)/PVP hydrogels presents any alterations also after 5 minutes of contact. Furthermore, abundant color absorption is shown by agar-agar gel, while few color traces were observed on the semi-IPN hydrogel surface.

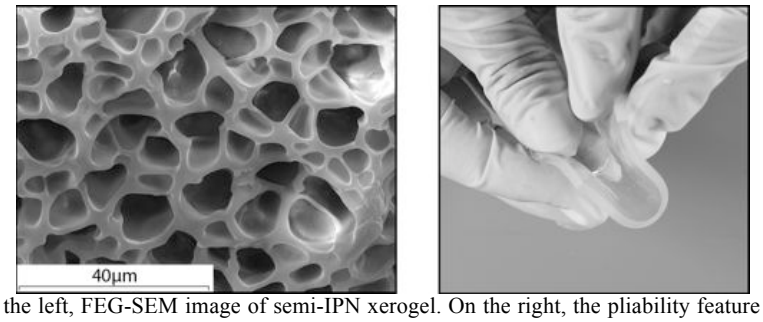

Figure 1. On the left, FEG-SEM image of semi-IPN xerogel. On the right, the pliability feature of the hydrogel is highlighted.

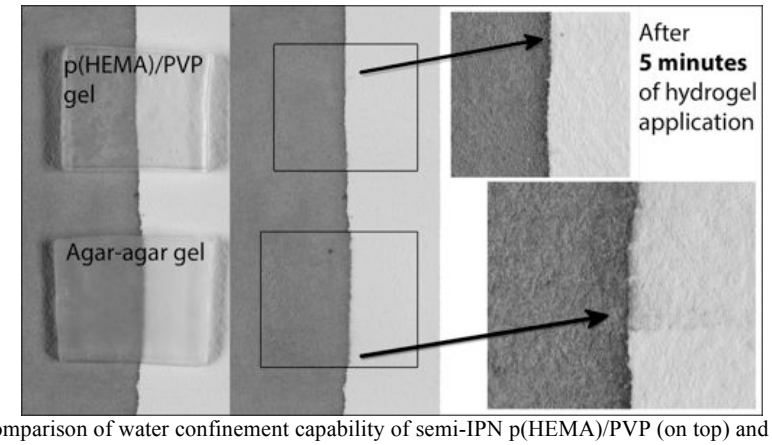

Figure 2. Comparison of water confinement capability of semi-IPN p(HEMA)/PVP (on top) and agar-agar (on bottom) hydrogels.

5 CONCLUSIONS

The assessment carried out on semi-IPN hydrogels has shown that these polymeric networks have most of the desired properties to achieve a high-controlled cleaning action, i.e. the appropriate equilibrium between release and retention properties. These features allow to obtain a real confinement of the cleaning system on the hydrogel-artifacts interface, and thus permit to use water based systems also on water–sensitive substrates, e.g. canvas paintings.

The direct comparison with the agar-agar hydrogel has highlighted that using semi-IPN hydrogels it is possible to obtain an enhanced control of the fluids penetration and to limit the interaction volume between cleaning system and treated surface.

REFERENCES

Baglioni, P., Dei, L., Carretti, E., Giorgi, R. 2009. Gels for the Conservation of Cultural Heritage. *Langmuir*. 25(15): 8373–8374.

Campani, E., Casoli, A., Cremonesi, P., Saccani, I., Signorini, E., 2007. L'uso di Agarosio e Agar per la preparazione di "Gel Rigidi". *Quaderni del Cesmar7 n.4*. Padova: Il Prato.

Carretti, E., Bonini, M., Dei, L., Berrie, B.H., Angelova, L.V., Baglioni, P., Weiss, R.G., 2010. New Frontiers in Materials Science for Art Conservation: Responsive Gels and Beyond. *Accounts of Chemical Research*. 43(6): 751-760 (references therein).

Domingues, J.A.L., Bonelli, N., Giorgi, R., Fratini, E., Gorel, F., Baglioni, P., (in preparation). Innovative hydrogels based on semi-interpenetrating p(HEMA)/PVP networks for the cleaning of water-sensitive cultural heritage artifacts. *Langmuir*.

Giorgi, R., Baglioni, M., Berti, D., Baglioni, P., 2010. New Methodologies for the Conservation of Cultural Heritage: Micellar Solutions, Microemulsions, and Hydroxide Nanoparticles. *Accounts of Chemical Research*. 43(6): 695-704 (references therein).

Pizzorusso, G., Fratini, E., Eiblmeier, J., Giorgi, R., Chelazzi, D., Chevalier, A., Baglioni, P., 2012. Physicochemical characterization of acrylamide/bisacrylamide hydrogels and their application for the conservation of easel paintings. *Langmuir*. 28(8): 3952−3961.

Phenix, A. & Sutherland, K. 2001. The cleaning of paintings: effects of organic solvents on oil paint films. *Reviews in Conservation*. 2: 47–60.

INTERNATIONAL JOURNAL OF CONSERVATION SCIENCE

ISSN: 2067-533X Volume 4, Special Issue, 2013: 715-722 www.ijcs.uaic.ro

INNOVATIVE METHOD FOR THE CLEANING OF WATER-SENSITIVE ARTIFACTS: SYNTHESIS AND APPLICATION OF HIGHLY RETENTIVE CHEMICAL HYDROGELS

Joana DOMINGUES, Nicole BONELLI,
Rodorico GIORGI, Emiliano FRATINI, Piero BAGLIONI*

Department of Chemistry "Ugo Schiff" and CSGI (Center for Colloid and Surface Science),
University of Florence, Via della Lastruccia 3, 50019 Sesto Fiorentino (FI), Italy.

Abstract

Cleaning is one of the most important processes for the conservation of cultural heritage artifacts, but also one of the most delicate and potentially damaging to the original materials. Nowadays, aqueous cleaning is usually preferred to cleaning with organic solvents, because it is environmental friendly and less aggressive to artifact's materials. However, in some circumstances, such as cleaning paper documents, easel paintings and textiles, water-based systems can be invasive. The interaction of water with the hydrophilic support favors mechanical stresses between substrate and paint layers, which can eventually lead to paint detachment or paint leaching. Water-based detergent systems (such as micellar solutions and oil-in-water microemulsions) offer several advantages in terms of selectivity and gentle removal of hydrosoluble (e.g. grime) and hydrophobic (e.g. aged adhesive) materials. The confinement and controlled release of these water-based systems is achieved through the synthesis and application of chemical hydrogels specifically designed for cleaning water-sensitive cultural heritage artifacts. These gels are based on semi-interpenetrating p(HEMA)/PVP networks. Semi-IPN hydrogels are prepared by embedding linear polyvinylpyrrolidone physically into a network of poly(2-hydroxyethyl methacrylate). Water retention and release properties were investigated. The micro-porosity was studied by Scanning Electron Microscopy. To demonstrate both efficiency and versatility of the selected hydrogels in confining the most appropriate water-based cleaning system a representative case study is presented.

Keywords: *Semi-IPN hydrogels; Cleaning; Nanocontainers; Gel structure.*

Introduction

In general, most of the materials and methods used for conservation treatments are initially designed for application in other fields and then adapted by restorers for their specific purposes. This implies that the common procedure may not have the most suitable features demanded by each particular case study. In the last decades our research group is being concerned in providing

* Corresponding author: baglioni@csgi.unifi.it

conservators new tools based on nanotechnology that are specifically designed to answer different issues in conservation of cultural heritage [1-3].

Usually, a cleaning process is carried out to remove superficial layers that may induce further degradation to the artifact. These layers can be hydrophilic (e.g. superficial grime) or hydrophobic (e.g. aged varnishes and adhesives). While the removal of hydrophilic layers is easily performed with aqueous methods, the removal of hydrophobic layers is commonly carried out through the use of pure organic solvents. Most organic solvents are toxic and do not allow a controlled cleaning since they can quickly diffuse into inner layers [4, 5].

Dissolving hydrophobic materials, such as polymers, through non-confined pure solvents can cause their penetration within artifacts' porous matrix. After solvent evaporation polymer residues may remain within the substrate porosity.

Nanostructured fluids (e.g. oil-in-water microemulsions, micellar solutions) have been developed by the CSGI (Center for Colloid and Surface Science) to address this problem [6-8]. A microemulsion is a high-performing cleaning tool since it can remove hydrophobic layers using a small amount of organic solvents. The microemulsion droplets contain the appropriate solvent able to swell or solubilize the polymeric layers, while the water in the dispersing phase can penetrate within the porous substrate of the artifact, avoiding the risk of redeposition of the dissolved polymers, because of its affinity with the hydrophilic pores of the surface.

The use of confining tools that are able to retain capillary penetration of water-based systems is particularly important in the specific case of water-sensitive substrates (e.g. paper manuscripts, canvas paintings).

Nowadays the most used confining methods in conventional conservation practice include the use of cellulose pulp poultices and some physical gels [9, 10] (cellulose derivatives, polyacrylic acids, polysaccharide-based gels, and others), which do not have the suitable retentive features for the cleaning of water-sensitive artifacts. For this reason, highly retentive chemical "sponges" that allow a controlled release of the cleaning system, limiting its action only to the first few layers of the painted surface, were developed. For this, efforts were focused on the polymer gel technology.

Gels can be divided into two major categories, depending on the nature of their bonds: physical and chemical gels. Physical gels are formed by electrostatic interactions between polymeric chains, so they are usually viscous systems that can respond to heat or be disrupted by mechanical forces. Polysaccharide based gels (e.g. agar-agar or gellan gum) are an example of physical gels and are, at present, one of the most promising tools used by conservators with the intent of retaining the cleaning agent [11]. These gels, however, are fragile and do not have the suitable retention features.

Chemical gels are, on the other hand, characterized by the presence of covalent bonds. They have a specific shape given during synthesis and have strong gel cohesion, so no gel residues are expected after treatment using chemical gels. Chemical gels are more versatile because depending on the components (monomer, cross-linker, liquid medium, etc.) and the quantitative proportions it is possible to obtain gels with different chemical-mechanical properties [12-14]. In the specific case of cleaning water-sensitive artifacts, the ideal container would be a highly retentive soft hydrogel. In this paper we present the potential application of highly retentive hydrogels based on semi-interpenetrating polymer networks (semi-IPN) composed by a cross-linked polymer network of polyhydroxyethylmethacrylate (p(HEMA)) and an interpenetrating linear polymer of polyvinylpyrrolidone (PVP) that does not form covalent bonds with HEMA. These two polymers are biocompatible materials, largely used in the biomedical and pharmaceutical areas. The amount of PVP modulates the hydrophilicity and softness of the final product, while p(HEMA), constituting the

three-dimensional network, largely determines the mechanical properties. A high equilibrium water content (EWC) of hydrogels, which is correlated to pore dimensions, and hydrophilicity of the polymer network, is consistent with high hydrogel softness. Moreover, polymer network hydrophilicity is related to hydrogels' retention capacity, because the interaction forces of aqueous system/polymer network may prevail over the ones of aqueous system/artifacts surface.

Materials and Methods

Synthesis of p(HEMA)/PVP hydrogels

HEMA monomer and the cross-linker N,N'methylenebisacrylamide (MBA) were mixed together in a water solution with linear PVP (average Mw~1300 kDa). The reaction mixture was bubbled with nitrogen for 5 minutes to remove oxygen and then radical initiator 2,2'-Azobis(2-methylpropionitrile) was added in a 1:0.01 monomer/initiator molar ratio. The reaction mixture was gently sonicated for 30 minutes in pulsed mode to eliminate possible gas bubbles. The polymerization reaction, started by thermal homolysis of the initiator, was performed for 4h at 60ºC. After polymerization, hydrogels were placed in containers with distilled water.

Table 1. Composition (w/w) of three representative semi-IPN p(HEMA)/PVP hydrogels already applied for cleaning of cultural heritage artifacts.

Hydrogel	HEMA	PVP	MBA	H_2O	Monomer/cross-linker ratio	HEMA/PVP ratio
H50	25.0%	24.9%	0.2%	49.9%	1:1 x 10^{-2}	1:1
H58	16.8%	25.1%	0.2%	57.9%	1:1.5 x 10^{-2}	1:1.5
H65	10.5%	24.5%	0.2%	64.9%	1:2 x 10^{-2}	1:2.3

Hydration cycle

To investigate how much water a semi-IPN hydrogel can load after synthesis until equilibrium is reached, hydrogel weight was registered at different times, as follows:

$$\text{Water uptake (\%)} = \frac{W_i - W_{0*}}{W_{0*}} \times 100 \quad (1)$$

where W_i is the hydrogel weight obtained at time *i*, W_{0*} is the hydrogel weight immediately after synthesis.

Fourier Transform Infrared Spectroscopy (FTIR)

A FTIR spectrometer (Thermo Nicolet Nexus 870) in attenuated total reflectance mode (ATR-FTIR), equipped with a Golden Gate diamond cell was used to verify the absence of gel residues after direct contact with canvas. Data were collected with a MCT detector with a sampling area of 150 μm^2. The spectra were obtained from 128 scans with 4 cm^{-1} of optical resolution.

Scanning Electron Microscopy (SEM)

A FEG-SEM ∑IGMA (Carl Zeiss, Germany) was used to acquire images from xerogels (freeze-dried hydrogels) using an acceleration potential of 1 kV and a working distance of 1.9 mm.

Results and Discussion

The investigated semi-IPN hydrogels were designed to address the problem of cleaning water-sensitive surfaces. Accordingly, the most important gel features are transparency, softness, high-retention and gel cohesion to avoid any gel residues on the surface after cleaning treatment. Each of these hydrogels' features is discussed in more detail further in this work.

Hydrogels' transparency and softness

Semi-IPN p(HEMA)/PVP hydrogels are transparent and soft, as highlighted in figure 1. The material's transparency is very important in restoration treatments because it allows the restorer a visual control of the cleaning process. These hydrogels can load as well other aqueous systems and pure solvents without losing their transparency. Their softness permits an acceptable adhesion to most surfaces, as illustrated in figure 1 (left). Furthermore, these hydrogels can remain attached to surfaces both in vertical position and upside down, allowing treatments on wall paintings or painted ceilings.

Fig. 1. Semi-IPN hydrogel (H65) on a travertine stone. On the left, the hydrogel applied in vertical position; on the right, the hydrogel removal is shown. It is worth noting that the stone surface is wet only in correspondence with the contact area.

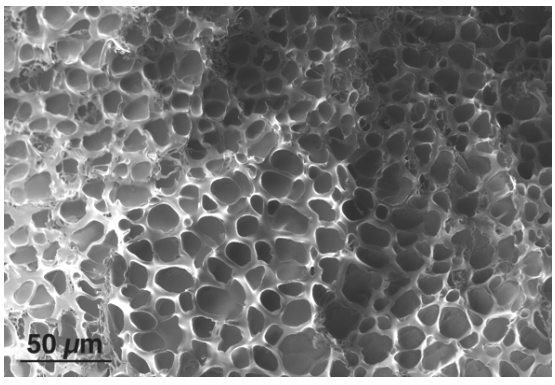

Fig. 2. SEM image of semi-IPN H65 hydrogel in xerogel form (lyophilized hydrogel).

Semi-IPN hydrogels present a mesoporosity that was investigated using a Scanning Electron Microscope (SEM). The SEM image of H65 xerogel's porosity is presented in figure 2. A sponge-like structure is noted, with pore dimensions varying from 5 to 40 μm. Hydrogels' porosity is mainly given by the presence of water during synthesis. Formulations with higher initial water amount in the reaction mixture show higher porosity.

Hydrogels' hydrophilicity and retention capacity

Three formulations were devised for addressing the specific demands of different case studies (see table 1). The main differences between gel formulations are the softness and retention capacity. The softer hydrogels are also the most hydrophilic. Hydrophilicity is correlated with the water content inside hydrogels, so less hydrophilic hydrogels have less water content. The water amount in the reaction mixture is 50% (w/w) in H50 and 65% (w/w) in H65. After the synthesis, the newly formed semi-IPN sponge can still load a high quantity of water until equilibrium water content (EWC) is reached. Curves in figure 3 show the difference in water loading capacity (i.e. hydrophilicity) of two hydrogel formulations (H50 and H65). H65 hydrogel, the most hydrophilic one, displays a water uptake of ~134%, while H50 have a water uptake of ~64%.

The hydration cycle permits to investigate the time required to reach the EWC after synthesis; all the investigated gel formulations need about 6 days. Only when the EWC is reached, can the hydrogels be used for cleaning procedures. Furthermore, if needed, it is possible to exchange the already water-loaded hydrogels with another water-based system, such as oil-in-water microemulsions, or pure organic solvents, by putting them in a filled container with the liquid to be loaded inside hydrogels. This exchange takes approximately 12h.

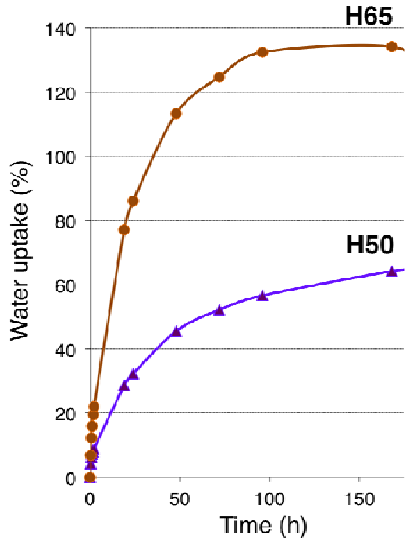

Fig. 3. Hydration cycle for two semi-IPN hydrogel formulations.

After 4h exposure to the air in a controlled environment (55% relative humidity and 20ºC), water-loaded hydrogels (shaped as a 1 cm square, with 2 mm thickness) still maintain a water content of around 90% with respect to EWC. This means that these hydrogels limit the

liquid evaporation rate and, thus, allow a longer contact between cleaning system and artifact's surface.

Hydrogels' cohesion

The cross-linked polymer network of semi-IPN hydrogels implies very high gel cohesion, which prevents gel residues on the surface after cleaning treatments.

To confirm this statement, ATR-FTIR spectra, shown in figure 4, were collected from a cotton canvas, which is a very hydrophilic surface, after direct contact with semi-IPN hydrogels. For instance, the characteristic intense bands assigned to the carbonyl stretching vibration of both HEMA and PVP (respectively 1724 and 1654cm^{-1}) are not visible in the spectra of cleaned canvas; this confirmed that no detectable gel residues are left on canvas due to gel contact.

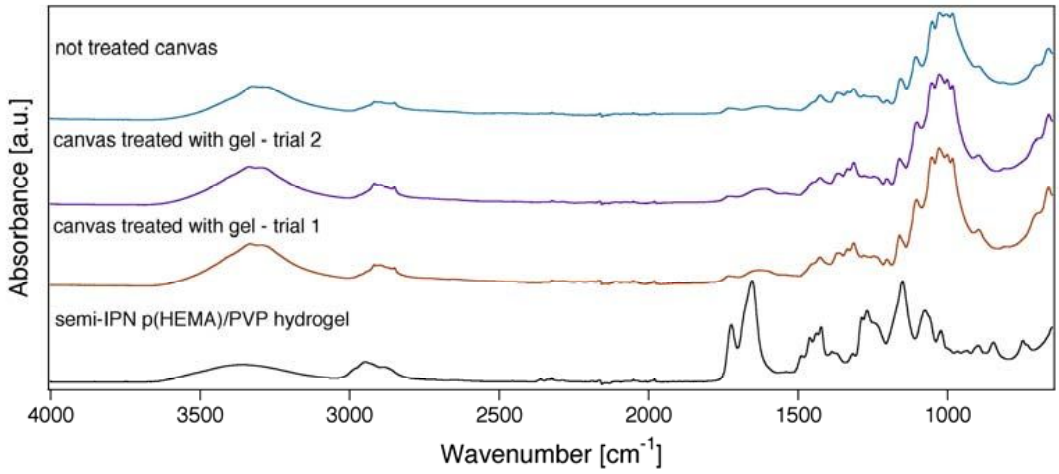

Fig. 4. ATR-FTIR spectra to verify the absence of gel residues on canvas after direct contact with semi-IPN hydrogels.

Cleaning tests

These semi-IPN hydrogels permit a highly controlled cleaning and could replace the common methods used in conservation, such as the use of a wetted cotton-swab (largely used for the application of water or other solvents directly over the painted surface). In order to make a comparison between these two techniques a mock-up sample of a water-sensitive material (canvas) was prepared. Acrylic and vinyl tempera were used to paint the canvas. On the top of the paint layer, a thin deposit of the hydrophilic artificial grime mixture developed by Wolbers [15] was applied. It is well known that acrylic and vinyl color applied on canvas tend to lose adhesion with the support when in contact with water. For that reason, this mock-up sample was a good reference material to check the efficiency of this new gel-based technique. Cleaning tests were carried out using different hydrogel formulations, and compared with a classic wetted cotton-swab cleaning. Results are summarized in figure 5. None of the hydrogel formulation led to color removal. The best cleaning result was achieved with formulation H65. On the other hand, evident color traces were noted on cotton-swab after its use (Fig. 5 right), due to the swelling and loss of adhesion of the paint layer favored by water.

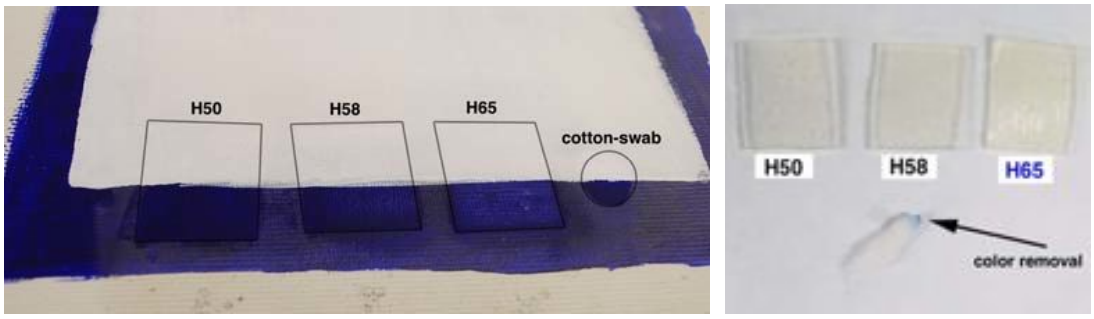

Fig. 5. Cleaning tests on a canvas painted with modern tempera (acrylic/vinyl resins) and coated with artificial grime. Cleaning was performed with water-loaded semi-IPN hydrogels applied for 5 minutes. Cotton-swab wetted with water was used for comparison purpose.

Conclusions

Chemical semi IPN hydrogels are a suitable tool to achieve a controlled cleaning action on water-sensitive cultural heritage artifacts. They are transparent and easy to manipulate, can load high quantities of water-based cleaning systems and keep them in contact with surfaces for the time required for the cleaning. Several advantages in respect to traditional cleaning methods (physical gels and cotton swab) were observed: due to the strong gel cohesion no residues are left on the surface after cleaning and no pigments removal was observed after contact with water-sensitive paint layers.

Funding Body

J. D. acknowledges financial support provided by Fundação para a Ciência e a Tecnologia (FCT) through a Ph.D. research grant (SFRH/BD/73817/2010). This work was partly supported by the CSGI, the European Union, Project NANOFORART (FP7-ENV-NMP-2011/282816) and the Ministry for Education and Research (MIUR, PRIN-2009P2WEAT).

References

[1] P. Baglioni, D. Chelazzi, R. Giorgi, G. Poggi, *Colloid and Materials Science for the Conservation of Cultural Heritage: Cleaning, Consolidation, and Deacidi cation*, **Langmuir**, **29**, 2013, pp. 5110−5122.

[2] P. Baglioni, D. Chelazzi (eds), **Nanoscience for the Conservation of Works of Art**, Royal Society of Chemistry, Oxfordshire, 2013.

[3] P. Baglioni, D. Berti, M. Bonini, E. Carretti, L. Dei, E. Fratini, R. Giorgi, *Micelle, Microemulsions, and Gels for the Conservation of Cultural Heritage*, **Advances in Colloid and Interface Science**, 2013, DOI 10.1016/j.cis.2013.09.008.

[4] N. Stolow, *Application of Science to Cleaning Methods: Solvent Action Studies on Pigmented and Unpigmented Linseed Oil Films*, **Recent Advances in Conservation, Proceedings of the IIC Rome Conference, Rome, Italy, 1961**, Butterworths, London, 1963, pp. 84−88.

[5] A. Phenix, K. Sutherland, *The Cleaning of Paintings: Effects of Organic Solvents on Oil Paint Films*, **Reviews in Conservation**, **2**, 2001, pp. 47−60.

[6] M. Baglioni, D. Berti, J. Teixeira, R. Giorgi, P. Baglioni, *Nanostructured Surfactant-Based Systems for the Removal of Polymers from Wall Paintings: A Small-Angle Neutron Scattering Study*, **Langmuir**, **28**, 2012, pp. 15193-15202.
[7] M. Baglioni, R. Giorgi, D. Berti, P. Baglioni, *Smart Cleaning of Cultural Heritage: a New Challenge for Soft Nanoscience*, **Nanoscale**, **4**, 2012, pp. 42-53.
[8] R. Giorgi, M. Baglioni, D. Berti, P. Baglioni, *New Methodologies for the Conservation of Cultural Heritage: Micellar Solutions, Microemulsions, and Hydroxide Nanoparticles*, **Accounts of Chemical Research, 43**, 2010, pp. 695-704.
[9] R. Wolbers, **Cleaning Painted Surfaces: Aqueous Methods**, Archetype, London, 2000.
[10] P. Cremonesi, **L'Uso di Tensioattivi e Chelanti nella Pulitura di Opere Policrome**, Il Prato, Padua, 2004.
[11] E. Campani, A. Casoli, P. Cremonesi, I. Saccani, E. Signorini, *Use of Agarose and Agar for preparing "Rigid Gels"*, **Quaderni del Cesmar 7**(4), Ed. Il Prato, Padova, 2007.
[12] M. Bonini, S. Lenz, E. Falletta, F. Ridi, E. Carretti, E. Fratini, A. Wiedenmann, P. Baglioni, *Acrylamide-Based Magnetic Nanosponges: A New Smart Nanocomposite Material*, **Langmuir**, **24**, 2008, pp.12644-12650.
[13] G. Pizzorusso, E. Fratini, J. Eiblmeier, R. Giorgi, D. Chelazzi, A. Chevalier, P. Baglioni, *Physicochemical Characterization of Acrylamide/Bisacrylamide Hydrogels and Their Application for the Conservation of Easel Paintings***, Langmuir**, **28**, 2012, pp. 3952-3961.
[14] J. Domingues, N. Bonelli, R. Giorgi, E. Fratini, F. Gorel, P. Baglioni, *Innovative Hydrogels Based on Semi-Interpenetrating p(HEMA)/PVP Networks for the Cleaning of Water-Sensitive Cultural Heritage Artifacts*, **Langmuir**, **29**, 2013, pp. 2746-2755.
[15] R. Wolbers, *The Use of a Synthetic Soiling Mixture as a Means for Evaluating the Efficacity of a Aqueous Cleaning Materials on Painted Surfaces*, **Conservation-Restauration Biens Culturels**, **4**, 1992, pp. 22-29.

Received: October, 11, 2013
Accepted: December, 07, 2013

Appl. Phys. A (2014) 114:705–710
DOI 10.1007/s00339-013-8150-0

Applied Physics A
Materials Science & Processing

Chemical semi-IPN hydrogels for the removal of adhesives from canvas paintings

Joana Domingues · Nicole Bonelli · Rodorico Giorgi · Piero Baglioni

Received: 9 July 2013 / Accepted: 8 November 2013 / Published online: 29 November 2013

Abstract Semi-interpenetrating (IPN) poly (2-hydroxyethyl methacrylate)/polyvinylpyrrolidone hydrogels were synthesized and used for the removal of adhesives from the back of canvas paintings. The high water retention capability and the specific mechanical properties of these gels allow the safe cleaning of water-sensitive artifacts using water-based detergent systems. The cleaning action is limited to the contact area and layer-by-layer removal is achieved while avoiding water spreading and absorption within water-sensitive substrates, which could lead, for example, to paint detachment. The use of these chemical gels also avoids leaving residues over the treated surface because the gel network is formed by covalent bonds that provide high mechanical strength. In this contribution, the physicochemical characterization of semi-IPN chemical hydrogels is reported. The successful application of an o/w microemulsion confined in the hydrogel for the removal of adhesives from linen canvas is also illustrated.

1 Introduction

Several conservation issues are continuously demanding innovative materials and techniques capable of providing efficient long-term preservation of cultural heritage artifacts. Cleaning is very challenging because of the difficulty in removing soiling materials with efficiency and with a high selective and controlled action. Wet cleaning provides several tools for gentle removal of unwanted materials, but the use of neat solvents has limitations due to the porosity of the artifact that favors the capillary absorption of the liquid phase, with the consequent spreading of the solubilized materials within the original artwork's materials [1]. Moreover, in the case of easel paintings, the low control of solvents penetration may cause swelling or leaching of the artifacts' organic materials [2].

Recently, several nanostructured fluids have been formulated with enhanced properties in terms of cleaning capability. Most of them are water-based systems efficient in the swelling, solubilization and removal of hydrophobic coatings, e.g. microemulsions, micellar solutions. Moreover, oil-in-water microemulsions guarantee the confinement of the specific solvent for the material to be removed within oil microemulsion droplets preventing the spreading into the artifact [3, 4]. These systems are very versatile and optimal for several applications, yet, in some cases, limitations could still persist. In fact, in the case of water-sensitive artifacts (e.g. paper manuscripts or canvas paintings), the strong interaction between the aqueous continuous phase of the microemulsion/micellar solution and the hydrophilic substrates can lead to deformations, halos and detachment of material. For this reason, in order to benefit from these nanofluids, it is of paramount importance to use highly retentive containers capable of efficiently confining these detergent systems, with the aim of limiting their cleaning action merely at the interface.

Solvent gels, i.e, solvents in their thickened state, are one of the present methods used by conservators to minimize solvent penetration into the artifact [5]. However, the use of solvent gels entails a considerable risk related to the residues that remain on the surface after cleaning. In fact, after the cleaning procedure it is always necessary to

J. Domingues · N. Bonelli · R. Giorgi · P. Baglioni (✉)
Department of Chemistry Ugo Schiff and CSGI,
University of Florence, Via della Lastruccia 3, Sesto Fiorentino,
50019 Florence, Italy
e-mail: baglioni@csgi.unifi.it

J. Domingues
e-mail: domingues@csgi.unifi.it

perform an appropriate removal of the residues through the use of organic solvent blends. To overcome this limitation, conservators and scientists have recently devised new confining methods, one of which is the use of polysaccharide-based physical gels (e.g. agar-agar, gellan gum) for the cleaning of various types of materials [6]. However, these physical gels do not exhibit the appropriate features for cleaning water-sensitive artifacts, since the weak bond interactions of the gel structure can lead to excessive water release. Chemical hydrogels, on the other hand, have a polymeric network constituted by covalent bonds and, therefore, exhibit improved mechanical features. Moreover, in latter studies chemical gels have shown to have high retention capability and controlled water release without leaving any gel residues on the artifact [7, 8]. Chemical gels can be shaped in the desired form during the synthesis and can load high amounts of liquid phase, without undergoing gel solubilization.

In this paper we report the innovative use of hydrogels based on semi-interpenetrating polymer networks (semi-IPN) loaded with an o/w microemulsion for the removal of aged adhesives from a backside of a canvas painting. In relation to previous acrylamide/bisacrylamide hydrogels [7], semi-IPN hydrogels have similar hydrophilic features, but are more resistant, transparent and are highly retentive and, therefore, appropriate for cleaning water-sensitive artifacts. In a previous work (see reference [8]) hydrophilic layers of grime were removed from a Thang-Ka (water-sensitive substrate based on tempera magra technique) using water-loaded semi-IPN hydrogels. In this paper we used p(HEMA)/PVP hydrogels to remove hydrophobic layers, such as aged polymers, using the appropriate detergent system (a microemulsion) confined into the gel network. We showed that these gels are very versatile and can be used to remove different kinds of materials from various types of water-sensitive substrates.

The semi-IPN hydrogels described here are constituted by a network of poly(2-hydroxyethyl methacrylate) [p(HEMA)], which contributes to the hydrogel mechanical strength, and the interpenetrated linear polymer polyvinylpyrrolidone (PVP), that contributes to the hydrogel hydrophilicity. Some of the most important characteristics of these hydrogels are the softness [9] and their capability to confine the cleaning action exclusively to the contact area, where only the first few layers of the artwork's surface are in contact with the solvent system [8] allowing a controlled layer-by-layer cleaning treatment. The hydrogels' capability to load different cleaning systems (e.g. pure and mixed solvent systems, micellar solutions, microemulsions) is shown here for the first time.

The case study reported is a lining removal. A lining consists of a structural treatment where a new canvas is attached to the backside of the canvas support (see Fig. 1, left). Aging of linings leads to an accelerated degradation of the painting caused by acid formation due to molecular decay of the used adhesives, so lining removal is often necessary. Adhesives removal is very stressful for the painting because, on one hand the use of pure solvents can transport the dissolved polymer into the canvas fibers and, in the worst cases, into the preparation layers (see Fig. 1, right) and, on the other, canvas can easily absorb water-based systems, leading to the swelling of the hydrophilic layers of the painted artifact, which may lead to paint detachment.

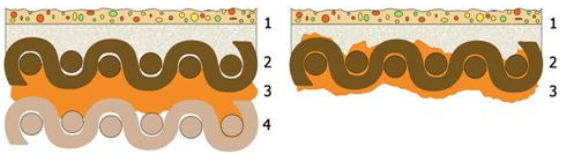

Fig. 1 Schematic cross-section of a painting with a lining (*left*) and after its removal using solvent technology (*right*). *1* Preparation and painted layers; *2* original canvas; *3* adhesive; *4* canvas used for lining

2 Experimental

2.1 Synthesis of hydrogels

The semi-IPN hydrogels were prepared by embedding PVP (average Mw $\approx$1,300 kDa) physically into the forming hydrogel network of HEMA. For this purpose HEMA monomer and the cross-linker *N*,*N*′-methylenebisacrylamide (MBA) were mixed together in a water solution with linear PVP. The reaction mixure was bubbled with nitrogen for 5 min to remove the oxygen and then the radical initiator α, α′-azoisobutyronitrile was added in a 1:0.01 monomer/initiator molar ratio. The reaction mixture was gently sonicated for 30 min in pulsed mode to eliminate the possible gas bubbles. Different formulations of hydrogels were prepared by varying the proportions of monomer/

Table 1 Compositions (w/w) of the selected semi-IPN hydrogels; HEMA/MBA and HEMA/PVP ratios

	H50	H58	H65
HEMA (%)	25.0	16.8	10.5
MBA (%)	0.2	0.2	0.2
PVP (%)	24.9	25.1	24.4
Water (%)	49.9	57.9	64.9
HEMA/MBA ratio	$1:1 \times 10^{-2}$	$1:1.5 \times 10^{-2}$	$1:2 \times 10^{-2}$
HEMA/PVP ratio	50/50	40/60	30/70

The acronym HXX refers to the XX percentage of water in the reaction mixture

cross-linker ratio with PVP and water percentages. The composition of the three investigated systems is reported in Table 1. The polymerization reaction by thermal homolysis of the initiator was performed for 4 h at 60 °C. After polymerization, the hydrogels were washed and placed in containers with distilled water.

Polysaccharide-based physical gels (agar–agar and gellan gum) were also prepared by dispersion of dry powders in water with 3 % (w/w). Powders were supplied by C.T.S. Italy (trademarks AgarArt and Kelcogel).

2.2 Physicochemical characterization

The gel content (G) gives the fraction between the mass of the final semi-IPN p(HEMA)/PVP hydrogel and the mass of the two components in the initial mixture, which can be calculated as follows [10]:

$$G\,(\%) = (W_d/W_0) \times 100 \quad (1)$$

where W_d is the dry weight of the hydrogel and W_0 is the weight of HEMA and PVP in the initial reaction mixture. The equilibrium water content (EWC) of hydrogels gives information on the polymer network hydrophilicity and can be calculated as follows:

$$\mathrm{EWC} = [(W_w - W_d)/W_w] \times 100 \quad (2)$$

where W_w is the weight of the water swollen hydrogel in equilibrium obtained at least 7 days after polymerization reaction.

Water release feature provides a better understanding of the retention capability of each gel system. The surfaces of fully swollen hydrogels were gently dried and the gel was put on three sheets of Whatman® filter paper inside a plastic Petri dish with lid to avoid water evaporation. The sheets of filter paper were weighed before and after 30 min of gel application.

The loading gel capacity toward different cleaning systems was calculated by immersing the lyophilized H58 hydrogel into the selected solvents. Squared hydrogel films of about 1 cm^2 and 2 mm of thickness were used. Both hydrogel weights and size were registered before and after immersion in the solvent to estimate the quantity of loaded solvent by each gel. The solvents were chosen from those commonly used by conservators [11].

A FTIR spectrometer (Thermo Nicolet Nexus 870) in attenuated total reflectance FT-infrared mode (ATR-FTIR), equipped with a Golden Gate diamond cell was used to investigate on possible gel residues after a cleaning treatment. Data were collected with an MCT detector with a sampling area of 150 μm^2. The spectra were obtained from 128 scans with 4 cm^{-1} of optical resolution.

A FEG-SEM ΣIGMA (Carl Zeiss, Germany) was used to acquire images from xerogels (freeze-dried hydrogels) using an acceleration potential of 1 kV and a working distance of 1.4 mm.

2.3 Removal of aged polymer adhesives

To evaluate the effectiveness of the prepared hydrogel systems, cleaning tests on model samples were performed. Linen canvas samples were previously treated with two different polymers widely used in lining procedure, Mowilith® DM5 (vinyl acetate/*n*-butyl acrylate copolymer) and Plextol® B500 (ethyl acrylate/methyl methacrylate copolymer). To simulate the natural aging process samples were submitted to an artificial aging as described in the literature [12].

The hydrogels were loaded with EAPC o/w microemulsion [1] through immersion for at least 12 h before application on canvas. This microemulsion is composed of water (73.3 wt%), sodium dodecyl sulfate (3.7 wt%), 1-pentanol (7.0 wt%), propylene carbonate (8.0 wt%) and ethyl acetate (8.0 wt%). The hydrogel loaded with the microemulsion EAPC was kept in contact with the canvas surface for 4 h. To avoid evaporation of the microemulsion, the hydrogel was covered with a plastic foil. A Whatman® filter paper was placed on the backside of the canvas to verify the absence of dissolved polymer or solvent diffusing through the canvas. After the gel application, the aged polymeric adhesive was swollen and softened and could be easily removed with gentle mechanical action.

3 Results and discussion

The three p(HEMA)/PVP hydrogels formulations here presented were designed to address different needs in conservation concerning cleaning. The gel content (G) in this type of hydrogels is usually low because there are no chemical bonds between polymer network and interpenetrated linear polymer, so any excess of the latter can be washed out. H50 hydrogel presents a G value of 90 % (Table 2), which is comparable with the G of acrylamide

Table 2 Some physicochemical properties of the selected p(HEMA)/PVP, acrylamide [7] and polysaccharide hydrogels

	G (%)	EWC (%)	Water release (mg/cm^2)
H50	90	72	8
H58	78	80	15
H65	74	87	16
Acrylamide "Hard"	95	95	27
Acrylamide "Soft"	88	97	56
AgarArt	-	97	30
Kelcogel	-	97	33

chemical gels. This is a considerable fact since there is a 50/50 p(HEMA)/PVP ratio. This sustains the presence of hydrogen bonds between HEMA and PVP [13]. However, increasing linear PVP amount with respect to HEMA leads to a substantial drop in *G* at a specific p/(HEMA)/PVP ratio, meaning that the available area of HEMA network is not enough to encompass more PVP.

In general, all the synthesized semi-IPN hydrogels are transparent and soft. The systems differ mainly in hydrophilicity, i.e., water loading and water release features. These properties can be tuned before synthesis by variation of their component ratios (HEMA/PVP, HEMA/cross-linker, water/reaction mixture). In particular, from H50 to H65 the hydrophilicity character increases as demonstrated by the EWC values reported in Table 2. The physical gels (AgarArt and Kelcogel) have an EWC of 97 %, which correlates with an excessive water release for cleaning water-sensitive substrates, as illustrated in a previous work [8]. In fact, water release test shows that physical gels release water at least twice as much as semi-IPN hydrogels. Acrylamide gels have a high EWC and show an higher water release with respect to semi-IPN hydrogels, which are for that reason more suitable for the cleaning of water-sensitive substrates.

Table 3 Amount of loaded solvents in hydrogel H58 and loading percentage with respect to the water loaded gel

	Solvent/xerogel (w/w)	%
Acetic acid	11.17	270
Benzyl alcohol	10.70	254
2-Methoxyethanol	4.02	33
Ethylene glycol	3.98	32
Ethanolamine	3.81	26
Water	3.02	0
Ethyl alcohol	2.97	−2
Propylene glycol	2.72	−10
Methyl alcohol	2.47	−18
2-Butanol	1.74	−42
Cyclohexane	n.l.	n.l.
Heptane	n.l.	n.l.
p-Xylene	n.l.	n.l.
Triethanolamine	n.l.	n.l.
Toluene	n.l.	n.l.
Acetone	n.l.	n.l.
Butyl acetate	n.l.	n.l.
2-Butoxyethanol	n.l.	n.l.
Methyl ethyl ketone	n.l.	n.l.
Propylene carbonate	n.l.	n.l.

n.l. not loaded

Semi-IPN p(HEMA)/PVP hydrogels are capable to load pure solvents as well. The loading capacity for some pure solvents is presented in Table 3. As expected, only the more polar solvents are loaded in semi-IPN hydrogels.

Mesoporosity was investigated through FEG-SEM images obtained from freeze-dried hydrogels (xerogels). It is known that some structure collapse may occur when ice forms. To verify this, EWC was calculated before and after freeze-drying process. A difference was noticed especially for H65 hydrogel that showed an EWC decrease of ca. 8 % that has to be considered when analyzing FEG-SEM images. FEG-SEM images of H50 and H65 hydrogels (Fig. 2) show the presence of a sponge-like structure. The difference between H50 and H65 hydrogels' porosity is mainly due to the quantity of water in the reaction mixture (50 and 65 % w/w, respectively), but also to PVP loss after polymerization, noted from *G* value, which contributes to larger pores due to the volume fraction of the macromolecule.

To confirm that these chemical gels do not leave residues on the surface after a cleaning treatment ATR-FTIR spectra were performed on canvas previously in contact with water-loaded semi-IPN gels. ATR-FTIR spectra reported in Fig. 3 show two reference spectra (a cotton canvas and a H50 hydrogel) and spectra from two canvas samples treated with H50 and H65. The characteristic carbonyl stretching vibration bands of HEMA and PVP are not present in the spectra of the treated canvases, proving that no detectable gel residues are left after the cleaning procedure.

The removal of aged adhesives from the back of canvas paintings can be done using oil-in-water microemulsions. However, in order to ensure a controlled cleaning process, the confinement of this cleaning tool inside hydrogels is

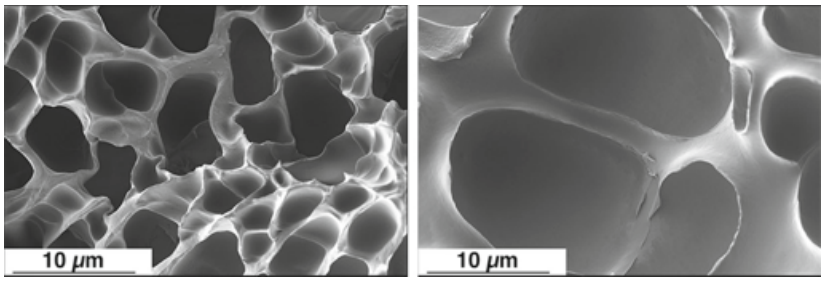

Fig. 2 FEG-SEM images of H50 (*left*) and H65 (*right*) xerogels

important to minimize fibers swelling due to contact with the water phase. It has been recently shown that an ethyl acetate/propylene carbonate based microemulsion (μEAPC) can be effectively loaded inside acrylamide hydrogels and provide an efficient removing of lining adhesives [7]. The use of p(HEMA)/PVP hydrogels loaded with this microemulsion was considered mainly because of the high water retention capability. The application of μEAPC loaded hydrogels H50 and H65 for the removal of aged adhesives is illustrated in Fig. 4.

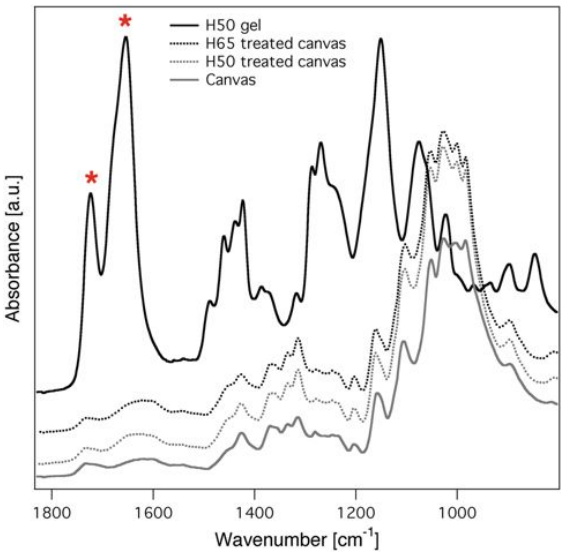

Fig. 3 ATR-FTIR fingerprint region spectra of a canvas, of H50 hydrogel and of canvases previously in contact with p(HEMA)/PVP hydrogels H65 and H50. Marked bands (*asterisk*) correspond to characteristic C=O stretching vibration of HEMA (1,724 cm^{-1}) and PVP (1,654 cm^{-1})

The artificially aged polymer adhesives, swollen after application of p(HEMA)/PVP hydrogels loaded with EAPC, are easily removed by gentle mechanical action. In Fig. 4 (centre and right), the enhanced swelling of these adhesives, after contact with the microemulsion confined inside hydrogels, is clearly detectable. In addition, the Whatman® filter paper placed on the backside of the canvas samples did not show traces of polymer transported by the microemulsion on the backside of the canvas. This confirms the hydrogel's effectiveness in confining the cleaning action only at the interface. The H65 hydrogel showed better efficacy in swelling both polymers making it the most appropriate confining tool for this kind of cleaning procedure under these circumstances. The required application time of 4 h allows the swelling and the partial solubilization of the polymer by the microemulsion. We have observed that a shorter application time results in a non complete swelling of the polymer leading to an inhomogeneous removal. The cleaning results are highlighted by optical microscopy images given in Fig. 5. The adhesive removal obtained through the application of H50 shows an incomplete cleaning action (Fig. 5, right) since the amount of microemulsion confined into the gel available for the cleaning is lower than in the H65 hydrogel. As a result, the

Fig. 4 Application of H50 hydrogel on the canvas glued with Plextol® adhesive, which, after swelling, could be removed by gentle mechanical action (*left* and *center*); removal of Mowilith® adhesive after application of H65 hydrogel (*right*)

Fig. 5 Optical microscopy images (×100 magnification) of the canvas with Plextol® before (*left*) and after removal of the aged adhesive using EAPC microemulsion confined in H65 (*center*) and H50 (*right*) hydrogels

canvas cleaned with H65 hydrogel presents a better cleaning, without visible damage of canvas fibers (Fig. 5, center).

4 Conclusions

Water-sensitive artifacts, i.e. artifacts that are constituted by hydrophilic materials, are always a concern for conservators that must apply gentle and controlled methods for efficient and safe removal of soiling materials, adhesives or aged varnishes. Chemical hydrogels based on semi-IPNs of p(HEMA)/PVP have demonstrated to be highly retentive and with good cleaning efficiency for the removal of hydrophobic layers, such as aged polymers, through the confinement of high-performing nanostructured fluids. This efficient combination of hydrogels and cleaning systems confined into the chemical gel network is a step forward in the conservation of cultural heritage and could be potentially applicable to different case studies.

Acknowledgements The authors acknowledge Dr. Chelazzi for providing the aged canvas samples. J. D. acknowledges financial support provided by *Fundação para a Ciência e a Tecnologia* (FCT) through a Ph.D. research grant (SFRH/BD/73817/2010). This work was partly supported by the CSGI, the European Union, Project NANOFORART (FP7-ENV-NMP-2011/282816) and the Ministry for Education and Research (MIUR, PRIN-2009-P2WEAT).

References

1. P. Baglioni, D. Chelazzi, R. Giorgi, G. Poggi, Langmuir **29**, 5110–5122 (2013)
2. A. Phenix, K. Sutherland, Rev. Conserv. **2**, 47–60 (2001)
3. M. Baglioni, R. Giorgi, D. Berti, P. Baglioni, Nanoscale **4**, 42–53 (2012)
4. M. Baglioni, D. Berti, J. Teixeira, R. Giorgi, P. Baglioni, Langmuir **28**, 15193–15202 (2012)
5. R. Wolbers, Cleaning painted surfaces: aqueous methods (Archetype, London, 2000).
6. E. Campani, A. Casoli, P. Cremonesi, I. Saccani, E. Signorini, Quaderni del Cesmar. **7**, 4 (2007)
7. G. Pizzorusso, E. Fratini, J. Eiblmeier, R. Giorgi, D. Chelazzi, A. Chevalier, P. Baglioni, Langmuir **28**, 3952–3961 (2012)
8. J.A.L. Domingues, N. Bonelli, R. Giorgi, E. Fratini, F. Gorel, P. Baglioni, Langmuir **29**, 2746–2755 (2013)
9. F. Yanez, A. Concheiro, C. Alvarez-Lorenzo, Eur. J. Pharm. Biopharm. **69**, 1094–1103 (2008)
10. S. Ming Kuo, S. Jen Chang, Y. Jiin Wang, J. Polym. Res. **6**, 191–196 (1999)
11. G.D. Smith, R. Johnson, WAAC Newsl. **30**, 11–19 (2008)
12. A. Chevalier, D. Chelazzi, P. Baglioni, R. Giorgi, E. Carretti, M. Stuke, M. Menu, R. Duchamp, in Proceedings of the ICOM-CC 15th Triennial Meeting, 22–26 September 2008, New Delhi, (Allied Publishers Pvt Ltd, New Delhi, 2008), p. 581
13. Y. Huang, J. Yang, Novel colloidal forming of ceramics (Springer, Berlin Heidelberg, 2011), p. 124